Asymmetric Migration Response and Its Implications in Big Shocks

Pin Sun*

July 7, 2025

Abstract

Standard migration models with a single migration elasticity imply that post-shock migration patterns mirror pre-shock behavior, regardless of the shock's magnitude—a prediction inconsistent with observed data. To address this limitation, I develop a nested logit migration framework in which nests are defined by both geographic and location's characteristics. This model allows migration elasticities to vary across locations—a feature that enables post-shock migration patterns to depend on the size of the shock. Using U.S. commuting-zone-level migration flow data, I document substantial heterogeneity in migration elasticities. I validate the model using the case of Hurricane Katrina in 2005, showing through simulation that the model's structure—featuring heterogeneous elasticities—can account for much of the persistently disproportionate migration responses observed over the decade following the disaster. Finally, the framework reveals that localized shocks generate more uneven spatial welfare losses compared to a single-elasticity model,

*School of Applied Economics, Renmin University of China; pin.sun@ruc.edu.cn. I am extremely grateful to my dissertation committees: Stephen Yeaple, Jonathan Eaton, Jingting Fan, Fernando Parro and Lilliard Richardson for their continuous guidance and encouragement. For very helpful discussions and suggestions, I also thank David Argente, Kirill Borusyak, Fabian Eckert, Michael Gechter, Elisa Giannone, Paul L. E. Grieco, Zibin Huang, Keisuke Hirano, Vijay Krishna, Omer Koru, Samuel Kortum, Qi Li, Nelson Lind, Douglas Noonan, Xinle Pang, Esteban Rossi-Hansberg, Bradley Setzler, Yuta Suzuki, Kohei Takeda, James Tybout, Thomas Zylkin, and seminar and conference participants for helpful comments and discussion. This work previously circulated with the title "Asymmetric migration response: an application in welfare analysis in climate change".

with high-migration-elasticity destinations disproportionately burdened due to overflow migrants from the affected origin.

JEL Codes: C68, J61, R13, R23

Keywords: Migration, Heterogeneous migration elasticities, Nested logit distribution, Katrina, Big shocks, Economic geography, Welfare analysis

1 Introduction

> *Migration is often regarded as a transformational adaptation strategy in response to climate-induced hydrological changes.* –IPCC (2022)

Individuals' migration responses are critical in shaping economic activities or determining the impact of local economic shocks across space. A large body of literature has examined the equilibrium effects of individuals' migration from various perspectives–for example, its contribution to aggregate productivity (Bryan and Morten, 2019), its role in smoothing adverse local shocks (Yagan, 2014), its influence on the effectiveness of place-based policies (Kline and Moretti, 2014; Gaubert et al., 2025), its capacity to mitigate the impact of climate change (Bilal and Rossi-Hansberg, 2023; Cruz and Rossi-Hansberg, 2024; Balboni, 2025), and its role in determining the distributional effect of trade shocks (Redding, 2016; Caliendo et al., 2019). A central parameter in these models of migration behavior is the migration elasticity, which governs how sensitively individuals respond to economic shocks across space.

A common simplifying assumption in this literature is that a single migration elasticity applies uniformly across all individuals and locations. In other words, migration behavior is assumed to be governed by a homogeneous elasticity, regardless of who is migrating, where they are migrating from or to, or the scale of shock they face. Under this assumption, when a localized shock occurs, all migration outflows from the affected area are expected to scale up proportionally, preserving the pre-shock distribution of destination choices. As a result, post-shock migration patterns mirror pre-shock ones and remain invariant to the shock's magnitude.

Introducing heterogeneity in migration elasticities, however, may lead to significantly different implications. For instance, consider individuals displaced by flooding. If low-risk destinations have relatively high migration elasticities, it becomes easier for displaced individuals to relocate and adapt to climatic risks. From the perspective of residents in those safer areas, however, a large and unrelated climatic shock elsewhere may lead to an overwhelming inflow of migrants, due to those same high elasticities—potentially imposing nonnegligible burdens on local communities.

In this paper, I develop a nested logit migration framework in which nests depend on both

geography and location's characteristics. This structure allows for heterogeneous migration responses, specifically through the heterogeneity in migration elasticities. I demonstrate the importance of accounting for this heterogeneity for accurately predicting the migration flows and evaluate the distributional welfare costs induced by the localized shocks across different regions.

To build intuition and illustrate the model's core mechanism, I begin with a stylized migration setting, which exhibits a crucial difference in the migration adjustment in response to a localized shock based on whether there is a single migration elasticity or heterogeneous elasticities. I find that allowing for different migration elasticities across locations can lead to distinctive model predictions. Specifically, a local shock can shift the migration pattern of the directly impacted location in my model with heterogeneous elasticities, whereas the post-shock migration behaviors remain the same as the pre-shock behaviors in the single-elasticity model. Furthermore, in the heterogeneous framework, the size of a localized shock determines how largely the post-shock migration pattern will deviate from the pre-shock one.

Motivated by the insight that the magnitude of a localized shock can fundamentally alter migration patterns under heterogeneous elasticities, I analyze the massive displacement caused by Hurricane Katrina. Focusing on migration out of New Orleans, the area most heavily hit by Hurricane Katrina, I document four stylized facts. The most important stylized fact is that Katrina migrants were more likely to move to areas that have characteristics similar to those of New Orleans: namely, urban places within the same U.S. Census Division (Division 7). In particular, this disproportionate response persists well beyond the year of Hurricane Katrina's occurrence. These patterns suggest potential heterogeneity in migration elasticities across space, especially between urban and rural areas, and across regional boundaries.

To assess whether these observed shifts can be attributed to underlying differences in migration elasticities rather than the confounding factors–such as moving barriers or fundamental changes in certain destinations–I conduct a reduced-form, triple difference-in-difference (DID) analysis regarding migration flows before versus after Hurricane Katrina. The results demonstrate the very different migration elasticities across alternative destinations. I find that the migration elasticities are much higher for urban locations in the same southern census division

as New Orleans, including Arkansas, Louisiana, Oklahoma, and Texas, than for rural areas or for more distant cities. Additionally, the triple DID analysis also reveals a persistent, Katrina-induced disproportionate migration response that extends well beyond the immediate aftermath of the disaster.

To explore the exact role of heterogeneous migration elasticities in shaping post-Katrina migration responses, I extend the model of Caliendo et al. (2019) by relaxing the single-elasticity assumption. As in the Caliendo et al. (2019) model, forward-looking individuals make discrete choice decisions about where to live based on their current location, the expected economic conditions in all locations, the costs of moving across locations, and idiosyncratic taste shocks. Where I deviate from the standard framework is in positing different nests in terms of these taste shocks. Specifically, I classify destinations into nests depending on the census division to which they geographically belong and their type, whether rural or urban. This nesting structure allows for variation in expected economic conditions to have heterogeneous effects on people's moving decisions based on where they currently reside. I refer to this extended framework as a "dynamic nested logit migration model."

Under this departure, the law of motion for bilateral migration rates becomes the product of two components: the probability of selecting a nest and the conditional probability of choosing a specific destination within that nest. Conceptually, agents first choose to which nest to go, anticipating that they will subsequently make the optimal destination choice within the nest; conditional on this nest choice, they select the best location within it. This structure implies that migration elasticities are differentiated: the migration elasticity between locations within the same nest is governed by the within-nest parameter, while the elasticity between locations in different nests is governed by the cross-nest parameter. Notably, if the within-nest and cross-nest parameters are assumed to be identical, my framework collapses to the standard single-elasticity model. In other words, the single-elasticity framework is a special case of the dynamic nested logit migration model.

Inspired by the structure of the migration rate's law of motion, I construct an empirical strategy to validate the nested specification and identify heterogeneous migration elasticities. Specifically, the law of motion for bilateral migration rates links observed migration patterns

to unobserved continuation values of destinations. I use this relationship to derive sufficient statistics for each destination's continuation value. These statistics are then substituted into the origin-specific value function—which can be expressed as a function of both flow utility and destination-specific continuation values—to eliminate unobserved components. This yields an estimating equation in which the elasticity parameters interact with observed variables and can be recovered through a tractable regression framework. This approach provides a direct test of the nested logit structure and a consistent method for estimating heterogeneous migration elasticities across space.

Leveraging a unique demographic dataset, I verify the validity of my model's nest setting and find that elasticities are very different across pairs of locations in sensible ways. I statistically reject the hypothesis of a single migration elasticity. The estimated migration elasticity for pairs of locations within a nest, called the within-nest migration elasticity, is significantly higher than the elasticity for pairs of places across different nests, called the cross-nest migration elasticity. For the purpose of comparison, this paper uses the same datasets to estimate the single migration elasticity under the existing framework. I find that the estimate is a level between my model's cross-nest and within-nest migration elasticities. This suggests that the classical model underestimates the within-nest migration adjustment but overestimates the cross-nest adjustment to a local shock.

Additionally, to address concerns that changes in bilateral moving costs associated with Hurricane Katrina might bias the estimated migration elasticities, I conduct a robustness check using a subsample that excludes the Katrina-affected period. The underlying idea is to rely solely on cross-sectional variation in economic conditions during normal times to identify migration elasticities, thereby mitigating concerns about shock-induced distortions in moving costs. The resulting elasticity estimates are highly consistent with the baseline results, lending further credibility to the model's structure and the presence of substantial heterogeneity in migration responses.

Equipped with the estimated migration elasticities, I apply the dynamic nested logit migration model to analyze the displacement effects of Hurricane Katrina. Specifically, I assess how much of the variation in the disproportionate migration responses of New Orleans residents

can be explained by heterogeneity in migration elasticities alone. The simulation results show that, while the standard single-elasticity model captures very limited aspects of post-Katrina migration dynamics, the dynamic nested logit framework explains a substantial portion of the disproportionate responses—both in terms of the immediate shift in migrant behavior and the transitional patterns observed in the triple DID empirical analysis.

I then turn to the economic implications of incorporating multiple migration elasticities. The analysis reveals that when migration elasticities are properly calibrated, adjustment to climate change shocks slows dramatically and the costs of adjustment are disproportionately borne by people living in areas to which displaced migrants from the shock origin exhibit higher migration elasticities. In the Katrina case, these are urban locations within the same census division as New Orleans—specifically, urban areas in Arkansas, Louisiana, Oklahoma, and Texas. Displaced individuals are more likely to relocate to within-nest destinations with higher migration elasticities, concentrating population pressure and imposing congestion costs on those areas. Over time, this burden gradually shifts toward lower-elasticity destinations, but the process unfolds more slowly than in a model with a uniform elasticity. As a result, when discounting welfare losses over time, high-elasticity regions bear greater costs and do so earlier in the adjustment path. For instance, in the Katrina case, the average welfare loss of places located in the same nest as New Orleans is substantially larger than what would be predicted under the standard single-elasticity model.

This paper contributes to the existing literature by demonstrating why and how migration behavior should be modeled in a more flexible way. I develop a dynamic nested logit migration framework that allows for heterogeneous migration elasticities across locations and demonstrate substantial heterogeneity in these elasticities across U.S. location pairs. By combining structural modeling, reduced-form evidence, and simulation-based analysis, my work shows that accounting for such heterogeneity is essential for understanding both the transitional dynamics and distributional outcomes across space following large, localized shocks. These findings highlight the importance of incorporating heterogeneous migration elasticities into models of spatial adjustment to such localized shocks.

My research contributes to several strands of literature. First, it advances the rapidly grow-

ing body of work utilizing quantitative spatial dynamic migration models to understand the spatial distribution of economic activity in response to localized shocks, including Artuç et al. (2010), Desmet and Rossi-Hansberg (2014), Desmet and Rossi-Hansberg (2015), Desmet et al. (2018), Caliendo et al. (2019), Caliendo et al. (2021), Conte et al. (2021), Cruz (2021), Bilal and Rossi-Hansberg (2023), Kleinman et al. (2023), Cruz and Rossi-Hansberg (2024) and Balboni (2025). Artuç et al. (2010) and Caliendo et al. (2019) analyze labor adjustment in response to trade shocks. Desmet and Rossi-Hansberg (2014) explore the relationship between the spatial distribution of economic activity and local innovations. Desmet et al. (2018) consider the welfare implications of relaxing cross-country migration restrictions, while others examine the effects of climate change across sectors (Desmet and Rossi-Hansberg, 2015; Conte et al., 2021; Cruz, 2021; Cruz and Rossi-Hansberg, 2024). Balboni (2025) studies the risks rising sea levels pose to coastal infrastructure, and Desmet et al. (2021) investigates associated population and economic shifts across space. Caliendo et al. (2021) quantify the welfare and migration effects of EU enlargement. Recent methodological advances include Bilal and Rossi-Hansberg (2023), who integrate heterogeneous agent dynamics and anticipatory behavior to model climate change adaptation, building on solution techniques from Bilal (2023), and Kleinman et al. (2023), who incorporate capital dynamics to examine how capital-labor interactions affect spatial responses to shocks. Both approaches rely on first-order approximations around a model baseline. I complement this literature by allowing more heterogeneous migration responses to economic shocks in the quantitative framework. This heterogeneity is particularly important for conducting quantitative analysis regarding the impact of big shocks. I also show that implementing such a quantitative analysis does not require heavy computational costs.

Second, my work also speaks to the literature examining the spatial consequences of large localized shocks, including Kline and Moretti (2014), Ahlfeldt et al. (2015), Burzyński et al. (2022), Fried (2022), Henkel et al. (2024), Redding and Sturm (2024), Hsiao (2025), and Takeda and Yamagishi (2025). Kline and Moretti (2014) investigate the long-run effects of one of the largest regional development projects in the U.S. history–the Tennessee Valley Authority–at both local and national levels. Ahlfeldt et al. (2015) analyze how Berlin's division and subsequent reunification reshaped economic activities within the city in terms of

employment and land values. Other work studies the long-term consequences of wartime destruction: Redding and Sturm (2024) examine long-lived spillover effects on neighboring areas, while Takeda and Yamagishi (2025) highlight the crucial role of agglomeration forces in Hiroshima's recovery after the atomic bombing. Other work focuses on large-scale natural disasters: Burzyński et al. (2022) explores the economic consequences of extreme weather events driven by climate change; Fried (2022) and Hsiao (2025) study the impacts of rising sea levels; and Henkel et al. (2024) analyzes the effects of post-disaster assistance policies. My contribution to this literature lies in showing how heterogeneity in migration elasticities shapes the distributional impact of such shocks across space.

Finally, this paper connects to research on heterogeneous spatial responses to local shocks. Monte et al. (2018) documents how local employment adjusts unevenly across space through migration and commuting in response to a local labor demand shock. Porcher (2022) studies the role of information frictions in heterogeneous migration responses. The closest to my work is Rodríguez-Clare et al. (2025), which develops a model that differentiates workers' cross-sector mobility elasticity from their cross-location mobility elasticity to understand unemployment impacts of the China shock under downward nominal wage rigidity. Expanding on this literature, I focus on heterogeneity in migration elasticities across locations at a more granular level. I derive a reduced-form expression that identifies the presence of such heterogeneity and demonstrate that migration elasticities vary systematically across regions and across the urban/rural divide. Importantly, I show that this heterogeneity implies that localized shocks can lead to deviations in post-shock migration patterns relative to pre-shock baselines—and that the size of these deviations depends on the magnitude of the shock.

The rest of the paper is structured as follows. Section 2 provides a stylized model that motivates the core research question. Section 3 describes the study's data sources and relevant empirical findings. The full-fledged nested logit migration model that incorporates heterogeneous migration elasticities is presented in Section 4. Section 5 delivers the identification and estimation strategy for the migration elasticities and reports estimated results. In Section 6, I demonstrate that the proposed model accounts for a significant share of the observed disproportionate migration responses in the Katrina case and likewise has different welfare and policy

implications. I conclude my work in Section 7.

2 A Stylized Model

The section fulfills three objectives. First, it demonstrates that differences in moving costs alone are insufficient to account for the observed migration patterns. Second, it provides intuition for how to identify locations' different substitution patterns; namely, heterogeneous elasticities. Finally, it motivates the next section's empirical analysis.

I begin by considering an economy with four locations–1, 2, 3, and 4–which are evenly distributed across two nests, **N** and **S**. Here, "nest" is used to represent those economic and non-economic attributes that are unobserved by economists. Locations within the same nest share similar unobserved characteristics. Specifically, Locations 1 and 2 are in nest **N**, while Location 3 and 4 are in nest **S**. In other words, Locations 1 and 2 share similar unobserved economic and non-economic attributes, while Locations 3 and 4 share similar counterparts. Residents in each location are likely to prefer places within the same nest when making moving decisions, due to these shared unobserved attributes.[1] This preference will be reflected in individuals' idiosyncratic tastes, which I will disscuss in this section.

In the economy, there is always a continuum of agents with measure one. These agents only survive one period. As shown in Figure 1, generation t is born at the beginning of period t. Given locations' fundamentals and generation t's realized idiosyncratic tastes over each place, generation t chooses their optimal destination. Upon moving to the optimal location, they become involved in producing a freely tradable homogeneous good with linear production technology that requires only labor input. Both the product and local labor market are perfectly competitive. Finally, they earn wages and obtain log utility by consuming the homogeneous product. At the start of period $t+1$, generation t is replaced by the new generation $t+1$ with the same distribution across locations. Namely, the initial location of generation $t+1$ is conditional on the distribution of generation t.

Specifically, individual i of generation t in birthplace j makes her migration decision ac-

[1] For example, this special taste could result from an individual's unique attraction to a particular type of location (Zerecero (2021), and Sprung-Keyser et al. (2022)), or from unobserved social networks embedded in a range of locations (Sahai and Bailey (2022), Tang (2024), and Zabek (2024)).

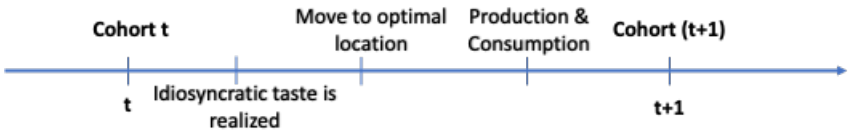


Figure 1

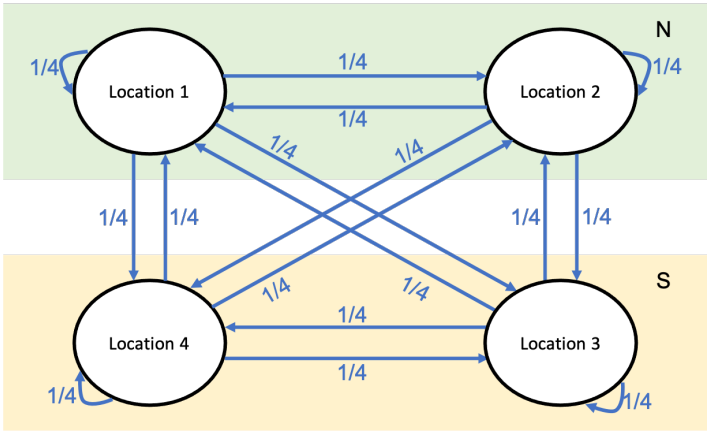


Figure 2

cording to

$$u_{it}^{j} = \max_{k \in \{1,2,3,4\}} \{\ln w_t^k - \tau_t^{kj} + \ln \varepsilon_{it}^{kj}\}, \tag{1}$$

where w_t^k is the real wage in destination k measured as units of the homogeneous product; τ_t^{kj} represents the moving cost from j to k; and ε_{it}^{kj} is individual i's idiosyncratic taste toward k, which is assumed to be drawn from an exogenous distribution right after her birth.

To simplify the analysis, I assume that the four locations offer the same wage and that all moving costs are identical. Obviously, we will arrive at the steady state in which people are evenly distributed across space and all outflows are identical, as presented in Figure 2. Note that this is independent of the specification of the idiosyncratic preference distribution, ε_{it}^{kj}. Let us assume that the economy is initially at the steady state.

Suppose now that there is a negative shock leading to wage decline in Location 1 at the beginning of period s. If all idiosyncratic tastes are independently drawn from a single distribution–namely, all locations share the same migration elasticity and individuals do not have special preferences for destinations within the nest–then, as evident in Figure 3 we will see that although all outflows of generation s from Location 1 increase relative to the steady state, the

ratio of any two of the outflows from Location 1 remains the same as that of the steady state, which is equal to 1. If we specify that distribution as a Fréchet distribution,[2] which is often used in the literature, we have the following proposition:

Proposition 1 *If idiosyncratic taste ε_{it}^{kj} is drawn from the following distribution,*

$$\begin{aligned}\mathbf{P}[\varepsilon_t^{kj} \leq a_k, k = 1,2,3,4] &= \Pi_{k\in\{1,2,3,4\}}\mathbf{P}[\varepsilon_t^{kj} \leq a_k] = \Pi_{k\in\{1,2,3,4\}} \exp\big(-a_k^{-\sigma}\big) \\ &= \exp\big(-\sum_{k\in\{1,2,3,4\}} a_k^{-\sigma}\big),\end{aligned} \tag{2}$$

then the partial derivative of the ratio of any two outflows from Location 1 w.r.t the change of Location 1's wage, w^{*1}

$$\frac{\partial\big(\frac{\mu^{*k1}}{\mu^{*h1}}\big)}{\partial \log w^{*1}} = 0, \forall k, h \in \{2,3,4\}, \tag{3}$$

where μ^{*k1} is the migration rate from Location 1 to Location k. Hence, the outflow migration pattern of individuals from Location 1 will not be influenced by changes in the origin location's wage, indicating an absence of asymmetric migration response. This holds even if there are heterogeneous wages and moving costs.

PROOF See Appendix A. ∎

Proposition 1 implies that if all destinations have the same migration elasticity, the fundamental change in origin location will not shift the migration behaviors of those who live there.

Instead of assuming independent draws,suppose that individuals born in Location 1 view Location 2—which lies in the same nest—as more similar or preferable than the two destinations in nest S due to some unobserved factors. That is, individuals tend to favor within-nest destinations, and their idiosyncratic preferences for those destinations are more strongly correlated. As shown in Figure 4 it is expected that the ratio of the migration flow from Location 1 to Location 2 to the counterpart to either of the two nest-**S** locations will be larger than 1, which

[2]In papers like Caliendo et al. (2019), researchers assume idiosyncratic tastes follow a Type-1 extreme value distribution because they do not take the log of the tastes. It is easy to show that the log distribution of a Fréchet distribution is a Type-1 extreme value distribution.

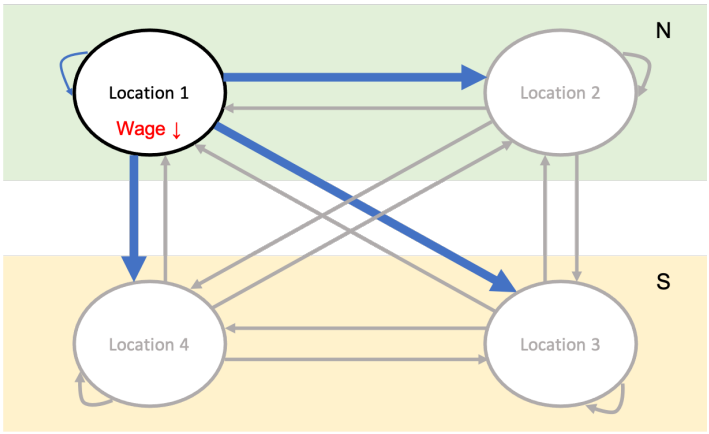


Figure 3: The Case of Uniform Preferences Across Locations

is different from the steady state. To formalize this heterogeneity in how migrants choose between destinations, I make the *sum* in equation (2) into nests and allow the migration elasticity to shift within a nest. I thus arrive at this proposition:

Proposition 2 *If idiosyncratic taste* ε_{it}^{kj} *is drawn from the following distribution,*

$$\mathbf{P}[\varepsilon_t^{kj} \leq a_k, k = 1,2,3,4] = \exp\left(-\left[\sum_{d\in\{N,S\}} \sum_{h\in D_d} \left((a_h)^{-\gamma}\right)^{\frac{\theta}{\gamma}} \right] \right), \gamma \geq \theta \tag{4}$$

where γ *represents within-nest locations' migration elasticity and* θ *is cross-nest locations' elasticity*[3]*, then the partial derivative of this migration flow ratio w.r.t the origin location's wage change,*

$$\begin{cases} \frac{\partial\left(\frac{\mu^{*31}}{\mu^{*41}}\right)}{\partial \log w^{*1}} = 0, \\ \frac{\partial\left(\frac{\mu^{*21}}{\mu^{*h1}}\right)}{\partial \log w^{*1}} = \frac{\theta-\gamma}{2} \quad \forall h \in \{3,4\}, \end{cases} \tag{5}$$

where μ^{*21} *denotes the migration rate from Location 1 to within-nest Location 2, and* μ^{*h1} *is the migration rate from Location 1 to cross-nest Location h. This suggests an asymmetric migration response to negative shocks in the origin, wherein migrants from Location 1 disproportionately favor relocating to within-nest Location 2 that exhibits a higher migration elasticity with respect to the origin. In particular, this response strengthens with larger origin*

[3]Here, it is assumed that $\gamma \geq \theta$. In other words, locations within the same region exhibit a higher degree of migration elascticity compared to those across different regions.

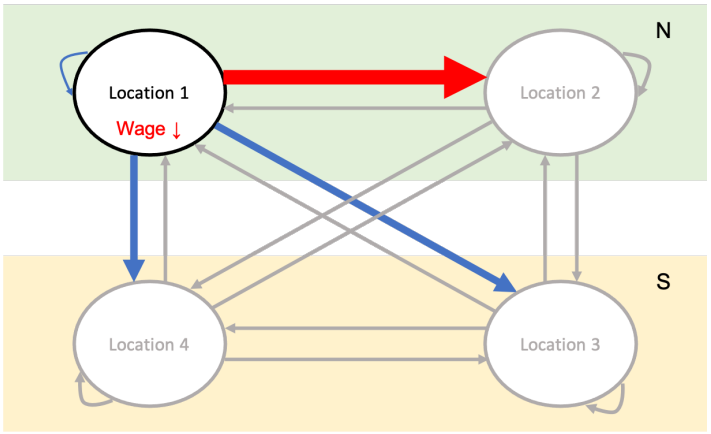


Figure 4: The Case of Unobserved Special States for Within-region Locations

shocks. This property holds even if there are heterogeneous wages and moving costs.[4]

PROOF See Appendix A. ■

Proposition 2 tells us that when a local shock happens, people from the directly impacted place will disproportionately relocate to destinations with higher migration elasticities relative to the origin.

Intuitively, the departure of post-shock migration behavior from pre-shock migration behavior results from the shift in the composition of migrants. In the initial steady state, those who choose to stay in their birthplace must have a strong idiosyncratic preference over the origin place. Because of the high correlation between within-nest idiosyncratic tastes, they also prefer the within-nest alternative locations over outside-nest destinations. When a negative local shock happens, a fraction of the people are forced to leave. The larger the shock, the bigger the fraction. Because of this correlation, they will disproportionately move to places within the same nest. As a result, the post-shock migration pattern deviates from the pre-shock one. The larger the shock, the bigger the deviation. However, when idiosyncratic draws are independent, those who choose to stay in the origin location because of their strong idiosyncratic preference over it but are forced to leave do not prefer one destination over others.

It follows from Propositions 1 and 2 that the change in migration behavior from before to after a shock helps to identify differences in migration elasticities across locations. If migration

[4]Note that when $\theta = \gamma$, equation (4) collapses to equation (2). In this sense, Proposition 1 is essentially a special case of Proposition 2.

elasticities vary across destinations, it is expected that there will be a big shift in the migration pattern after some big shocks. This expectation motivates the next section's analysis.

3 Empirical Evidence

By empirically analyzing the impact of Hurricane Katrina on New Orleanian migration behaviors, this section provides evidence of heterogeneity in migration elasticities across destinations. It consists of two subsections. In the first subsection, I describe the multiple data sources used in this study. The second subsection centers on four stylized facts related to Hurricane Katrina.

3.1 Data

The geographic unit of analysis is the commuting zone (CZ), which is defined in this study as a local labor market.[5] There are 722 CZs in the contiguous United States that encompass all metropolitan and nonmetropolitan areas. For analyzing CZ-level migration behaviors, this paper relies on data from multiple sources.

The first data source is the Internal Revenue Service's (IRS) county-to-county outflow dataset from 2000 to 2019. This is the only publicly available dataset that can be used to construct annual CZ-level bilateral migration flows. However, one of its drawbacks is that the IRS omits any bilateral flow that does not meet a particular threshold. Before 2013, the threshold was 10; since then, the threshold has been 20. Because of this, although theoretically we should observe all 722×722(=521,284) bilateral migration flows, we can observe only those flows above the threshold. After county-level data is aggregated at the CZ level, there are fewer than 25,000 (4.8%) observations annually before 2013 and approximately 14,000 (2.7%) annually after that (except in 2016, when there were about 16,400). A large drop in the post-2013 period resulted from the rising threshold in 2013.

To mitigate the impact of the IRS's deletion policy, I adjust the original data by imputing certain bilateral migration flows based on information about each county's total number of

[5] A commuting zone, as initially conceptualized by Tolbert and Sizer (1996), consists of multiple contiguous counties and is characterized by strong commuting ties within the CZ and weak commuting ties across CZs.

migrants (more details in Appendix B). With this process, the number of available migration flow observations increases to more than 35,700 annually. I exploit this imputed CZ-to-CZ bilateral migration flow dataset to document some stylized facts in Subsection 3.2.

Another drawback of the publicly accessible IRS migration flow data is that the data do not include demographic information such as age. This could affect the migration estimation that relies on wage variation in Section 5. To handle this issue, I discipline the imputed migration flow data using the second data source, which is a demographic dataset from a private company, Infutor Inc., that covers more than 180 million individuals annually ranging from 2014 to 2019. It includes rich demographic information such as date of birth and residential address. Based on this information, I create the CZ-to-CZ migration flow data for individuals aged 25-55 over the 2014-2018 period. In contrast to the IRS data, the data I use, even when limited to individuals aged 25-55, include more than 100,000 non-zero bilateral migration flow observations annually. As a validity test, I calculate the correlation between IRS and Infutor migration flow data during the 2014-2018 period at both the county and CZ levels. My calculation shows high correlation with values of 0.986 and 0.988, respectively.[6] Eventually, I combine the 2014-2018 Infutor migration flow data with the 2004-2013 imputed IRS data to create a dataset for the migration elasticity estimation and the quantitative analysis.

In addition to using the two aforementioned data sources, I use the 5 percent sample of the U.S. census in 2000 and annual American Community Survey (ACS) data over the 2005-2019 period from Steven Ruggles and Sobek (2022) for the elasticity estimation. These datasets provide a wide range of individual-level economic and demographic information including ages, wages, and housing costs. Importantly, they also report the Public Use Microdata Area (PUMA) in which each household unit is located. Exploiting the crosswalk between PUMAs and CZs by Autor and Dorn (2013), I calculate CZ-level 25-55-year-old employee wages and living costs from 2005 to 2019, which I then use for the migration elasticity estimation (see Section 5).

Finally, to identify the role of mobility in helping people to adapt to climate change, I exploit two flood risk measures provided by the First Street Foundation (FSF). The FSF reports

[6]These correlations are calculated conditional on non-zero migration flows in IRS data, as I am unable to verify whether zero flows there reflect true zeros or missing data.

the total number of parcels inside the Special Hazard Flood Area (SFHA) for each county in the contiguous United States. SFHAs, areas designated by the Federal Emergency and Management Agency (FEMA), have at least a 1% annual chance of being flooded. In most of this study, I use the percentage of properties inside SFHAs as a proxy for each CZ's flood risk exposure. To complement this measure, I use a flood risk measure developed independently by the FSF that takes into account climate change.

3.2 Empirical Facts

Motivated by the difference between a model with and without heterogeneity in locations' migration elasticities, as shown in Section 2, in this subsection I examine whether migration elasticities differ across locations by analyzing the effect of Hurricane Katrina on New Orleanian migration patterns. Before documenting the details, I briefly discuss the background.

Hurricane Katrina, one of the most powerful hurricanes in U.S. history, struck the Gulf Coast region in late August 2005, making landfall as a Category III storm about 50 miles southeast of New Orleans. The storm had a devastating impact on Gulf Coast residents, with at least 1,833 deaths and more than $100 billion in property damages (NWS (2016)). Figure 5 illustrates the trajectory of Hurricane Katrina, with the red star on the map indicating the location of New Orleans.

Among the impacted regions, New Orleans, which is situated largely below sea level, suffered the worst damage. A large storm surge produced by Katrina overwhelmed the levee system protecting New Orleans from flooding and led to 80% of New Orleans being flooded (Deryugina et al. (2018)). This unprecedented damage triggered massive displacement of New Orleans residents. From one month before Katrina to five months afterward, the city of New Orleans lost 278,833 residents, or 63.8% of its total population at the time (Frey and Singer (2006)).

This dramatic population decline can be seen in the yearly IRS data. The CZ to which the city of New Orleans belongs lost about 20% of its population in 2005.[7] As presented in Figure

[7]The bigger difference of 63.8% in Frey and Singer (2006) may be because there were many temporary evacuees who returned to New Orleans within a year and thus are not accounted for in the Frey and Singer (2006) measure. The New Orleans CZ consists of nine parishes (analogous to counties), one rural and eight urban. They

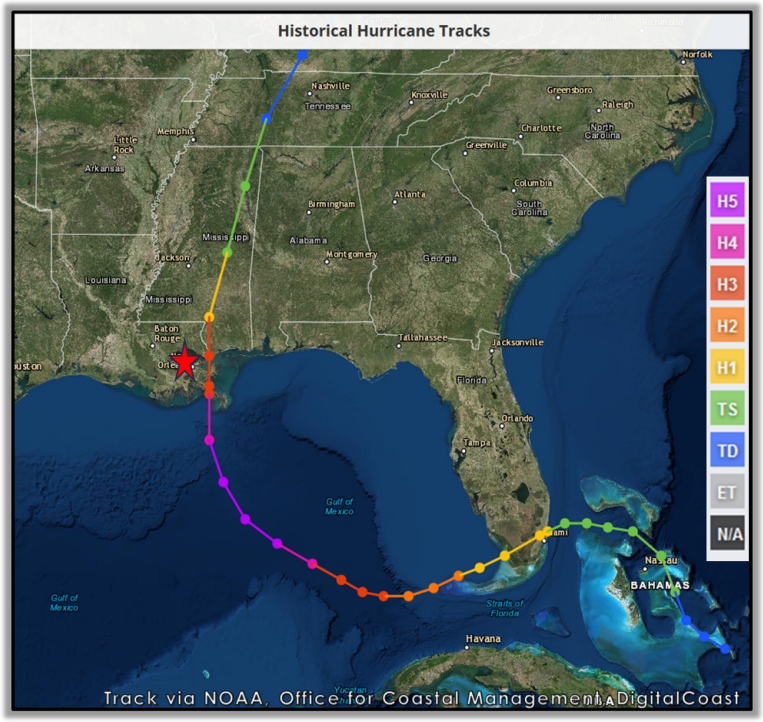


Figure 5: Hurricane Katrina Path

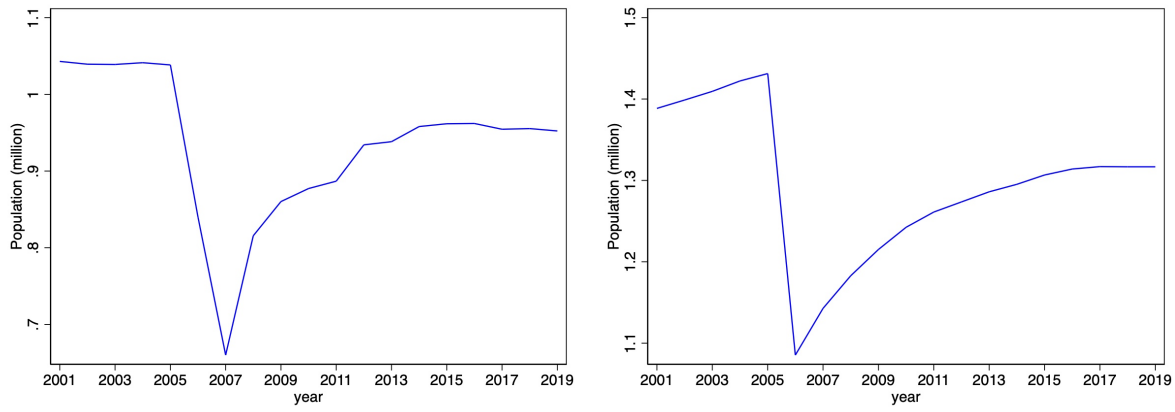
Source: NOAA.

6a, the population of New Orleans CZ had not yet returned to its 2004 level even thirteen years after Hurricane Katrina. A similar trend is evident in the Census estimated yearly population data, as shown in Figure 6b.[8] Given the generally low U.S. migration rate and its continuous decline for almost four decades (Molloy et al. (2011)), the dramatic migration movement induced by Hurricane Katrina provides a unique opportunity to examine whether the existing framework modeling individuals' migration behaviors operates as expected or whether the hypothesis embedded in that framework needs to be modified to account for significant differences in pre- and post-Katrina migration behavior. By exploiting the imputed IRS CZ-to-CZ migration flow data, I document the following four stylized facts:

***Fact 1**: After the New Orleans CZ was hit by Hurricane Katrina, the outmigration rate*

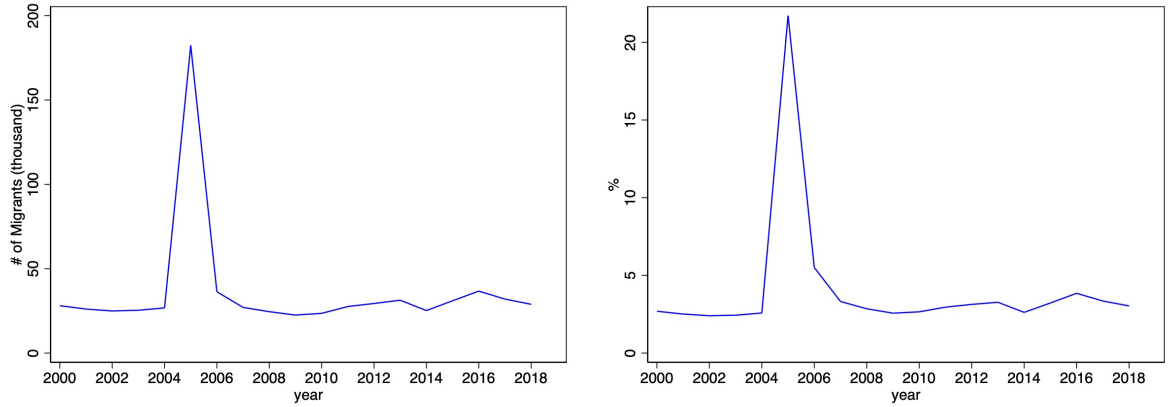
are Jefferson Parish, Orleans Parish (in which the city of New Orleans is located), Plaquemines Parish, St. Bernard Parish, St. Charles Parish, St. James Parish, St. John the Baptist Parish, St. Tammany Parish, and Washington Parish (rural).

[8]The discrepancy in population levels between the IRS and Census data primarily reflects differences in coverage: IRS data includes mainly working-age individuals who file tax returns, while Census data encompasses the entire population. Additionally, the Census does not publicly provide bilateral migration flow data, so we rely solely on IRS data for the subsequent empirical analysis.



(a) IRS Data (b) Census Data

Figure 6: New Orleans CZ's Yearly Population



(a) Number of Migrants (b) Migration Rate

Figure 7: New Orleans CZ's Yearly Migration Outflow

jumped to more than eight times its pre-Katrina level.

Over the 2004-2005 period, the time just before the occurrence of Katrina, the overall outmigration rate in the New Orleans CZ was 2.58%. [9] However, as shown in Figure 7a, a year later it jumped to 21.72%. In terms of the change in the number of migrants, as evident in Figure 7b, the IRS recorded more than 182,300 outmigrants from the New Orleans CZ in 2005, which is 5.8 times larger than 26,800, the number recorded in 2004.

[9] Although Katrina happened in late August 2005, its effect on migration flows is not expected to be reflected in the IRS 2004-2005 data because pre-2011 IRS data is based exclusively on income tax returns filed before the end of September. This is shown in the fact that the reported overall outmigration rate in New Orleans in 2004 is almost the same as the one in 2003, 2.44%.

City	2000	2001	2002	2003	2004	2005	2006	2007
Houston, TX	31.1	33.5	30.8	34.1	34.0	53.8	47.5	42.7
Atlanta, GA	16.7	17.5	18.2	17.7	17.5	16.4	16.1	14.3
Dallas, TX	14.4	11.1	12.2	10.8	12.1	18.0	17.1	13.6
Los Angeles, CA	7.3	7.9	9.0	9.4	7.8	2.1	3.0	4.4
Washington DC	7.9	7.3	6.4	6.9	7.2	1.8	3.4	5.0
Miami, FL	4.8	5.4	5.7	5.5	5.5	1.0	2.3	3.9
New York, NY	5.0	5.5	5.0	5.1	5.3	1.0	2.4	4.3
Chicago, IL	4.3	3.8	4.6	4.0	4.1	1.4	2.1	3.6
Austin, TX	4.2	3.9	3.3	3.2	3.3	3.6	4.4	5.2
San Francisco, CA	4.3	4.0	4.9	3.2	3.2	0.8	1.7	3.0
Total	100 (8,412)	100 (7,278)	100 (6,546)	100 (6,490)	100 (7,304)	100 (78,487)	100 (11,931)	100 (7,334)

# of yearly migrants in parentheses;

Table 1: Distribution of New Orleans CZ Yearly Migrants (%)

Fact 2: *The migration pattern in New Orleans CZ was stable before Hurricane Katrina, but it dramatically shifted afterward. Notably, this shift persisted for at least three years.*

Table 1 presents the pre- and post-Katrina distributions of yearly migration from the New Orleans CZ over the top ten big city destinations where New Orleanians often move. Each element represents the percentage for which a particular destination accounts. The final row is the summation and the number in brackets is the number of New Orleans migrants moving to these ten cities. As evident in Table 1, the New Orleans CZ's migration pattern across the top ten big city destinations before Hurricane Katrina was stable. After Hurricane Katrina happened, however, the migration behavior dramatically changed. Cities like Austin, Dallas, and Houston came to accept disproportionately more migrants from New Orleans than the other remaining seven destinations. Importantly, this pattern of disproportionate relocation persisted through at least 2007, well beyond the immediate aftermath of the disaster.

Based upon what we learned in Section 2, the substantial shift in the migration pattern after Hurricane Katrina suggests the potential heterogeneity of locations' migration elasticity, which is discussed in detail in ***Fact 4***.

Fact 3: *The flood risk exposure of migrants from the New Orleans CZ increased 15.7%.*

Under FEMA's risk measure, the average flood risk exposure of New Orleans migrants was 0.062 in 2004. However, after Katrina struck New Orleans, the risk rose to 0.072.[10] I observe

[10]The average is the mean of each migration destination's flood risk exposure weighted by migrants from the

a similar situation based on the FSF's own risk measure: that is, that New Orleans evacuees' risk exposure rose from 0.107 in 2004 to 0.112 in 2005. The inability to avoid flood risk is primarily attributed to the migration of numerous New Orleans evacuees to high flood risk areas, such as Houston, Texas. This indicates that New Orleanians did not necessarily relocate to escape flood risk, suggesting that flood risk was not a predominant factor directly influencing migration decisions.[11]

Fact 4*: New Orleanian migrants disproportionately relocated to urban places in Census Division 7.*

Proposition 1 and 2 in Section 2 suggest that ***Fact 2***'s findings imply the potential heterogeneity of location's migration elasticity. To verify this, we need to identify the "nest" mentioned in Section 2 that can classify locations based on unobserved economic and non-economic factors. The "census division", developed by the U.S. Census Bureau to divide the whole U.S. territory into nine areas, as presented in Figure 8, would be a strong candidate for this nest definition.[12] These divisions are argued to be based on the economic and non-economic similarity of locations' characteristics (Blanchard and Katz (1992) and Kim (1995)). This delineation has been utilized in different studies (Blanchard and Katz (1992), Kim (1995), Autor et al. (2013), and Fan and Bakkensen (2022)).[13] Empirical migration pattern observed in the Hurrican Katrina case also favor using census divisions as nests. The three destinations in

New Orleans CZ. To calculate these two numbers, I drop all Katrina-impacted destinations. If a county in a CZ was eligible for either the Public or Individual Assistance Program offered by FEMA after Hurricane Katrina, I considered that destination CZ to be a Katrina-impacted place. There are 32 such CZs in total.

[11]Pang and Sun (2024) investigate and model the influence of flooding risk on migration behavior.

[12]The nine census dividisions are Census Division 1 (New England: Connecticut, Maine, Massachusetts, New Hampshire, Rhode Island, Vermont), Census Division 2 (Middle Atlantic: New Jersey, New York, and Pennsylvania), Census Division 3 (East North Central: Indiana, Illinois, Michigan, Ohio, and Wisconsin), Census Division 4 (West North Central: Iowa, Kansas, Minnesota, Missouri, Nebraska, North Dakota, and South Dakota), Census Division 5 (South Atlantic: Delaware, District of Columbia, Florida, Georgia, Maryland, North Carolina, South Carolina, Virginia, West Virginia), Census Division 6 (East South Central: Alabama, Kentucky, Mississippi, and Tennessee), Census Division 7 (West South Central: Arkansas, Louisiana, Oklahoma, and Texas), Census Division 8 (Mountain: Arizona, Colorado, Idaho, New Mexico, Montana, Utah, Nevada, Wyoming), and Census Division 9 (Pacific: Alaska, California, Hawaii, Oregon and Washington).

[13]Blanchard and Katz (1992) use census divisions to group the U.S. states and study the spatial employment responses to adverse shocks. Kim (1995) explore the long-run trends in U.S. regional specialization based upon census divisions. Autor et al. (2013) exploit census divisions to control for region-specific trends in their study of the impact of China trade shock on U.S. employment. Fan and Bakkensen (2022) employ census divisions to study the household sorting in response to hurricane risk.

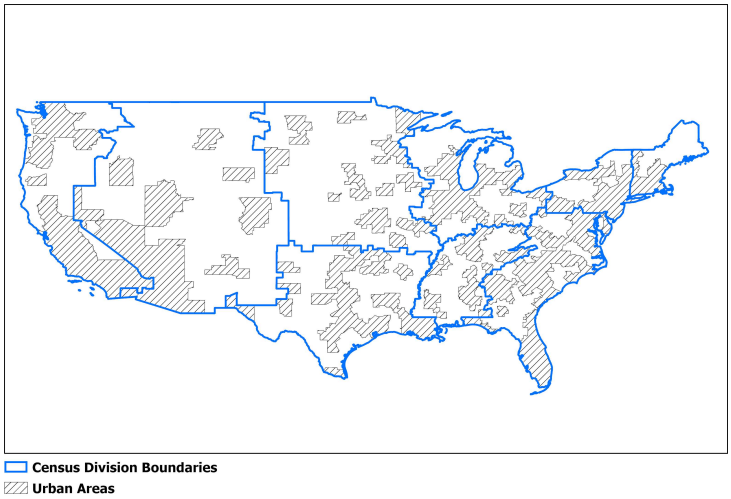


Figure 8: Census Divisions and Urban Areas

Table 1– Austin, Dallas, and Houston– which received disproportionately more New Orleans' migrants than other major cities, are all in the same census division as New Orleans (Census Division 7, or the "West South Central" census division).[14] The percentage of New Orleans migrants for which it accounts increased from the pre-Katrina 47.5% in 2004 to 66.8% in 2005.

Since this study covers the entire contiguous U.S. at a fine geographic unit and rural places differ from urban places even within the same census division, I also use locations' type– rural or urban–as another element to define the nest in this research. In other words, the nest is defined by two factors: the census division to which a location belongs and whether the location rural or urban.[15] This results in a total of eighteen nests in the study. This nest structure is supported by the data. Of those migrating to Census Division 7, most chose urban places as their destination. Urban CZs in Census Division 7 accepted 63.4% of the migrants from New Orleans, a substantial increase over the 44% pre-Katrina rate, whereas rural CZs accepted only 3.4%, a rate even less than the pre-Katrina 3.5%. The fraction of migrants moving to urban CZs in Census Division 7 remained higher than the pre-Katrina fraction till 2013.

For instance, the Houston CZ, an urban CZ in Census Division 7, became the most popular destination for post-Katrina New Orleans migrants, accepting more than 23% of the total evacuees from the New Orleans CZ. In comparison to the number of pre-Katrina migrants from New Orleans to the Houston CZ in 2004, the number of migrants in 2005 was 1500%

[14]Census Division 7 includes four states, Arkansas, Louisiana, Oklahoma, and Texas. The classification of CZs into census divisions is documented in Appendix B.

[15]The definitions of rural and urban CZs are documented in Section 5.

greater, marking the biggest change among those CZs receiving New Orleanians in 2005.[16] The second-biggest shift was observed with the Dallas CZ, which is another Texas urban CZ in Census Division 7.

In order to further validate my nest structure, I also analyze the massive migration outflows caused by another historic hurricane event, Hurricane Andrew, which devastated the Miami CZ in Census Division 5 in 1992. The results show that post-Andrew migrants also disproportionately moved to those within-nest destinations, specifically to urban CZs in Census Division 5. In addition to the empirical evidence, I develop an econometric identification strategy, documented in Section 5, to test the validity of the nest structure in this study.

One may argue that the observed shift in New Orleanians' migration behavior post-Katrina could reflect changes in destination attractiveness rather than differential responses to the disaster. For instance, positive localized shocks in Austin, Dallas and Houston could have attracted more migrants from New Orleans. Alternatively, lower moving barriers to nearby locations could possibly account for the post-Katrina migration behaviors. To rule out these confounding factors, I use the following triple difference approach to identify whether Hurricane Katrina caused disproportionate movement to urban places in Census Division 7:

$$Y_{ijt} = \alpha_{ij} + \alpha_{c(j)t} + \alpha_{it} + \sum_{k=\underline{c}}^{\bar{c}} \alpha_k \mathbb{1}_{\{t=2005+k\}} \times \mathbb{I}_j + \sum_{k=\underline{c}}^{\bar{c}} \beta_k \mathbb{1}_{\{t=2005+k\}} \times \mathbb{I}_j \times \mathbb{I}_{N(i)} + u_{ijt}, \quad (6)$$

where Y_{ijt} denotes the log of migrants from origin j to destination i in year t; α_{ij} is the origin-destination fixed effect that controls for time-invariant bilateral migration frictions such as geographic proximity. $c(j)$ indicates the census division to which origin j belongs, and $\alpha_{c(j)t}$ is the origin location's census-division-time fixed effect that captures shocks common to all origins within a census division. α_{it} is the destination-time fixed effect that that absorbs any changes in destination-specific pull factors over time; $\mathbb{1}_{\{t=2005+k\}}$ is the Katrina event dummy that k equals to 0 when Hurricane Katrina occurred; $\mathbb{I}_j$ is a dummy variable indicating whether origin j is the New Orleans CZ; $\mathbb{I}_{N(i)}$ is a dummy indicator that equals 1 if the nest to which destination i belongs is the Census-Division-7$\times$Urban nest; and $\underline{c}$ represents the lead period

[16] In terms of migration rate, the post-Katrina migration rate from the New Orleans CZ to the Houston CZ increased by 1900%.

and is set to -4, whereas $\bar{c}$ is the lag period that is equal to 8.

The coefficient α_k captures the average change in the number of New Orleans' outmigrants to each destination caused by Hurricane Katrina in year $2005+k$. Of the triple difference coefficients, β_k, which measure the differential change in New Orleans' migrants to urban destinations in Census Division 7 (within-nest) relative to other destinations (outside-nest), is my focus. Based upon Proposition 2 in Section 2, if migration elasticities vary across locations, Hurricane Katrina would cause disproportionate migration to urban places in Census Division 7 (within-nest). We expect to see significantly positive values in β_k after 2005. Figure 9 reports the estimated coefficients β_k, with β_{-1} normalized to zero. The results show a pronounced asymmetric migration response: New Orleans migrants were significantly more likely to relocate to urban CZs within Census Division 7 after Katrina. The magnitude is non-negligible. The coefficient in 2005 is 0.65, suggesting that all else being equal, when a shock like Katrina happens, the change in outflow from New Orleans to an urban CZ in Census Division 7 is, on average, 65% higher than it is to any rural CZ or any urban CZ outside of Census Division 7.[17] This pattern supports the presence of heterogeneous migration elasticities across locations. Notably, the asymmetric migration response persisted significantly for at least three years after Hurricane Katrina.

One may also be concerned that refugee support policies implemented in Texas might have influenced migration behavior in ways unrelated to underlying migration elasticities. For example, the Houston municipal government provided emergency shelters in the Houston Astrodome and the George R. Brown Convention Center to accommodate evacuees from New Orleans. The Texas state government further supported evacuees by waiving standard documentation requirements for school enrollment and arranging transportation from New Orleans to various Texas cities. These interventions may have reduced bilateral mobility frictions specifically between New Orleans and Texas destinations. To address this concern, I re-estimate the triple-difference specification excluding all commuting zones in Texas. The resulting estimates, reported in Figure 10, remain highly consistent with the baseline results in Figure 9. In addition, I conduct robustness checks using the PPML estimator and the original IRS migration data, as presented

[17] The estimated α_k are reported in Appendix B.

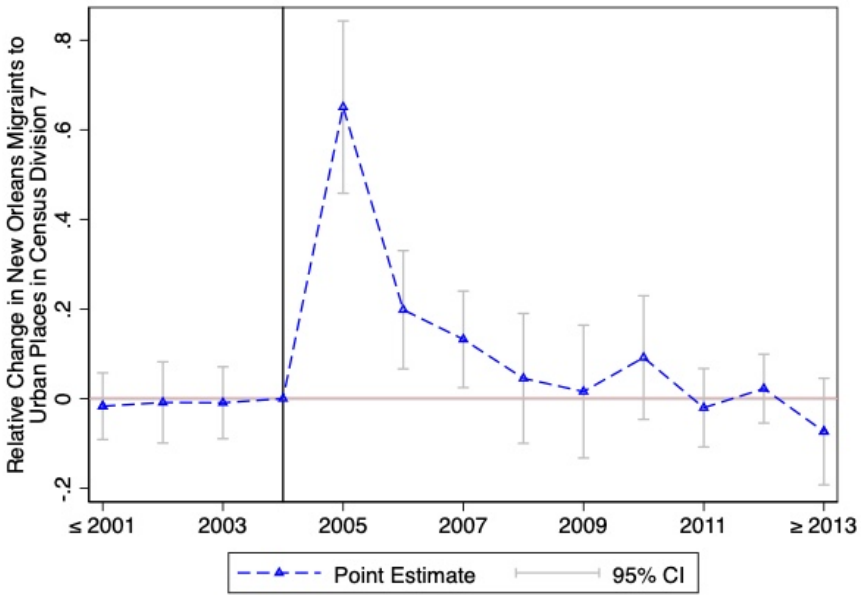


Figure 9: Estimated Triple DID Effects of Hurricane Katrina on Migrants from New Orleans CZ

in Appendix B, which also confirm the main findings. Furthermore, in Section 5, where I identify heterogeneous migration elasticities, I restrict the analysis to a subperiod that excludes the Katrina years to rule out any potential changes in bilateral migration costs induced by the storm. The estimates from that subperiod remain consistent with the baseline results.

The empirical findings in this section suggest the potential existence of heterogeneity in migration elasticities across locations. New Orleanians' disproportionate migration response to Hurricane Katrina tells us that there are both regional and rural-urban differences in terms of locations' migration elasticity. These differences necessitate a more flexible framework that can rationalize such an asymmetric migration response. [18] Importantly, the asymmetric migration response found in the Katrina case is not unique. I observe a similar pattern in the migration aftermath of another historic hurricane, Hurricane Andrew, which devastated the Miami CZ in Census Division 5 in 1992 and led to massive outflows. Details can been found in Appendix B.

[18] My findings also indicate that Katrina migrants did not successfully move away from flood risk; on the contrary, they chose destinations such as Houston, Texas, which are areas of similarly high flood risk. The average flood risk of urban places in Census Division 7 is 0.095, substantially higher than the overall average, 0.056.

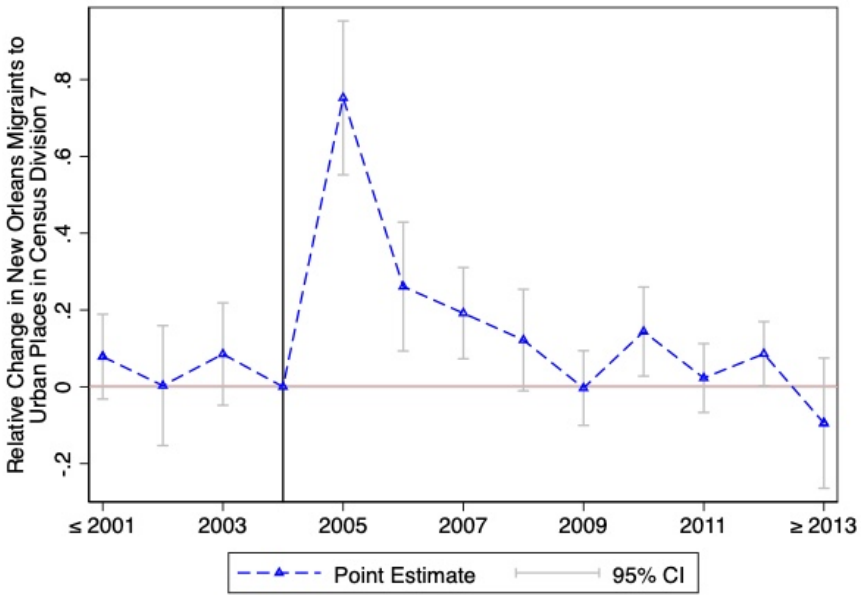


Figure 10: Estimated β_k Coefficients Excluding Texas CZs

4 Dynamic Nested Logit Migration Model

In this section, I develop a dynamic nested logit migration model, building on Caliendo et al. (2019), that incorporates heterogeneity in migration elasticities across locations. The key innovation is to allow migration elasticities to differ between within-nest and cross-nest destinations, capturing potential shifts in migration patterns following localized shocks.

In the model, time is discrete and infinitely lived agents have perfect foresight. The world is composed of J CZs, indexed by j or k. Each CZ represents a competitive local labor market. I allow for mobility across different CZs. Each period, a forward-looking individual decides whether to stay where she is or to move to a different location. Her migration decision is governed by two components: a component that is same for everyone in the same origin location, which consists of the destination's expected continuation value and moving cost; and her realized idiosyncratic preference over that destination. The moving cost is a function of the origin and destination locations and is additive, measured in terms of utility. The idiosyncratic taste is assumed to be drawn periodically from an exogenous distribution and therefore is time-varying. Formally,

$$v_{it}^{j} = u(C_t^j) + \max_{k\in\{1,..,J\}} \left\{\beta \mathbf{E}[v_{it+1}^{k}] - \tau_t^{kj} + \ln \varepsilon_{it}^{kj}\right\}, \tag{7}$$

where v_{it}^{j} is the lifetime utility of individual i living in location j at time t; $u(C_t^j)$ is the flow utility of consuming local goods C_t^j; β is the discount factor; τ_t^{kj} denotes the migration cost from j to k with $\tau_t^{jj} = 0$; and ε_{it}^{kj} is the idiosyncratic taste over k at t. $\mathbf{E}[.]$ is the expectation taken over future realizations of the idiosyncratic shock. Thus, $\mathbf{E}[v_{it}^{k}]$ represents the lifetime utility of a representative agent in location k. Let $V_t^k \equiv \mathbf{E}[v_{it}^{k}]$.[19]

An agent's idiosyncratic taste, ε_{it}^{kj}, is drawn from a given distribution each period. Because her taste is time-variant, she may prefer a location much more at one time than another time depending on the exact realized level. This property, therefore, aims to capture any aspect of the agent's personal situation that may influence the direction or timing of her moving decision independently of the income effect. It also helps to generate the gradual response of the economy to a shock (Cameron et al. (2007)). Additionally, introducing the log term of the idiosyncratic taste into the formula generates negative levels so as to capture the fact that gross migration flows are in excess of net flows, which is often seen in the data.

The main departure from existing studies comes from this idiosyncratic preference setting. In contrast to the assumption in studies such as Caliendo et al. (2019) that the idiosyncratic preference is *i.i.d.* over time, locations, and individuals and drawn from a single logit distribution, in this study, such preference draws of within-nest destinations are allowed to be more strongly correlated with each other. The nest depends on both geography and a location's particular characteristics and is defined as a pair of one of nine possible census divisions and one of two possible location types, rural and urban. In total, then, there are 18 nests. Concretely, the idiosyncratic tastes $(\varepsilon_t^{1j}, \ldots \varepsilon_t^{Jj})$, are drawn from a generalized extreme value distribution,

$$\mathbf{P}[\varepsilon_t^{kj} \leq a_k, k = 1, \ldots, J] = \exp\left(- \Big[\sum_{m \in M} \Big(\sum_{h \in D_m} (a_h)^{-\gamma_m} \Big)^{\frac{\theta}{\gamma_m}} \Big] \right), \tag{8}$$

where M denotes the set of nests that is used to categorize the CZs. Here, the total number of nests is 18. D_m is the set of CZs within nest m. The parameter γ_m represents within-nest locations' migration elasticity, while θ is cross-nest locations' migration elasticity. Equation

[19] It may be helpful to consider the following narrative. At the beginning of each period, the aggregate states across locations are realized. Individuals then receive wages through production and choose their optimal consumption baskets. In the middle of each period, agents learn the levels of both the relocation costs, τ_t^{kj}, and their own idiosyncratic tastes, ε_{it}^{kj}, and then make their migration decisions. They pay the migration costs and enjoy the idiosyncratic preference at the end of each period, wherever they have landed.

(8)'s specification requires that $\gamma_m \geq \theta$ hold. Namely, within-nest places' elasticity must be higher than that of their cross-nest counterparts.

If $\gamma_m > \theta \forall m$, within-nest idiosyncratic taste draws are implicitly more analogous to each other than cross-nest idiosyncratic taste draws. In other words, when agents only make within-nest migration decisions, their optimal within-nest destination choices are less likely to be driven by their own idiosyncratic preference shocks toward within-nest destinations than they are by places' economic conditions. Later I show that γ_m is the within-nest migration elasticity that governs the sensitivity of flows to within-nest destinations in response to the origin location's income shock, whereas θ is the cross-nest migration elasticity that determines the response of flows to outside-origin-location-nest destinations. If $\gamma_m = \theta \forall m$, equation (8) collapses to the idiosyncratic preference distribution often seen in the existing literature that assumes a uniform migration elasticity across locations.

As shown in Appendix C, under this setting, I can derive a closed-form solution to the migration rate's law of motion. The migration rate from j to k at time t, denoted as μ_t^{kj}, equals

$$\mu_t^{kj} = \underbrace{\frac{\exp(\gamma_m \beta V_{t+1}^k - \gamma_m \tau_t^{kj})}{\sum_{h \in D_m} \exp(\gamma_m \beta V_{t+1}^h - \gamma_m \tau_t^{hj})}}_{\text{Conditional probability choosing destination } k} \times \underbrace{\frac{\exp(\theta \tilde{V}_{t+1}^{mj})}{\sum_{s \in M} \exp(\theta \tilde{V}_{t+1}^{sj})}}_{\text{Probability selecting nest } m}, \quad k \in D_m \tag{9}$$

where $\tilde{V}_{t+1}^{mj}$ denotes the expected value of moving to nest m for an agent who lives in j, expressed as

$$\tilde{V}_{t+1}^{mj} = \ln\Big(\sum_{h \in D_m} (\exp(\gamma_m \beta V_{t+1}^h - \gamma_m \tau_t^{hj}) \Big)^{\frac{1}{\gamma_m}}. \tag{10}$$

In this way, the migration rate becomes a product of the probability of selecting the nest to which the destination belongs and the conditional probability of choosing that destination within the nest. This framework has an intuitive interpretation. The moving decision consists of two stages, as depicted in Figure 11. The first stage is choosing a nest, which is the second term in equation (9). The object, $\tilde{V}_{t+1}^{mj}$, is the expected nest-m value of an agent in j who anticipates that she will make the optimal choice within nest m. All else being equal, the higher the value of $\tilde{V}_{t+1}^{mj}$, the more likely it is that the agent moves to nest m. The second stage entails

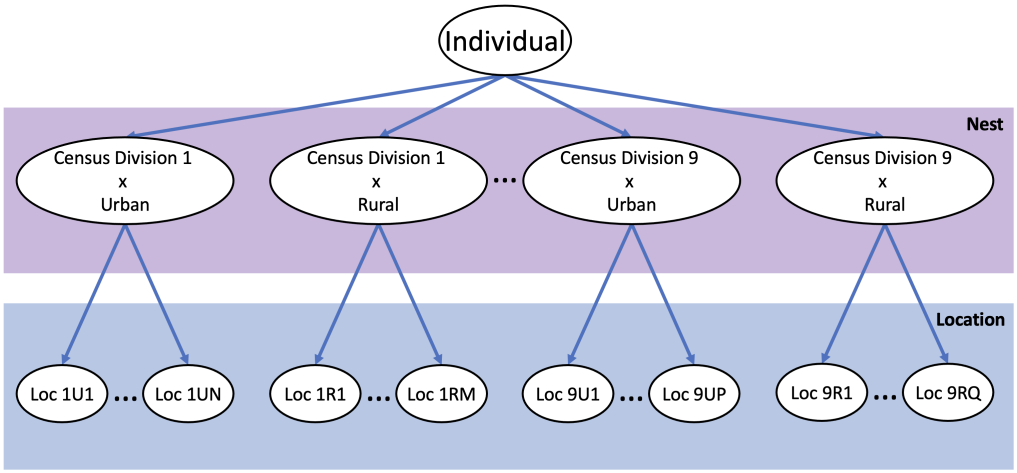


Figure 11: Individuals' Migration Decision

selecting the optimal location within the nest, conditional on the nest choice. This optimal location is the first term in equation (9). All else being equal, a higher lifetime utility (i.e., net moving cost) in destination k will attract more migrants. Due to this nested logit structure, I call my migration model a "dynamic nested logit migration model."

Equation (9) indicates that the parameter θ is the nest-level migration elasticity that governs the adjustment of migration flows to a nest in response to a local shock, while γ_m is the within-nest elasticity determining how the flows to locations within the same nest m react to the shock. Therefore, if origin CZ j and destination CZ j belong to the same nest m, the migration elasticity between them is equal to γ_m. If they are located in different nests, because the adjustment of migration flows between them is controlled by the first-stage nest choice, the migration elasticity is equal to θ. For instance, the elasticity between the New Orleans CZ and the Houston CZ, both of which belong to the Census Division 7-Urban nest, or between two rural places in the same census division, is equal to the within-nest migration elasticity. However, the elasticity governing the flow from the New Orleans CZ to either a rural destination anywhere in the United States or an urban destination outside Census Division 7 is equal to θ. Introducing the nested logit structure into the idiosyncratic taste draws allows for heterogeneity in migration elasticities that depends on both the origin and destination locations. Later I identify θ as the "cross-nest migration elasticity" and γ_m as the "within-nest migration elasticity". Additionally, if $\gamma_m = \theta \forall m$, the first term's denominator in equation (9) will cancel out the second term's numerator and the formula will collapse to the migration rate formula in the extant literature.

Again, this verifies that the single-elasticity framework is simply a special case of my model.

I derive a similar proposition as Proposition 2 in Section 2 indicating that a local shock can lead to distinctive migration responses between within-nest and outside-nest destinations:

Proposition 3 *When a local shock affects location j's fundamentals, A^j_{t+1}, and thereby alters its value function, V^j_{t+1}, then all else being equal, the partial differentiation of the ratio of the migration flow to destinations k and h, $\frac{\mu_t^{mj}}{\mu_t^{hj}}$ w.r.t A^j_{t+1}, is given by*

$$\frac{\partial\left(\frac{\mu_t^{kj}}{\mu_t^{hj}}\right)}{\partial A^j_{t+1}} = \begin{cases} 0, & \text{if } j \in D_d, k, h \notin D_d, \\ \beta(\theta-\gamma_d)\frac{\mu_t^{kj}}{\mu_t^{hj}}\frac{\mu_t^{jj}}{\sum_{f\in D_d}\mu_t^{fj}}\frac{\partial V^j_{t+1}}{\partial A^j_{t+1}}, & \text{if } j,k \in D_d, j \neq k, h \notin D_d. \end{cases} \tag{11}$$

This proposition suggests that a decrease in the origin location's continuation value will bring about a change in the ratio of the flow to a within-nest destination relative to the flow to a outside-nest one. The magnitude of such a change depends on the difference between the cross-nest migration elasticity, θ, and the within-nest elasticity, γ_d, as well as the pre-shock ratio and the conditional non-migration rate. However, the ratio of the flows to any two outside-nest destinations remains at the pre-shock level.

As documented in Section 2, the post-shock ratio change results from the change in the composition of migrants from the origin location after the shock. A negative local shock forces people who have a strong idiosyncratic preference over the origin place to start to leave now. They will primarily move to destinations that are similar to the origin location: that is, within-nest locations. As a result, the distribution of post-shock migrants differs from the pre-shock distribution. The larger the shock, the more likely it is that such people leave and the bigger the difference there is between the pre-shock and the post-shock distributions. The gap between the within-nest locations' elasticity parameter, γ_m, and the cross-nest one, θ, determines the extent to which migrants differentiate between within-nest and outside-nest destinations in their migration choices.

However, the single-elasticity model does not embrace the post-shock ratio change property because all destinations' migration elasticity is identical. The ratio of flows to any two destinations (excluding the origin location) is independent of the impact of the origin location's

shock according to the following proposition:

Proposition 4 *In the single-migration-elasticity model, when a local shock affects location j's fundamentals, A^j_{t+1}, and thereby alters its value function, V^j_{t+1}, then all else being equal, all its outflows will scale up at the same proportion. Specifically,*

$$\frac{\partial \log \mu_t^{kj}}{\partial A^j_{t+1}} = \beta \bar{\sigma} \mu_t^{jj} \frac{\partial V^j_{t+1}}{\partial A^j_{t+1}}, k \neq j \tag{12}$$

where $\bar{\sigma}$ is the single migration elasticity. Therefore,

$$\frac{\partial \left(\frac{\mu_t^{kj}}{\mu_t^{hj}}\right)}{\partial A^j_{t+1}} = 0, \forall k, h \neq j. \tag{13}$$

Proposition 4 shows that the post-shock percentage change in the migration rate from the impacted location to any of the alternative locations is always the same: it is a function of the discount factor, the single migration elasticity, and the non-migration rate. Accordingly, the migration behavior of migrants from the origin place follows the same pattern as it did before the shock.

To further concisely explain the additional margin introduced in my framework enabling it to account for the asymmetric migration response post-Hurricane Katrina, I use the expression formula in Equation (9). By dividing the two migration flows from the same origin j – one to a within-nest location k and the other to an outside-nest destination h–I derive the following ratio:

$$\frac{\mu_t^{kj}}{\mu_t^{hj}} = \frac{\exp(\gamma_d \beta V^k_{t+1} - \gamma_d \tau_t^{kj}) \times [\sum_{i \in D_m} \exp(\gamma_m \beta V^i_{t+1} - \gamma_m \tau_t^{ij})]}{\exp(\gamma_m \beta V^h_{t+1} - \gamma_m \tau_t^{hj}) \times [\sum_{f \in D_d} \exp(\gamma_d \beta V^f_{t+1} - \gamma_d \tau_t^{fj})]} \times \frac{\exp\left(\theta \tilde{V}^{dj}_{t+1}\right)}{\exp\left(\theta \tilde{V}^{mj}_{t+1}\right)}$$

Replacing $\sum_{i \in D_m} \exp(\gamma_m \beta V^i_{t+1} - \gamma_m \tau_t^{ij})$ using Equation (10) yields

$$= \underbrace{\frac{\exp(\gamma_d \beta V^k_{t+1} - \gamma_d \tau_t^{kj})}{\exp(\gamma_m \beta V^h_{t+1} - \gamma_m \tau_t^{hj})}}_{\text{The ratio of two destinations' expected lifetime value}} \times \underbrace{\frac{\exp\left((\theta - \gamma_d)\tilde{V}^{dj}_{t+1}\right)}{\exp\left((\theta - \gamma_m)\tilde{V}^{mj}_{t+1}\right)}}_{\text{The ratio of two nests' expected lifetime value}}, \tag{14}$$

$j, k \in D_d, j \neq k, h \notin D_d,$ and $h \in D_m$.

Therefore, the migration flow ratio becomes the product of the ratio of the expected lifetime values of the two destinatons, and the ratio of expected lifetime values of their corresponding nests. This implies that any shock in origin j can directly affect this ratio via the origin nest value, $\tilde{V}_{t+1}^{dj}$. For instance, a negative shock in origin j can lead to a decrease in $\tilde{V}_{t+1}^{dj}$ and as a result, because $\theta < \gamma_d$ in my dynamic nested logit framework, this ratio $\frac{\mu_t^{kj}}{\mu_t^{hj}}$ increases, indicating that people disproportionately move to within-nest destinations. However, this property does not exist in the single-elasticity model, where $\theta = \gamma_m \forall m$. In this case, the ratio collapses to be only the ratio of the expected lifetime value of the two destinations: $\frac{\mu_t^{kj}}{\mu_t^{hj}} = \frac{\exp(\gamma_d \beta V_{t+1}^k - \gamma_d \tau_t^{kj})}{\exp(\gamma_m \beta V_{t+1}^h - \gamma_m \tau_t^{hj})}$. Hence, any shock in the origin does not directly affect this ratio. This clearly explains why my nested logit model can account for more migration patterns than the single-elasticity model.

In addition to incorporating the difference in migration flow property, my dynamic nested logit model presents a distinction in the value function formula. Using the algebra shown in Appendix C, I can rewrite the value function, V_t^j, as a function of destination k,

$$V_t^j = u(C_t^j) + \beta V_{t+1}^k - \tau_t^{kj} \underbrace{-\frac{\gamma_m - \theta}{\theta \gamma_m} \ln\Big(\sum_{h \in D_m} \mu_t^{hj}\Big) - \frac{1}{\gamma_m} \ln\left(\mu_t^{kj}\right) + \frac{\bar{E}}{\theta}}_{\text{Average idiosyncratic taste over destination } k \text{ conditional on moving there from } j} , \quad k \in D_m, \tag{15}$$

where $\bar{E}$ is the Euler-Mascheroni constant. This formula, which holds for any destination k, tells us that the expected value of location j at time t is equal to the current flow utility, the discounted expected continuation value of destination k at $t+1$ net the moving cost, and three non-negative adjustment terms. The three adjustment components account for the probability that destination k is not the optimal choice. In fact, their summation is equal to the conditional average of idiosyncratic taste over destination k for those who initially live in origin j but decide to move to k (for details, see Appendix C).

A critical property of this conditional mean is that when j and k belong to different nests, a negative shock in j leads to a decrease in the conditional average because both the probability of moving to k's nest m, $\sum_{h \in D_m} \mu_t^{hj}$, and the unconditional probability of going to k, μ_t^{kj}, should rise. However, if destination k is located in origin j's nest, then the change direction of the conditional average of idiosyncratic taste is not as obvious because the likelihood of staying

in j's nest and the unconditional probability of moving to k shift in opposite directions; namely, the former decreases and the latter increases. Because of this difference between within-nest and cross-nest destinations in the conditional average of idiosyncratic taste, which is associated with the fact that equation (15) must hold for all destinations in equilibrium, when a negative shock happens to j, a within-nest destination's migration rate, μ_t^{kj}, can adjust faster than cross-nests' migration rate. This mechanism confirms that, as my model shows, the post-shock migration pattern is different from the pre-shock one and furthermore, that migrants from the origin location disproportionately move to within-nest destinations after such a shock.

Moreover, how much faster the flows to within-nest destinations, μ_t^{kj}, is dependent on $\frac{\theta}{\gamma_m}$ according to the following proposition:

Proposition 5 *When a local shock affects location j's fundamentals, A_{t+1}^j, and thereby alters its value function, V_{t+1}^j, all else being equal, then the partial differentiation of the log probability moving to destination k's nest m, $\ln \mathscr{N}_t^{mj} (\equiv \ln\left(\sum_{h\in D_m} \mu_t^{hj}\right))$ w.r.t A_{t+1}^j, is given by*

$$\frac{\partial \ln \mathscr{N}_t^{mj}}{\partial A_{t+1}^j} = \begin{cases} -\beta\theta\mu_t^{jj}\frac{\partial V_{t+1}^j}{\partial A_{t+1}^j}, & \text{if } j \notin D_m \\ \beta\theta\mu_t^{jj}\frac{1-\mathscr{N}_t^{mj}}{\mathscr{N}_t^{mj}}\frac{\partial V_{t+1}^j}{\partial A_{t+1}^j}, & \text{if } j \in D_m. \end{cases} \tag{16}$$

Since the term relevant to the probability of moving to destination k's nest m in the conditional average of idiosyncratic taste is the only red component in equation (15), this proposition implies that the impact of that nest likelihood on the conditional mean is determined by $\frac{\gamma_m-\theta}{\gamma_m}$. The smaller the ratio of $\frac{\theta}{\gamma_m}$, the larger the effect, and therefore, the faster the within-nest destination μ_t^{kj} can react compared to its cross-nest counterpart.

This property does not hold if $\gamma_m = \theta \forall m$, which is the single-elasticity framework. The red term related to the probability of moving to a particular destination's nest disappears and equation (15) collapses to the value function expression in existing studies:

$$V_t^j = u(C_t^j) + \beta V_{t+1}^k - \tau_t^{kj} \qquad \underbrace{-\frac{1}{\theta}\ln\mu_t^{kj} + \frac{\bar{E}}{\theta}}_{\text{Average idiosyncratic taste over destination } k \text{ conditional on moving there from } j} \quad , \ k \in D_m. \tag{17}$$

Since this equation must hold for all destinations, all conditional averages of idiosyncratic taste (except for the origin one) must shift in the same direction. Again, this explains why the post-shock migration pattern remains the same as the pre-shock one in the single-elasticity model.

5 Identification and Estimation

The previous section showed that allowing for richness in migration elasticities across locations can explain more features in the data. However, with this richness comes the challenge of identifying these different migration elasticities. In this section, I document my methodology with which to identify and estimate heterogeneous elasticities.

The identification strategy hinges on the following. If V_t^j and V_{t+1}^k are known, then subtracting βV_{t+1}^k from both sides in equation (15) can help us to simultaneously estimate γ_m and θ using a simple regression. Of course, while V_t^j and V_{t+1}^k cannot be observed directly, there is a term in equation (9) related to the value function, $\beta\gamma_m V_{t+1}^k$. As long as we know the variation in μ_t^{kj}, we can obtain sufficient statistics for $\beta\gamma_m V_{t+1}^k$. We can then multiply both sides in equation (15) by $\beta\gamma_m$ and subtract $\beta^2\gamma_m V_{t+1}^k$ from both sides in the expression to identify the migration elasticities. This is the identification strategy.

Specifically, the identification strategy consists of two stages, making it similar to the single-elasticity estimation approach in Artuç and McLaren (2015) and Caliendo et al. (2021). The first stage is to map the migration rate, μ_t^{kj}, to the observed variable and exploit its variation to obtain the sufficient statistics for the value function.[20] Concretely, the theoretical migration rate is related to the observed number of migrants. The number of migrants is given by

$$Q_t^{kj} = L_{jt}\mu_t^{kj}e_{kjt}, \tag{18}$$

where Q_t^{kj} denotes the number of migrants from origin j to destination k at time t; L_{jt} is j's

[20]The idea of inferring the continuation value from observed behavior rather than computing it directly is in the spirit of the conditional choice probability estimator developed by Hotz and Miller (1993). However, this study's approach is simpler because I do not need to use non-parametric methods to estimate the choice probabilities. Rather, I use the Poisson pseudo-maximum likelihood(PPML) method for inferring those continuation values. This is a convenient and efficient alternative to the conditional choice probability, especially for problems involving large choice sets.

population; and the error term e_{kjt} captures any deviation between the observations and theory.

For the identification, I assume that migration cost τ_t^{kj} is time-invariant during the sample period but allowed to bilaterally vary between origin and destination.[21] As evident in Appendix D, Q_t^k can be expressed as three types of fixed effects,

$$Q_t^{kt} = \exp(\Gamma_{k,t} + \Phi_{j,m,t} + F_{k,j})e_{kjt}, k \in D_m \tag{19}$$

where $\Gamma_{k,t}$ is the destination-time fixed effect; $\Phi_{j,m,t}$ is the origin-nest-time fixed effect; and $F_{k,j}$ is the origin-destination fixed effect. The destination-time fixed effect includes sufficient statistics for the destination's continuation value, $\beta\gamma_m V_{t+1}^k$, while the origin-nest-time fixed effect contains sufficient statistics for the origin's continuation value, $\beta\gamma_m V_{t+1}^j$. These two types of fixed effects are used to construct a reduced-form equation for the migration elasticity estimation in the second stage. To identify these fixed effects, we can log-linearize equation (19) and estimate them; however, doing so would yield biased estimators due to potential heteroskedasticity in the error term and the many-zero issue in the migration flow data. To overcome this issue, similar to Silva and Tenreyro (2006), I use PPML for identifying these fixed effects.

In the second stage, I multiply both sides in equation (15) by $\beta\gamma_m$ and then use the destination-time and origin-nest-time fixed effects to replace the current and next periods' lifetime utility terms, respectively. By performing some algebraic calculations associated with the assumption that all within-nest migration elasticities are identical–namely, $\gamma_m = \gamma \ \ \forall m$–I can derive the following reduced-form framework for the migration elasticity identification,[22]

$$\begin{aligned}\widehat{\Gamma}_{k,t} + \beta\widehat{\Phi}_{j,m,t+1} - \beta \ln L_{jt+1} = \beta\gamma u(C_{t+1}^k) + \alpha_{kj} + \alpha_t \\ + \alpha_1 \ln(\frac{\mu_{t+1}^{jk}}{\mu_{t+1}^{jj}}) + \beta(1-\frac{\gamma}{\theta})\ln(\sum_{h\in D_m}\mu_{t+1}^{hk}) + \tilde{e}_{kjt}, \ \ k,j \in D_m,\end{aligned} \tag{20}$$

where α_{kj} denotes the origin-destination fixed effect; α_t is the time fixed effect; and u_{kjt} is the error term. Equation (20) implies that the within-nest γ and cross-nest migration elasticity θ

[21] The time-invariant assumption has also been used to estimate the single migration elasticity in Caliendo et al. (2021). It is possible to allow the moving cost to be time-varying if we know its specific structure.

[22] Details can be found in Appendix D.

can be simultaneously identified using the time variation in the flow utility, $u(C^k_{t+1})$, and the log probability of staying in the origin's nest, $\ln(\sum_{h\in D_m}\mu^{hk}_{t+1})$.

Meanwhile, the coefficient of the log probability of staying in the origin's nest, $\ln(\sum_{h\in D_m}\mu^{hk}_{t+1})$, helps to validate my model's specification. If the coefficient is significantly strictly positive, then the within-nest elasticity γ is strictly smaller than the cross-nest elasticity θ, which violates the condition of the nest structure. Therefore, my model suffers from a misspecification issue. If the coefficient is statistically insignificant, then the within-nest and cross-nest migration elasticity are identical, $\gamma = \theta$. In other words, the standard modeling assumption of uniform migration responsiveness across destinations–namely, that there is one single migration elasticity–holds in the real world.

After deriving the estimated fixed effects in the first stage using PPML method and annual commuting-zone-to-commuting-zone migration flow data from 2000 to 2019 (as processed in Section 3), I specify the flow utility as log real wages, $u(C^k_{t+1}) = \log w^k_{t+1}$, and set the discount factor to $\beta = 0.98$. I then run a linear regression regarding equation (20). Yet estimating this equation by ordinary least-squares (OLS) may lead to biased estimates because of the potential endogeneity in the error term (e.g., unobserved endogenous amenities). To address this issue, I employ the following Bartik-style instrument, B_{kt}, for the real wage:

$$B_{kt} = \sum_{ind} w_{ind,-k,t} \frac{Emp_{ind,k,2000}}{Emp_{k,2000}}, \tag{21}$$

where $w_{ind,-k,t}$ represents the average log wage of 25-55-years-old employed workers in industry *ind* at time t, excluding workers in k. $Emp_{ind,k,2000}$ stands for the number of workers in industry *ind* in CZ k in 2000, and $Emp_{k,2000}$ represents the total number of workers in CZ k in 2000. The calculation of this wage and employment information is based on the ACS data.

Simultaneously, the average log probability of staying in the origin location's own nest among all destinations' neighboring CZs between 100 and 200 kilometers away instruments for the log probability of staying in the origin nest.[23]

The OLS and instrumental variable (IV) estimates for the two coefficients related to migra-

[23]To calculate the distance between CZs, I use each CZ's population centroid. This centroid is the population-weighted average of all counties' population centroids within a CZ. The county's centroid is taken from the U.S. census.

	OLS	IV
log real wage	0.2966 ***	1.2815***
	(0.0204)	(0.1956)
log probability of staying in origin's nest	-9.5902***	-43.7162***
	(0.8576)	(3.0971)
Cragg-Donald F-statistic		731.58***

Standard errors in parentheses. $*p < 0.1, **p < 0.05, ***p < 0.01$
Clustered at origin-by-destination.

Table 2: Estimated Coefficients

tion elasticities are reported in Table 2. As previously documented, the statistical significance in the coefficient of the log probability of staying in the origin's nest demonstrates the presence of heterogeneity in the migration elasticity. Its negative sign justifies my model's specification that the within-nest migration elasticity, γ, is indeed larger than its cross-nest counterpart, θ. If we map these estimates in Column 2 of Table 2 to the migration elasticities, we will have the first row's output in Table 3. The results show that the within-nest migration elasticity, γ, equal to 1.31, is substantially larger than the cross-nest elasticity, θ, equal to 0.03. This implies that that migrants are more responsive to changes in conditions within the same nest than to those in other nests. In other words, the adjustment of migration flows to similar destinations occurs much more readily than adjustments to dissimilar locations.

To the best of my knowledge, this is the first study to document such heterogeneity in migration elasticities at the U.S. commuting-zone level. While there is no directly comparable estimate, an indirect benchmark is provided by Caliendo et al. (2019), who estimate a single annual migration elasticity of 0.495 at the U.S. state level—falling between my within- and cross-nest estimates.

	Within-nest Migration Elasticity	Cross-nest Migration Elasticity
Nested Logit Migration Model	1.31***	0.03***
	(0.1996)	(0.0020)[24]
Single-elasticity Migration Model	0.31***	0.31***
	(0.0649)	(0.0649)

Standard errors in parentheses. $*p < 0.1, **p < 0.05, ***p < 0.01$

Table 3: Estimated Annual Migration Elasticities

These empirical estimates not only confirm the existence of heterogeneous migration elas-

[24]This is based on the variance of $\beta(1-\frac{\gamma}{\theta})$ in Column 2 in Table 2. Here, I use that variance associated with the estimated level of γ to calculate the standard deviation of θ.

ticities but also have important implications for understanding real-world migration dynamics. As documented in Section 4, this huge distinction between the within-nest and cross-nest migration elasticities may lead to a large deviation in the post-shock origin location's migration pattern from the pre-shock one after a big shock like Hurricane Katrina happens. In the case of Hurricane Katrina, this implies that much of the observed shift in New Orleanians' migration behavior can be attributed to heterogeneity in migration elasticities across destinations. Details are provided in the next section.

As a comparison, I derive a reduced-form equation that is similar to equation (20) for identifying the single migration elasticity in existing work.[25] This reduced-form equation is given by

$$\widehat{\Gamma}'_{kt} + \beta\widehat{\Phi}'_{jt+1} - \beta \ln L_{jt+1} = \beta\bar{\sigma}u(C^k_{t+1}) + \alpha_{kj} + \alpha_t + \alpha'_1 \ln(\frac{\mu^{jk}_{t+1}}{\mu^{jj}_{t+1}}) + \varepsilon'_{kjt}, \tag{22}$$

where $\widehat{\Gamma}'_{kt}$ is the estimated destination-time fixed effect; and $\beta\widehat{\Phi}'_{jt+1}$ is the estimated origin-time fixed effect. Both of the fixed effects can still be estimated using PPML, as in my model. α_{kj} is the origin-destination fixed effect and α_t is the year fixed effect. $\bar{\sigma}$ is the single migration elasticity of interest.

Because all places share the same migration elasticity in the single-elasticity framework, there is no nest-related term as seen in equation (20). In fact, we can interpret this single-elasticity identification formula, equation (22), as a special case of my model's identification framework. This is because when $\gamma = \theta$, the nest-related term in equation (20) will drop out due to the zero coefficient; D_m becomes the set of all locations. Finally, in an approach similar to my model's estimation method, I instrument the log real wage, which represents the flow utility, with the same Bartik-version variable, B_{kt}, in equation (21). In this way, I estimate the single migration elasticity, $\bar{\sigma}$.

The second row of Table 3 reports the estimated $\bar{\sigma}$, 0.31. It is a value between my model's within-nest migration elasticity, 1.31, and the cross-nest one, 0.03. This makes sense because the single elasticity should behave as the average of the two types of migration elasticity. On

[25] Details are provided in Appendix D.

top of this, its 95% confidence interval overlaps with neither my model's within-nest elasticity interval nor the cross-nest one. Therefore, the conventional migration model substantially underestimates the within-nest migration elasticity but overestimates the cross-nest migration elasticity.

In Appendix D, I also conduct several robustness tests regarding my model's elasticity estimators. For example, I re-estimate the model using Infutor data from 2014 to 2019. While the magnitude of localized shocks influences the extent of post-shock migration deviations, Proposition 1–5 show that even in normal periods, cross-locational variation can reveal heterogeneity in migration elasticities, which aids identification. As an additional robustness check, I incorporate endogenous amenities into the analysis. In all cases, the results remain consistent with the main findings.

6 Quantitative Assessment

In the previous section, I exploited my methodology to identify the heterogeneity in migration elasticities–specifically, differences in how migrants respond to various destination options across commuting zones (CZs). The results indicate that, when a localized shock occurs, migrants are more responsive to destinations within the same nest than to those outside it. The objective of this section is to leverage the quantitative analysis to show that the heterogeneity in migration elasticities identified in my framework alone can account for a substantial portion of the disproportionate migration response in the Katrina case and also delivers different welfare and policy implications.

To do so, I close my dynamic nested logit migration model with this general-equilibrium setting. On the consumer side, in addition to making migration decisions, agents in location j consume two goods each period: a homogeneous good, c_{jt}, and a local housing service, h_{jt}. Under the logarithmic preference assumption, the flow utility can be expressed as

$$u(C_t^j) = \log((\frac{c_{jt}}{1-\zeta})^{1-\zeta}(\frac{h_{jt}}{\zeta})^{\zeta}), \tag{23}$$

where ζ is the housing expenditure share, which is set to 0.3 in this study.

On the production side, a representative firm in location j produces this homogeneous product, which is freely tradable, using linear technology $A_{jt}L_{jt}$ with only labor input. Here, A_{jt} is the productivity in location j. Meanwhile, a representative local housing service supplier sets the housing supply price, P_{jt}, according to

$$P_{jt} = \bar{P}_j L_{jt}^{\eta_j}, \tag{24}$$

where η_j is the inverse elasticity of the housing supply; L_{jt} is the population in j; and $\bar{P}_j$ denotes all those time-invariant factors affecting the housing price in j. Here, I set each CZ's inverse elasticity of housing supply, η_j, to be the population-weighted average of county-level elasticities from Monte et al. (2018).

In the labor market, individuals supply a unit of labor inelastically to homogeneous good producers and receive a competitive market wage, W_{jt}. In equilibrium, $W_{jt} = A_{jt}$. If we choose the homogeneous product as numeraire, then individuals' real wage in location j is

$$\omega_{jt} = \frac{A_{jt}}{\bar{P}_j^{\zeta} L_{jt}^{\eta_j \zeta}}. \tag{25}$$

This equation can be used to invert the model and recover the unobserved changes in A_{jt} implied by the observed data, under the assumption that Hurricane Katrina only affected New Orleans' homogeneous goods productivity, A_{jt}, but not the housing market. Importantly, this assumption is not restrictive in my model setting, as it can be easily shown that the scenario affecting only goods' production is isomorphic to a scenario where Hurraince Katrina impacts both the housing and goods market. Given this, we can solve for the change in A_{jt} from the observed time series of CZ-level real wages in the ACS data and the local population size indicated in the IRS data according to the following formula implied by equation (25):

$$\dot{A}_{jt+1} \equiv \frac{A_{jt+1}}{A_{jt}} = \frac{\omega_{jt+1}}{\omega_{jt}} \left(\frac{L_{jt+1}}{L_{jt}}\right)^{\eta_j \zeta}. \tag{26}$$

Through this model inversion approach, I find that the New Orleans CZ's productivity declined 44% in 2006. I attribute this change to the impact of Hurricane Katrina. Note that this percent-

age is independent of the migration model specification. Namely, we would arrive at the same percentage, a 44% productivity decline, regardless of whether we used my model or the single-elasticity model. Next, I simulate the scenario in which there is only a permanent productivity change in the New Orleans CZ's economy due to Hurricane Katrina, conditional on the pre-Katrina state. Solving for all the transitional dynamics in this dynamic discrete-choice model can be challenging because it often requires pinning down the values of many unobserved fundamentals. However, the following two propositions show that we can employ dynamic-hat algebra, as seen in Caliendo et al. (2019) and Caliendo et al. (2021), to solve for the aforementioned simulation in my dynamic nested logit migration framework setting. In this case, we do not need to estimate the levels of fundamentals.

Proposition 6 *Conditional on an initial allocation of the economy, (L_0, μ_{-1}), and given an anticipated convergent sequence of changes in fundamentals, $\{\dot{\Theta}_t\}_{t=1}^{\infty}$, the solution to the dynamic labor market equilibrium in time difference does not require information on the value of fundamentals $\{\Theta_t\}_{t=0}^{\infty}$ and solves the following system of nonlinear equations:*

$$\frac{\dot{\mu}_{t+1}^{kj}}{\dot{\mathscr{N}}_{t+1}^{mj}}|_{k\in D_m} = \frac{(\dot{U}_{t+2}^{k})^{\gamma_m\beta}(\dot{\tau}_{t+1}^{kj})^{-\gamma_m}}{\sum_{s\in D_m}\mu_t^{sj}(\dot{U}_{t+2}^{s})^{\gamma_m\beta}(\dot{\tau}_{t+1}^{sj})^{-\gamma_m}}, \quad \mathscr{N}_t^{mj} \equiv \sum_{h\in D_m}\mu_t^{hj} \tag{27}$$

$$\dot{\mathscr{N}}_{t+1}^{mj} = \frac{\left(\sum_{n\in D_m}\frac{\mu_t^{nj}}{\mathscr{N}_t^{mj}}(\dot{U}_{t+2}^{n})^{\gamma_m\beta}(\dot{\tau}_{t+1}^{nj})^{-\gamma_m}\right)^{\frac{\theta}{\gamma_m}}}{\sum_{s\in M}(\mathscr{N}_t^{sj})^{\frac{\gamma_s-\theta}{\gamma_s}}(\sum_{n\in D_s}\mu_t^{nj}(\dot{U}_{t+2}^{n})^{\gamma_s\beta}(\dot{\tau}_{t+1}^{nj})^{-\gamma_s})^{\frac{\theta}{\gamma_s}}}, \tag{28}$$

$$\dot{U}_{t+1}^{j} = \dot{\omega}^{j}(\dot{L}_{t+1}, \dot{\Theta}_{t+1})\left[\sum_{n\in M}\left[(\mathscr{N}_t^{nj})^{\frac{\gamma_n-\theta}{\gamma_n}}\left[\sum_{f\in D_n}\mu_t^{fj}(\dot{U}_{t+2}^{f})^{\gamma_n\beta}(\dot{\tau}_{t+1}^{fj})^{-\gamma_n}\right]^{\frac{\theta}{\gamma_n}}\right]\right]^{\frac{1}{\theta}}, \tag{29}$$

$$L_{kt+1} = \sum_j \mu_t^{kj}L_{jt}, \tag{30}$$

where $U_t^j \equiv \exp(V_t^j)$; and $\dot{\tau}_{t+1}^{kj} = \exp(\tau_{t+1}^{kj} - \tau_t^{kj})$. $\mathscr{N}_t^{mj}$ is the migration rate from location j to nest m. $\dot{\omega}(\dot{L}_{t+1}, \dot{\Theta}_{t+1})(\omega_{jt} = \frac{A_{jt}}{\bar{P}_j^{\zeta}L_{jt}^{\eta_j\zeta}})$ is the change in the real wage, which can be solved as a function of the change in $\dot{L}_{t+1}$ and $\dot{\Theta}_{t+1}$. □

This proposition indicates that without knowing the levels of fundamentals, I can solve the model for a given sequence of changes in fundamentals using only initial-period data. Here, the set of fundamentals $\Theta_t \equiv (A, \tau, \bar{P})$ includes productivity, moving cost, and time-invariant

housing price factors. Using Proposition 6, I solve for a scenario in which the fundamentals remain the same as the pre-Katrina ones. This scenario serves as the baseline economy.

I use the next proposition to solve for a counterfactual economy in which the New Orleans CZ experiences an unexpected productivity change in 2006 due to Hurricane Katrina. First, I introduce new notation. Let $\hat{y}_{t+1} \equiv \dot{y}'_{t+1}/\dot{y}_{t+1}$ be the ratio of time changes between the counterfactual equilibrium, $\dot{y}'_{t+1} \equiv y'_{t+1}/y'_t$, and the initial equilibrium, $\dot{y}_{t+1} \equiv y_{t+1}/y_t$.

Proposition 7 *Given a baseline economy, $\{L_t, \mu_{t+1}\}_{t=0}^{\infty}$, and a counterfactual convergent sequence of changes in fundamentals, $\{\hat{\Theta}_t\}_{t=1}^{\infty}$, solving for the counterfactual sequential equilibrium $\{L'_t, \mu'_{t-1}\}_{t=1}^{\infty}$ does not require information on the baseline fundamentals. The solution to this equilibrium in turn solves the following system of nonlinear equations:*

$$\dot{\mu}_{t+1}^{'kj}|_{k\in D_m} = \frac{\sum_{h\in D_m} \mu_t^{'hj} \dot{\mu}_{t+1}^{'hj}}{\sum_{s\in D_m} \mu_t^{'sj} \dot{\mu}_{t+1}^{sj} (\hat{U}_{t+2}^{s})^{\gamma_m\beta} (\hat{\tau}_{t+1}^{sj})^{-\gamma_m}} \dot{\mu}_{t+1}^{kj} (\hat{U}_{t+2}^{k})^{\gamma_m\beta} (\hat{\tau}_{t+1}^{kj})^{-\gamma_m}, \tag{31}$$

$$\hat{\mathscr{N}}_{t+1}^{mj} = \frac{\left[\sum_{h\in D_m} \mu_t^{'hj} \dot{\mu}_{t+1}^{hj} (\hat{U}_{t+2}^{h})^{\gamma_m\beta} (\hat{\tau}_{t+1}^{hj})^{-\gamma_m}\right]^{\frac{\theta}{\gamma_m}} (\mathscr{N}_{jt}^{'m})^{-\frac{\theta}{\gamma_m}} (\dot{\mathscr{N}}_{t+1}^{mj})^{-\frac{\theta}{\gamma_m}}}{\sum_{d\in M} (\mathscr{N}_t^{'dj})^{\frac{\gamma_d-\theta}{\gamma_d}} (\dot{\mathscr{N}}_{t+1}^{dj})^{\frac{\gamma_d-\theta}{\gamma_d}} \left[\sum_{f\in D_d} \mu_t^{'fj} \dot{\mu}_{t+1}^{fj} (\hat{U}_{t+2}^{f})^{\gamma_d\beta} (\hat{\tau}_{t+1}^{fj})^{-\gamma_d}\right]^{\frac{\theta}{\gamma_d}}} \tag{32}$$

$$\hat{U}_{t+1}^{j} = \hat{\omega}_{jt+1}(\hat{L}_{t+1}, \hat{\Theta}_{t+1}) \left[\sum_{s\in M} (\mathscr{N}_t^{'sj})^{\frac{\gamma_s-\theta}{\gamma_s}} (\dot{\mathscr{N}}_{t+1}^{sj})^{\frac{\gamma_s-\theta}{\gamma_s}} \left[\sum_{f\in D_s} \mu_t^{'fj} \dot{\mu}_{t+1}^{fj} (\hat{U}_{t+2}^{f})^{\gamma_s\beta} (\hat{\tau}_{t+1}^{fj})^{-\gamma_s}\right]^{\frac{\theta}{\gamma_s}}\right]^{\frac{1}{\theta}} \tag{33}$$

$$L_{kt+1} = \sum_j \mu_t^{'kj} L_{jt}, \tag{34}$$

where $U_t^j \equiv \exp(V_t^j)$, and $\omega_{jt} = \frac{A_{jt}}{\bar{P}_j^{\zeta} L_{jt}^{\eta_j\zeta}}$. □

Proposition 7 shows that without knowing the levels of fundamentals in the baseline economy, I can solve counterfactuals from unanticipated changes to the baseline economy's fundamentals. The baseline fundamentals can be either time-varying or constant. In my Katrina simulation case, the baseline fundamentals are constant: they are the same as the initial-period ones. The change in fundamentals in the counterfactual is the unexpected productivity decline in the New Orleans CZ caused by Hurricane Katrina.

Therefore, from Proposition 7, I can derive the model-generated post-shock migration flow data in the counterfactual economy. Meanwhile, I can replicate the simulation strategy to obtain

the post-shock migration flow data under the single-elasticity model setting. In order to evaluate my model's performance in predicting the post-Katrina migration pattern observed in the data, I exploit the two model-generated migration flow datasets and rerun the triple DID analysis in equation (6) of Section 3.

The results are reported in Figure 12. The red line represents my model's estimates, while the blue line is the single-elasticity model's estimates. The gray area is the 95% confidence interval of the point estimators in Figure 9 of Section 3. Clearly, my dynamic nested logit framework captures a significantly larger share of the variation in the disproportionate migration response following Hurricane Katrina than the conventional model. This improvement is due to the model's flexibility in allowing migration behavior to vary depending on the type of destination. In my framework within-nest destinations like Austin, Dallas, and Houston are more likely to be chosen than cross-nest places like New York for New Orleanians; accordingly, when Hurricane Katrina occurs, New Orleanians will disproportionately move to these within-nest places. This will not happen in the single-elasticity model that assumes all destinations in the United States share a uniform migration elasticity. This feature is confirmed by Propositions 3 and 4 in Section 4.

Another important implication from Figure 12 concerns whether introducing the dynamic version can avoid the main drawback of the constraint in the idiosyncratic taste draw in the static setting (the idiosyncratic taste is assumed to be independently drawn from a Fréchet distribution), called *independence from irrelevant alternatives* (IIA). In IIA, for any two alternative destinations, the ratio of the probabilities of choosing each of the two stays constant and does not depend on any other alternatives. Arcidiacono and Miller (2011) argue that the dynamic setting can resolve the IIA issue because the choice probabilities there depend on differences in choice-specific value functions like equation (17) that include the characteristics of all the alternatives. However, Figure 12 tells us that that argument does not hold, at least not in the Katrina case, because the blue line is nearly aligned with the zero horizontal line. This suggests that IIA still holds. In contrast, my dynamic nested logit framework, which introduces additional structure through the nest-specific migration responsiveness, is able to account for a substantial share of both the immediate and persistent disproportionate migration patterns

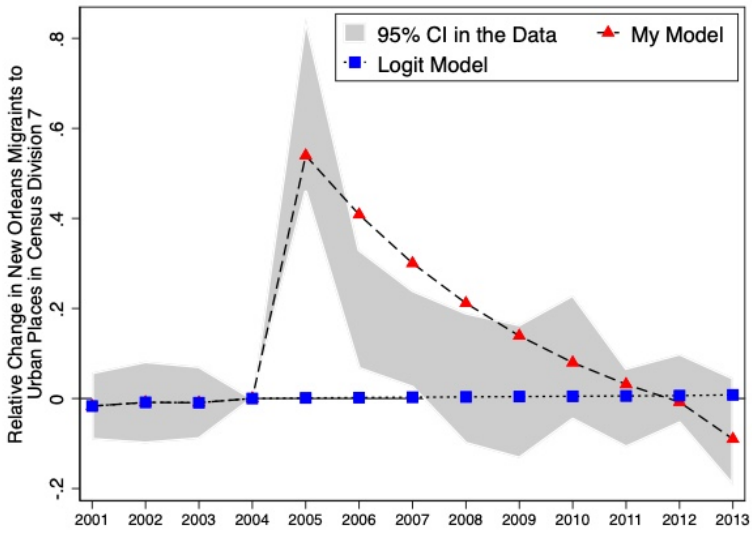


Figure 12: Triple DID Estimates Comparison

observed after Katrina. These findings underscore the necessity of allowing more flexibility in modeling idiosyncratic taste draws—particularly in the context of large, localized shocks.

In addition to explaining the post-Katrina migration pattern differently, my model delivers distinctive welfare implications for those who initially live in the migration destinations before the shock. The welfare change in my framework for agents residing in location j, measured in terms of consumption-equivalent variation, $\widehat{W}^j$, can be written as

$$\widehat{W}^j = \sum_{s=1}^{\infty} \beta^s \ln\left(\frac{\hat{C}_s^j}{(\hat{\mu}_s^{jj})^{1/\gamma_m}}\right) + \frac{\theta-\gamma_m}{\gamma_m\theta} \sum_{s=1}^{\infty} \beta^s \ln\left(\hat{\mathscr{N}}_s^{mj}\right), \quad j \in D_m. \tag{35}$$

When $\gamma_m = \theta \forall m$, we will arrive at the welfare change formula in the conventional model, written as

$$\widehat{W}^j = \sum_{s=1}^{\infty} \beta^s \ln\left(\frac{\hat{C}_s^j}{(\hat{\mu}_s^{jj})^{1/\theta}}\right). \tag{36}$$

This confirms that the single-elasticity framework is essentially a special case of my dynamic nested logit migration model.

Figure 13 illustrates the welfare change for those who originally live in the migration destinations before the shock. Panel 13a is the map of welfare change distribution in my frame-

work, while Panel 13b is that of the single-elasticity model.[26] In each panel's map, the gray boundaries represent each CZ's borders, the blue lines are census divisions' boundaries, and the shaded areas indicate urban places. Red means a welfare loss and green indicates a welfare gain.

As we can see, the welfare losses in my model are concentrated in destinations located in the nest to which the New Orleans CZ belongs. This is because the post-shock overflow of New Orleans migrants into those within-nest destinations causes a large congestion effect in within-nest places. This effect results in increased housing prices and dampened real wages. Local residents cannot easily avoid such a negative effect through migration due to the low cross-nest migration elasticity. In contrast, in the single-elasticity model, the welfare losses are relatively evenly distributed across the contiguous United States. This is because, under a uniform migration elasticity, individuals are assumed to adjust more flexibly across all destinations. Additionally, both models reveal modest welfare gains (less than 0.1 %) in certain nearby areas that historically have strong migration linkages with New Orleans, even though these areas lie outside its nest. These welfare gains occur because the initial post-shock migration disproportionately flows either to within-nest destinations (in my model) or to distant locations (in the conventional model), reducing immediate pressure on nearby areas. Since welfare is evaluated for the original local residents, the temporary alleviation of inflow-related congestion leads to a slight, though limited, welfare improvement in these adjacent zones.

Table 4 summarizes the CZ-level welfare changes in both my model and the single-elasticity model.[27] The first column presents the welfare loss in the New Orleans CZ. The models deliver very similar levels of loss. Intuitively, this makes sense because introducing heterogeneity in locations' migration elasticity changes agents' idiosyncratic preference over each destination and the disproportionate migration response in my framework is their optimal moving choice.

However, in the second column, which corresponds to the welfare loss in destinations (excluding the New Orleans CZ) located in the nest to which New Orleans CZ belongs, we observe a substantially larger average welfare loss in my model than in the conventional model. As il-

[26] Appendix E provides a snapshot of the census division to which New Orleans belongs.

[27] In the quantitative analysis, I integrate all CZs with fewer than 6,000 people each in a nest to form a single special CZ. This is why the number of observations in the table is fewer than the total number of CZs in the United States.

	New Orleans	New Orleans Nest		Other Nests		All	
	mean	mean	sd	mean	sd	mean	sd
Nested Logit Migration Model	-47.7700	-0.0553	0.0761	0.0001	0.0075	-0.0024	0.0211
Single-elasticity Migration Model	-51.7500	0.0000	0.0180	-0.0003	0.0042	-0.0003	0.0056
Observations	1	30		627		657	

New Orleans is excluded in Column 2-4

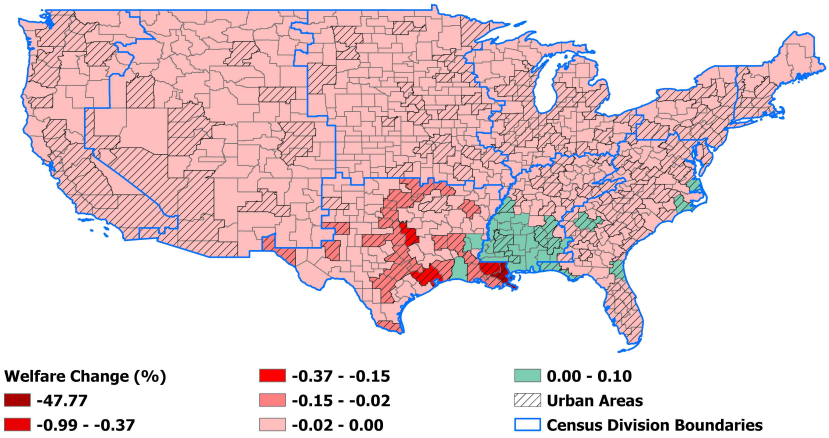
Table 4: Summary of Welfare Changes in the Katrina Case (%)

lustrated in Figure 13, this is due to the large congestion effect induced by excessive inflows of New Orleanians as well as the difficulty of moving away from such a effect for local residents. The welfare loss in each of these within-nest destinations in my framework is not simply a model-implied phenomenon. In fact, it has been documented in previous studies. Using monthly CPS data from September 2000 to August 2006, McIntosh (2008) finds that the influx of Katrina migrants led to a 1.8% decline in wages in the Houston metro area.[28] In contrast, as seen in the third column, places' welfare outside of New Orleans' nest is rarely impacted in my framework because of the low cross-nest migration elasticity. As a result of these asymmetric welfare implications between within-nest and cross-nest destinations, we expect to see a larger dispersion in the welfare change overall, which is indeed confirmed in the last column.

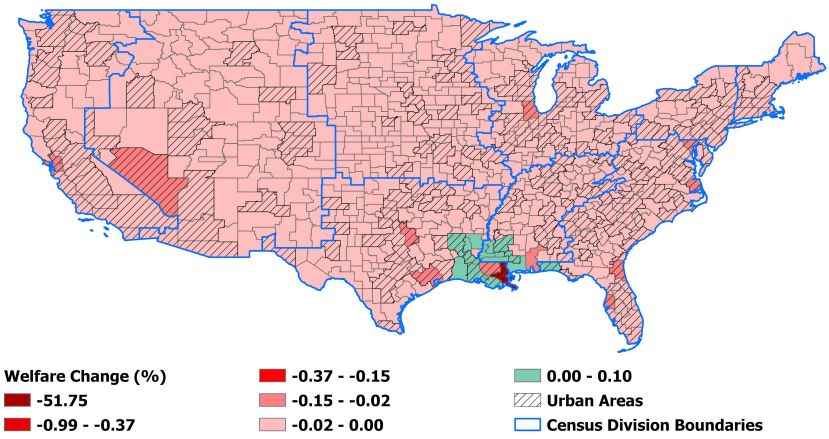
The final step I take in this exercise is to investigate how long after the shock that it takes the economy to converge to the new steady state in my model and in the conventional one, respectively. Specifically, I look at the overall population adjustment in the nest in which the New Orleans CZ is located.[29] Figure 14 plots the transitional path in each of the two models. The blue line represents my model and the red line shows the single-elasticity model. The y axis represents the percentage of population adjustment in the New Orleans nest up to period t, calculated as $\frac{Pop_{no,t}-Pop_{no,0}}{Pop_{no,\infty}-Pop_{no,0}} \times 100$, where $Pop_{no,t}$ is the population of New Orleans nest at time t, $Pop_{no,0}$ is the initial population and $Pop_{no,\infty}$ is the steady-state population. Clearly, my model's adjustment is dramatically slower than that of the conventional model. For instance, the adjustment in the single-elasticity framework is almost done after 100 years, but it takes

[28] Using a similar regression method based upon annual data for 2004 and 2005, my dynamic nested logit model predicts a 0.12% wage decline, substantially higher than the 0.07% predicted by the single-elasticity model. The discrepancy with McIntosh (2008) likely results from the inclusion of temporary evacuees in their monthly data, which the annual IRS migration flow data used in my model cannot capture. This is supported by their estimate of approximately 166,000 evacuees in the Houston metro area, while the IRS records only about 42,000 Katrina refugees.

[29] In Appendix E, I also report the transitional dynamics for population size in both the New Orleans CZ and its nest.



(a) Dynamic Nested Logit Migration Model



(b) Single-elasticity Migration Model

Figure 13: Welfare Changes in the Katrina Case

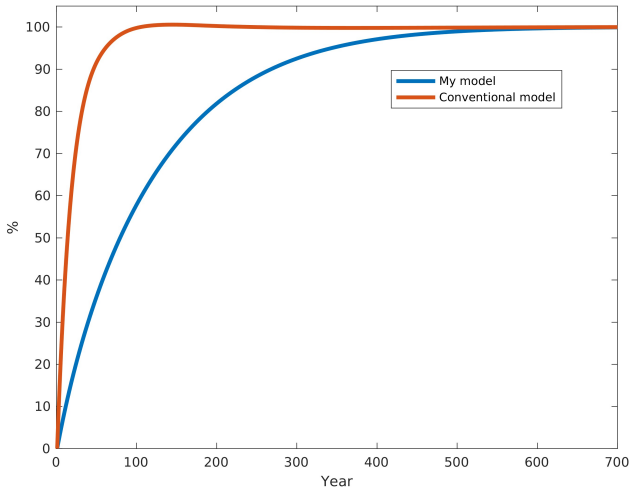


Figure 14: Population Adjustment in New Orleans Nest (Katrina Case)

more than 500 years to converge to the new steady state in my model. The much smaller cross-nest migration elasticity in my model compared to the classical model means that residents who live in the New Orleans nest before the shock but also bear most of welfare losses take a much longer time to move out of the nest than they would otherwise.

In Appendix F, I extend the analysis to a more comprehensive general-equilibrium setting that incorporates costly trade in goods, multiple production sectors, input-output linkages, and capital dynamics. Using an illustrative calibration, I demonstrate that the qualitative findings presented in this section remain robust to these additional complexities.

7 Conclusion

Migration plays a critical role in helping individuals adapt to localized shocks. This paper develops a dynamic nested logit migration framework that introduces greater behavioral flexibility by allowing for heterogeneity in migration elasticities across destinations. In this setting, a localized shock triggers a disproportionate outflow of migrants toward destinations with higher migration elasticities. As a result, the post-shock migration pattern deviates from the pre-shock one, with the extent of this deviation depending on the shock's magnitude. In contrast, the conventional single-elasticity framework, widely used in the migration literature, lacks this feature: all migration outflows scale proportionally with the size of the shock, leaving the relative dis-

tribution of migrants across destinations unchanged regardless of the shock's severity.

Motivated by this theoretical departure, I empirically examine migration behavior in the aftermath of Hurricane Katrina in 2005. Using a triple DID approach, I find strong evidence that the post-Katrina migration pattern of New Orleanians differed markedly from the pre-Katrina baseline, suggesting the presence of underlying heterogeneity in migration elasticities across destinations. Moreover, this disproportionate response persisted well beyond the immediate aftermath of the disaster.

To formalize this insight, I develop a dynamic nested logit migration model in which the nest structure is defined by both geographic and locational characteristics—specifically, the combination of Census division and urban/rural classification. Within this framework, I allow migration elasticities to differ between destinations within the same nest and those outside it. The model predicts—and the empirical evidence supports—that migration elasticities are higher for within-nest destinations than for cross-nest ones.

This additional flexibility introduces the challenge of identifying these heterogeneous migration elasticities. To address this, I derive a reduced-form estimation strategy that exploits variation in observed migration flows and destination characteristics. This methodology not only facilitates the estimation of migration elasticities but also provides a validation check for the model's assumed nest structure. Applying this method to a rich dataset of commuting-zone-to-commuting-zone migration flows, I find substantial variation in elasticities across locations, with consistently higher responsiveness to within-nest destinations.

I then apply the dynamic nested logit migration model—incorporating the estimated heterogeneous migration elasticities—to the case of Hurricane Katrina. Using a model inversion and simulation approach, I show that this framework explains a substantially larger share of the observed deviation in post-shock migration patterns than conventional single-elasticity models. In particular, it captures not only the immediate disproportionate relocation of Katrina migrants but also the persistence of these patterns over time.

The model yields distinct implications for welfare and adjustment dynamics. When migration elasticities differ across destinations, welfare losses tend to be geographically concentrated in locations with higher elasticities, which attract more migrants and experience greater con-

gestion effects. Moreover, spatial adjustment to local shocks becomes slower, as individuals are less responsive to destinations with lower migration elasticities.

This study also has several limitations. Although the current framework captures key patterns in the Katrina case, it does so using a relatively simplified structure of migration elasticity heterogeneity. Future research could enrich this framework to allow for more nuanced variation in responsiveness across destinations, though maintaining tractability in such extensions poses a significant challenge. A second limitation concerns the nest structure itself. Although I provide an empirical strategy to validate the proposed nests, it does not guarantee that the chosen structure is optimal. Developing a method to identify the optimal nest structure remains an important avenue for future work. Lastly, while heterogeneity in migration elasticities plays a major role in explaining the asymmetric response, it may not be the only factor. Exploring additional mechanisms behind such disproportionate adjustments would further enhance our understanding.

Taken together, this paper combines structural modeling, reduced-form estimation, and quantitative simulation to show that allowing for heterogeneous migration elasticities is critical to understanding both the transitional dynamics and the spatial distribution of outcomes following large, localized shocks. These findings underscore the importance of incorporating this heterogeneity into spatial models to better inform both theory and policy.

References

Adao, R., C. Arkolakis, and F. Esposito (2019). General equilibrium effects in space: Theory and measurement. Technical report, National Bureau of Economic Research.

Ahlfeldt, G. M., S. J. Redding, D. M. Sturm, and N. Wolf (2015). The economics of density: Evidence from the berlin wall. *Econometrica 83*(6), 2127–2189.

Arcidiacono, P. and R. A. Miller (2011). Conditional choice probability estimation of dynamic discrete choice models with unobserved heterogeneity. *Econometrica 79*(6), 1823–1867.

Artuç, E., S. Chaudhuri, and J. McLaren (2010). Trade shocks and labor adjustment: A structural empirical approach. *American Economic Review 100*(3), 1008–45.

Artuç, E. and J. McLaren (2015). Trade policy and wage inequality: A structural analysis with occupational and sectoral mobility. *Journal of International Economics 97*(2), 278–294.

Autor, D. and D. Dorn (2013). The growth of low-skill service jobs and the polarization of the us labor market. *American Economic Review 103*(5), 1553–97.

Autor, D., D. Dorn, and G. H. Hanson (2013). The china syndrome: Local labor market effects of import competition in the united states. *American Economic Review 103*(6), 2121–68.

Balboni, C. (2025). In harm's way? infrastructure investments and the persistence of coastal cities. *American Economic Review 115*(1), 77–116.

Bilal, A. (2023). Solving heterogeneous agent models with the master equation. Technical report, National Bureau of Economic Research.

Bilal, A. and E. Rossi-Hansberg (2023). Anticipating climate change across the united states. Technical report, National Bureau of Economic Research.

Blanchard, O. and L. Katz (1992). Regional evolutions. *Brookings Papers on Economic Activity 23*(1), 1–76.

Bryan, G. and M. Morten (2019). The aggregate productivity effects of internal migration: Evidence from indonesia. *Journal of Political Economy 127*(5), 2229–2268.

Burzyński, M., C. Deuster, F. Docquier, and J. De Melo (2022). Climate change, inequality, and human migration. *Journal of the European Economic Association 20*(3), 1145–1197.

Caliendo, L., M. Dvorkin, and F. Parro (2019). Trade and labor market dynamics: General equilibrium analysis of the china trade shock. *Econometrica 87*(3), 741–835.

Caliendo, L., F. Parro, L. D. Opromolla, and A. Sforza (2021). Goods and factor market integration: a quantitative assessment of the eu enlargement. *Journal of Political Economy 129*(12), 3491–3545.

Cameron, S., S. Chaudhuri, and J. McLaren (2007). Trade shocks and labor adjustment: theory. Technical report, National Bureau of Economic Research.

Conte, B., K. Desmet, D. K. Nagy, and E. Rossi-Hansberg (2021). Local sectoral specialization in a warming world. *Journal of Economic Geography 21*(4), 493–530.

Cruz, J. L. (2021). Global warming and labor market reallocation. Technical report, Working Paper.

Cruz, J.-L. and E. Rossi-Hansberg (2024). The economic geography of global warming. *Review of Economic Studies 91*(2), 899–939.

Deryugina, T., L. Kawano, and S. Levitt (2018). The economic impact of hurricane katrina on its victims: Evidence from individual tax returns. *American Economic Journal: Applied Economics 10*(2), 202–33.

Desmet, K., R. E. Kopp, S. A. Kulp, D. K. Nagy, M. Oppenheimer, E. Rossi-Hansberg, and B. H. Strauss (2021, April). Evaluating the economic cost of coastal flooding. *American Economic Journal: Macroeconomics 13*(2), 444–86.

Desmet, K., D. K. Nagy, and E. Rossi-Hansberg (2018). The geography of development. *Journal of Political Economy 126*(3), 903–983.

Desmet, K. and E. Rossi-Hansberg (2014). Spatial development. *American Economic Review 104*(4), 1211–43.

Desmet, K. and E. Rossi-Hansberg (2015). On the spatial economic impact of global warming. *Journal of Urban Economics 88*, 16–37.

Diamond, R. (2016). The determinants and welfare implications of us workers' diverging location choices by skill: 1980-2000. *American Economic Review 106*(3), 479–524.

Eaton, J. and S. Kortum (2002). Technology, geography, and trade. *Econometrica 70*(5), 1741–1779.

Fan, Q. and L. A. Bakkensen (2022). Household sorting as adaptation to hurricane risk in the united states. *Land Economics 98*(2), 219–238.

Frey, W. H. and A. Singer (2006). *Katrina and Rita impacts on gulf coast populations: First census findings*. Citeseer.

Fried, S. (2022). Seawalls and stilts: A quantitative macro study of climate adaptation. *The Review of Economic Studies 89*(6), 3303–3344.

Gaubert, C., P. M. Kline, D. Vergara, and D. Yagan (2025). Place-based redistribution. Technical report, Working Paper.

Henkel, M., E. Kwon, and P. Magontier (2024). The unintended consequences of post-disaster policies for spatial sorting. Technical report, Working Paper.

Hotz, V. J. and R. A. Miller (1993). Conditional choice probabilities and the estimation of dynamic models. *The Review of Economic Studies 60*(3), 497–529.

Hsiao, A. (2025). Sea level rise and urban adaptation in jakarta. Technical report, Working Paper.

Kim, S. (1995). Expansion of markets and the geographic distribution of economic activities: the trends in us regional manufacturing structure, 1860–1987. *The Quarterly Journal of Economics 110*(4), 881–908.

Kleinman, B., E. Liu, and S. J. Redding (2023). Dynamic spatial general equilibrium. *Econometrica 91*(2), 385–424.

Kline, P. and E. Moretti (2014). Local economic development, agglomeration economies, and the big push: 100 years of evidence from the tennessee valley authority. *The Quarterly Journal of Economics 129*(1), 275–331.

McIntosh, M. F. (2008). Measuring the labor market impacts of hurricane katrina migration: Evidence from houston, texas. *American Economic Review 98*(2), 54–57.

Molloy, R., C. L. Smith, and A. Wozniak (2011). Internal migration in the united states. *Journal of Economic Perspectives 25*(3), 173–96.

Monte, F., S. J. Redding, and E. Rossi-Hansberg (2018). Commuting, migration, and local employment elasticities. *American Economic Review 108*(12), 3855–90.

NWS (2016). National weather service hurricane katrina. https://www.weather.gov/mob/katrina. accessed: 2022-06-15.

Pang, X. and P. Sun (2024). Moving into risky floodplains: The spatial implication of flood relief policies. Technical report, Working Paper.

Porcher, C. (2022). Migration with costly information. Technical report, Working Paper.

Redding, S. J. (2016). Goods trade, factor mobility and welfare. *Journal of International Economics 101*, 148–167.

Redding, S. J. and D. M. Sturm (2024). Neighborhood effects: Evidence from wartime destruction in london. Technical report, National Bureau of Economic Research.

Rodríguez-Clare, A., M. Ulate, and J. P. Vasquez (2025). Trade with nominal rigidities: Understanding the unemployment and welfare effects of the china shock. *Journal of Political Economy*, forthcoming.

Sahai, H. and M. Bailey (2022). Social networks and spatial mobility: Evidence from facebook in india. Technical report, Working Paper.

Silva, J. S. and S. Tenreyro (2006). The log of gravity. *The Review of Economics and Statistics 88*(4), 641–658.

Sprung-Keyser, B., N. Hendren, S. Porter, et al. (2022). *The radius of economic opportunity: Evidence from migration and local labor markets*. US Census Bureau, Center for Economic Studies.

Steven Ruggles, Sarah Flood, S. F. R. G. J. P. M. S. and M. Sobek (2022). Ipums usa: Version 12.0.

Takeda, K. and A. Yamagishi (2025). The economic dynamics of city structure: evidence from hiroshima's recovery. Technical report, Working Paper.

Tang, Y. (2024). To follow the crowd? benefits and costs of migrant networks. Technical report, Working Paper.

Tolbert, C. M. and M. Sizer (1996). Us commuting zones and labor market areas: A 1990 update. Economic Research Service Staff Paper 9614.

Yagan, D. (2014). Moving to opportunity? migratory insurance over the great recession. *Working Paper*.

Zabek, M. (2024). Local ties in spatial equilibrium. *American Economic Journal: Macroeconomics 16*(2), 287–317.

Zerecero, M. (2021). The birthplace premium. Technical report, Working Paper.

A A Stylized Model

• Proposition 1

PROOF It is easy to show that the migration rate from j to k, μ_t^{kj}, is equal to

$$\mu_t^{kj} = \frac{\exp(\sigma \log w_t^k - \sigma \tau^{kj})}{\sum_{h\in\{1,2,3,4\}} \exp(\sigma \log w_t^h - \sigma \tau^{hj})}. \tag{37}$$

Hence,

$$\frac{\mu_t^{kj}}{\mu_t^{hj}} = \frac{\exp(\sigma \log w_t^k - \sigma \tau^{kj})}{\exp(\sigma \log w_t^h - \sigma \tau^{hj})}, \ \ \forall h,k \in \{1,2,3,4\}. \tag{38}$$

This indicates $\forall h,k \notin j$, the ratio $\frac{\mu_t^{kj}}{\mu_t^{hj}}$ is independent of the change in origin location's w_t^j, and as a result, $\frac{\partial\left(\frac{\mu^{*k1}}{\mu^{*h1}}\right)}{\partial \log w^{*1}} = 0, \forall k,h \in \{2,3,4\}$. ■

• Proposition 2

PROOF Using the proof in Appendix C, we have the migration rate from j to k, μ_t^{kj}, equal to

$$\mu_t^{kj} = \underbrace{\frac{\exp(\gamma \log w_t^k - \gamma \tau^{kj})}{\sum_{h\in D_d} \exp(\gamma \log w_t^h - \gamma \tau^{hj})}}_{\text{Conditional probability choosing location } k} \times \underbrace{\frac{\left(\sum_{h\in D_d} \exp(\gamma \log w_t^h - \gamma \tau^{hj})\right)^{\frac{\theta}{\gamma}}}{\sum_{s\in\{N,S\}} \left(\sum_{m\in D_s} \exp(\gamma \log w_t^m - \gamma \tau^{mj})\right)^{\frac{\theta}{\gamma}}}}_{\text{Probability selecting nest } D_d}, k \in D_d \tag{39}$$

where D_d is the set of locations in region d. Therefore,

$$\frac{\mu_t^{kj}}{\sum_{h\in D_d} \mu_t^{hj}}|_{k\in D_d} = \frac{\exp(\gamma \log w_t^k - \gamma \tau^{kj})}{\sum_{h\in D_d} \exp(\gamma \log w_t^h - \gamma \tau^{hj})} \tag{40}$$

Hence, $\forall h,k \notin j$,

$$\begin{aligned}
\frac{\partial\left(\frac{\mu_t^{kj}}{\mu_t^{hj}}\right)}{\partial \log w_t^j}|_{k,h\in D_s} &= \frac{\partial\left(\frac{\mu_t^{kj}}{\mu_t^{hj}}\right)}{\partial w_t^j} w_t^j \\
&\text{Equation (39)} \Rightarrow \\
&= \frac{\partial\left[\frac{\exp(\gamma \log w_t^k - \gamma\tau^{kj})}{\exp(\gamma \log w_t^h - \gamma\tau^{hj})}\right]}{\partial w_t^j} \times w_t^j \\
&= 0.
\end{aligned} \tag{41}$$

$$\frac{\partial\left(\frac{\mu_t^{kj}}{\mu_t^{hj}}\right)}{\partial \log w_t^j}|_{k,j\in D_d,h\in D_s,s\neq d} = \frac{\partial\left(\frac{\mu_t^{kj}}{\mu_t^{hj}}\right)}{\partial w_t^j} w_t^j$$

Equation (39)$\Rightarrow$

$$\begin{aligned}
&= \frac{\partial\left[\frac{\exp(\gamma \log w_t^k - \gamma\tau^{kj})}{\exp(\gamma \log w_t^h - \gamma\tau^{hj})} \frac{\left(\sum_{h\in D_d}\exp(\gamma \log w_t^h - \gamma\tau^{hj})\right)^{\frac{\theta}{\gamma}-1}}{\left(\sum_{m\in D_s}\exp(\gamma \log w_t^m - \gamma\tau^{mj})\right)^{\frac{\theta}{\gamma}-1}}\right]}{\partial w_t^j} \times w_t^j \\
&= (\frac{\theta}{\gamma}-1)\frac{\exp(\gamma \log w_t^k - \gamma\tau^{kj})}{\exp(\gamma \log w_t^h - \gamma\tau^{hj})} \frac{\left(\sum_{h\in D_d}\exp(\gamma \log w_t^h - \gamma\tau^{hj})\right)^{\frac{\theta}{\gamma}-2}}{\left(\sum_{m\in D_s}\exp(\gamma \log w_t^m - \gamma\tau^{mj})\right)^{\frac{\theta}{\gamma}-1}} \exp(-\gamma\tau^{jj})\gamma(w_t^j)^{\gamma-1} \times w_t^j \\
&= (\theta-\gamma)\frac{\exp(\gamma \log w_t^k - \gamma\tau^{kj})}{\exp(\gamma \log w_t^h - \gamma\tau^{hj})} \frac{\left(\sum_{h\in D_d}\exp(\gamma \log w_t^h - \gamma\tau^{hj})\right)^{\frac{\theta}{\gamma}-1}}{\left(\sum_{m\in D_s}\exp(\gamma \log w_t^m - \gamma\tau^{mj})\right)^{\frac{\theta}{\gamma}-1}} \frac{\exp(\gamma \log w_t^j - \gamma\tau^{jj})}{\sum_{h\in D_d}\exp(\gamma \log w_t^h - \gamma\tau^{hj})}
\end{aligned}$$

Equation (39) and (40) $\Rightarrow$

$$= (\theta-\gamma)\frac{\mu_t^{kj}}{\mu_t^{hj}} \frac{\mu_t^{jj}}{\sum_{f\in D_d}\mu_t^{fj}}. \tag{42}$$

■

B Data

• Data cleaning process

To impute certain county-to-county flows, I first collect the list of all bilateral non-zero flows

over the 2000-2018 period. Then I introduce the assumption that all bilateral flows in this list are non-zero annually. Therefore, based on the censored IRS flow data, I can identify those flows that should be non-zero but were dropped by IRS due to the deletion policy. After that, because each county's overall outflow to the United States is available in the IRS data, I evenly allocate the value of the overall outflow net the sum of observed bilateral flows to those non-zero flows deleted by IRS. If the imputed level is higher than the threshold, I restrict it to 9 before 2013 and 19 after that.

• Classification of commuting zones

The contiguous United States is divided into nine census divisions. Census divisions' borders are drawn along states' boundaries. Because there are some CZs spanning multiple states' boundaries and these states sometimes belong to different census divisions, I map these CZs to the census division that covers the largest share of a CZ's population.

The classification of a CZ as urban or rural is based on the 2013 Rural-Urban Continuum Codes released by the U.S. Department of Agriculture. The U.S. Department of Agriculture classifies each county as a either metro or non-metro county. In this study, if a CZ has more metro counties than non-metro counties, it is defined as an urban CZ. There is one exception, however: the CZ to which the city of Las Vegas belongs. Although there are more non-metro than metro counties in the Las Vegas CZ, the Las Vegas CZ is classified as an urban CZ. This classification brings the total of U.S. CZs to 221 urban CZs and 520 rural CZs.

• PPML method for estimating triple DID effects

The triple DID estimators based on PPML method and original IRS data are reported in Table 5.

• Estimated α_k in the triple DID equation (6)

Figure 15 plots estimated coefficients, α_k, that measure how Hurricane Katrina affected the outflows from the New Orleans CZ to a destination that is not an urban place in Census Division 7.

• The impact of Hurricane Andrew

Figure 16 plots the estimated coefficients indicating the disproportionate migration response of Miami CZ migrants induced by Hurricane Andrew in 1992. Because publicly accessible IRS

Table 5: PPML Estimators for the Katrina Triple DID Effects

	Adjusted IRS Data		Original IRS Data	
	(1) Migration Flows	(2) Migration Flows w/n Texas Destinations	(3) Migration Flows	(4) Migration Flows w/n Texas Destinations
2000	-0.077	-0.104	-0.113	-0.159*
	(0.055)	(0.070)	(0.078)	(0.095)
2001	-0.086	-0.078	-0.102	-0.077
	(0.057)	(0.068)	(0.076)	(0.098)
2002	-0.093	-0.060	-0.111	-0.068
	(0.061)	(0.056)	(0.074)	(0.082)
2003	-0.043	0.008	-0.036	0.032
	(0.057)	(0.063)	(0.074)	(0.089)
2005	0.897***	0.406***	0.794***	0.354**
	(0.125)	(0.113)	(0.115)	(0.140)
2006	0.410***	0.349***	0.451***	0.378***
	(0.081)	(0.066)	(0.115)	(0.094)
2007	0.212***	0.336***	0.286***	0.432***
	(0.061)	(0.065)	(0.071)	(0.079)
2009	0.035	0.130**	0.102	0.202**
	(0.079)	(0.064)	(0.089)	(0.086)
2010	0.083	0.155**	0.158*	0.230***
	(0.070)	(0.060)	(0.083)	(0.085)
2011	-0.033	0.059	-0.018	0.081
	(0.068)	(0.065)	(0.080)	(0.091)
2012	0.002	0.121**	0.002	0.123
	(0.070)	(0.060)	(0.079)	(0.085)
2013 $\leq$	-0.130***	-0.025	0.106	0.303***
	(0.049)	(0.047)	(0.069)	(0.074)
Constant	6.821***	6.850***	7.056***	7.090***
	(0.001)	(0.001)	(0.001)	(0.001)
Origin-by-Destination FE	Yes	Yes	Yes	Yes
Destination-by-Year FE	Yes	Yes	Yes	Yes
Origin's-Division-by-Year FE	Yes	Yes	Yes	Yes
New-Orlean-by-Year FE	Yes	Yes	Yes	Yes
# of Obs	668,643	556,600	352,424	293,269

Standard errors in parentheses

$*p < 0.1, **p < 0.05, ***p < 0.01$

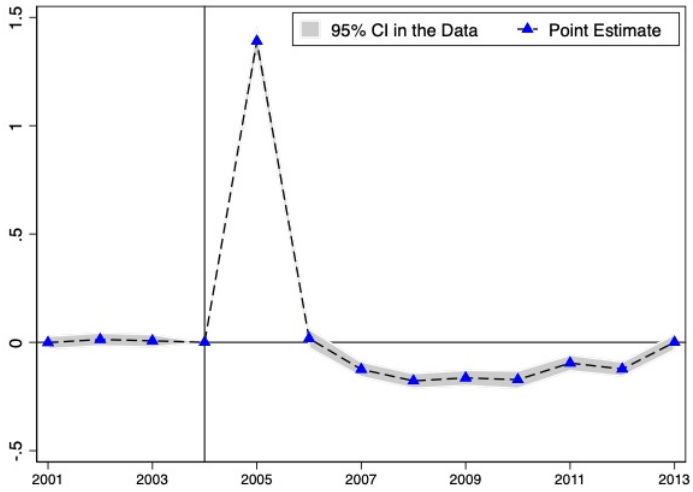


Figure 15: Estimated α_k

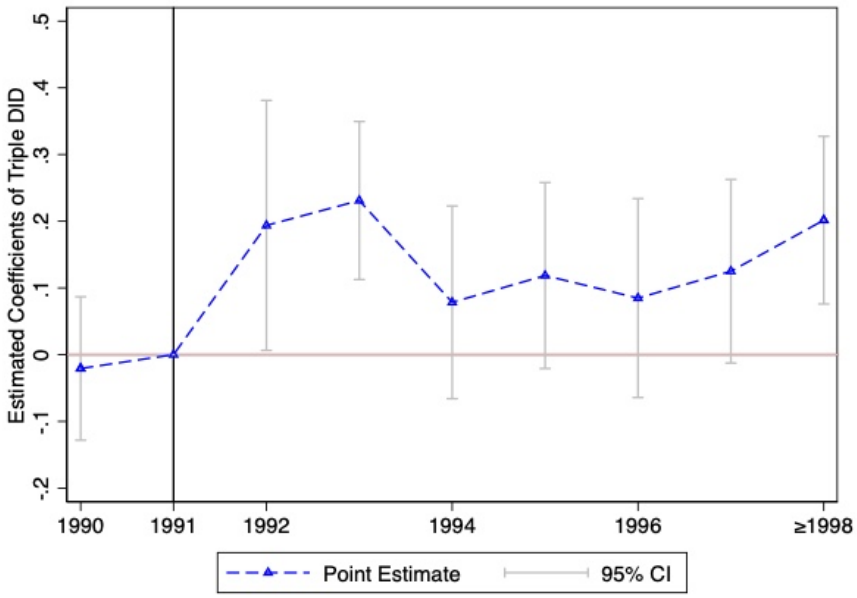


Figure 16: Treatment Effect for Migrants from Miami CZ

data are only available beginning in 1990, the triple DID analysis is conducted after that. The result in Figure 16 suggests that Hurricane Andrew caused Miami CZ migrants to disproportionately move to urban destinations in Census Division 5, the division in which the Miami CZ is located.

C Migration Model

• Migration rate

Let me define a function $G(.)$ such that

$$G(x_1,...,x_J) = \sum_{m\in M}\Big(\sum_{h\in D_m}(x_h)^{\frac{\gamma_m}{\theta}}\Big)^{\frac{\theta}{\gamma_m}}. \tag{43}$$

Therefore, the Generalized Extreme Value distribution in equation (8) can be formularized as

$$\mathbf{P}[\varepsilon_t^{kj} \leq a_k, k = 1,\ldots,J] = \exp[-G(a_1^{-\theta},\ldots,a_J^{-\theta})]. \tag{44}$$

And the first-order partial derivative of $G(.)$ *w.r.t* x_k is given by

$$\frac{\partial G}{\partial x_k}|_{x_k \in D_m} = \Big(\sum_{h \in D_m} (x_h)^{\frac{\gamma_m}{\theta}} \Big)^{\frac{\theta}{\gamma_m}-1} (x_k)^{\frac{\gamma_m}{\theta}-1}. \tag{45}$$

The fraction of individuals relocating from location j to k at time t, μ_t^{kj}, is equal to

$$\mu_t^{kj} = \lim_{a\to\infty} \mathbf{P}[\max_{i\in\{1,..,J\}} \ln \varepsilon^{ij} + \beta V_{t+1}^i - \tau_t^{ij} - \beta V_{t+1}^k + \tau_t^{kj} \leq \ln a \text{ and } \ln \varepsilon^{kj} =$$

$$\max_{i\in\{1,..,J\}} (\ln \varepsilon^{ij} + \beta V_{t+1}^i - \tau_t^{ij} - \beta V_{t+1}^k + \tau_t^{kj})]$$

Let $\ln y^{ij} = \ln \varepsilon^{ij} + \beta V_{t+1}^i - \tau_t^{ij} - \beta V_{t+1}^k + \tau_t^{kj}$

$= \lim_{a\to\infty} \mathbf{P}[\max_{i\in\{1,..,J\}} \ln y^{ij} \leq \ln a \text{ and } \ln y^{kj} = \max_{i\in\{1,..,J\}} \ln y^{ij}]$

By the monotonicity property,

$= \lim_{a\to\infty} \mathbf{P}[\max_{i\in\{1,..,J\}} y^{ij} \leq a \text{ and } y^{kj} = \max_{i\in\{1,..,J\}} y^{ij}]$

$= \lim_{a\to\infty} \mathbf{P}[y^{kj} \leq a \text{ and } y^{kj} = \max_{i\in\{1,..,J\}} y^{ij}]$

$= \lim_{a\to\infty} \mathbf{P}[y^{kj} \leq a \text{ and } y^{ij} \leq y^{kj}, \forall i \neq k]$

$= \lim_{a\to\infty} \int_0^a \mathbf{P}[y^{ij} \leq t, \forall i \neq k | y^{kj} = t] \frac{\partial}{\partial t} \mathbf{P}[y^{kj} \leq t] dt$

By Bayes' rule, $\mathbf{P}[y^{ij} \leq t, \forall i \neq k | y^{kj} = t] = \dfrac{\frac{\partial}{\partial t}\mathbf{P}[y^{ij} \leq c, \forall i \neq k \text{ and } y^{kj} \leq t]|_{c=t}}{\frac{\partial}{\partial t}\mathbf{P}[y^{kj} \leq t]}$

$= \lim_{a\to\infty} \int_0^a \frac{\partial}{\partial t} \mathbf{P}[y^{ij} \leq c, \forall i \neq k \text{ and } y^{kj} \leq t]|_{c=t} dt$

Equation (44) $\Rightarrow \mathbf{P}[y^{kj} \leq a_k, k = 1, \ldots, J] = \exp[-G(< a_m^{-\theta} \exp[\theta(\beta V_{t+1}^m - \tau_t^{mj} - \beta V_{t+1}^k + \tau_t^{kj})] >)]$

$= \int_0^\infty \frac{\partial}{\partial a_k} \exp[-G(< a_m^{-\theta} \exp[\theta(\beta V_{t+1}^m - \tau_t^{mj} - \beta V_{t+1}^k + \tau_t^{kj})] >)]|_{a_m=t,\forall m} dt$

$= \int_0^\infty \exp[-G(< a_m^{-\theta} \exp[\theta(\beta V_{t+1}^m - \tau_t^{mj} - \beta V_{t+1}^k + \tau_t^{kj})] >)]$

$\times G_k(< a_m^{-\theta} \exp[\theta(\beta V_{t+1}^m - \tau_t^{mj} - \beta V_{t+1}^k + \tau_t^{kj})] >) \theta a_k^{-\theta-1}|_{a_m=t,\forall m} dt$(where $G_k = \dfrac{\partial G}{\partial x_k}$)

$= \int_0^\infty \exp[-G(< t^{-\theta} \exp[\theta(\beta V_{t+1}^m - \tau_t^{mj} - \beta V_{t+1}^k + \tau_t^{kj})] >)]$

$\times G_k(< t^{-\theta} \exp[\theta(\beta V_{t+1}^m - \tau_t^{mj} - \beta V_{t+1}^k + \tau_t^{kj})] >) \theta t^{-\theta-1} dt$

By the homogeneous degree 1 of $G(.)$ and degree 0 of G_k^j

$$
\begin{aligned}
&= \int_0^{\infty} \exp[-t^{-\theta}\exp(-\theta\beta V_{t+1}^{k} + \theta\tau_t^{kj})G(<\exp[\theta(\beta V_{t+1}^{m} - \tau_t^{mj})]>)] \\
&\quad \times G_k(<\exp[\theta(\beta V_{t+1}^{m} - \tau_t^{mj})]>)\theta t^{-\theta-1}dt \\
&= \Bigg[\exp\big[-t^{-\theta}\exp(-\theta\beta V_{t+1}^{k} + \theta\tau_t^{kj})G(<\exp[\theta(\beta V_{t+1}^{m} - \tau_t^{mj})]>)\big] \\
&\frac{\exp(\theta\beta V_{t+1}^{k} - \theta\tau_t^{kj})G_k(<\exp[\theta(\beta V_{t+1}^{m} - \tau_t^{mj})]>)}{G(<\exp[\theta(\beta V_{t+1}^{m} - \tau_t^{mj})]>)}\Bigg]_0^{\infty} \\
&= \frac{\exp(\theta\beta V_{t+1}^{k} - \theta\tau_t^{kj})G_k(<\exp[\theta(\beta V_{t+1}^{m} - \tau_t^{mj})]>)}{G(<\exp[\theta(\beta V_{t+1}^{m} - \tau_t^{mj})]>)}
\end{aligned} \tag{46}
$$

Substituting euqation (43) and (45) into it yields

$$
\begin{aligned}
&= \frac{\exp(\gamma_m\beta V_{t+1}^{k} - \gamma_m\tau_t^{kj})\big(\sum_{h\in D_m}(\exp(\gamma_m\beta V_{t+1}^{h} - \gamma_m\tau_t^{hj})\big)^{\frac{\theta-\gamma_m}{\gamma_m}}}{\sum_{s\in M}\big(\sum_{h\in D_m}\exp(\gamma_s\beta V_{t+1}^{h} - \gamma_s\tau_t^{hj})\big)^{\frac{\theta}{\gamma_s}}} \\
&= \underbrace{\frac{\big(\sum_{h\in D_m}(\exp(\gamma_m\beta V_{t+1}^{h} - \gamma_m\tau_t^{hj})\big)^{\frac{\theta}{\gamma_m}}}{\sum_{s\in M}\big(\sum_{h\in D_s}\exp(\gamma_s\beta V_{t+1}^{h} - \gamma_s\tau_t^{hj})\big)^{\frac{\theta}{\gamma_s}}}}_{\text{The probability selecting nest } D_m}\ \underbrace{\frac{\exp(\gamma_m\beta V_{t+1}^{k} - \gamma_m\tau_t^{kj})}{\sum_{h\in D_m}\exp(\gamma_m\beta V_{t+1}^{h} - \gamma_m\tau_t^{hj})}}_{\text{The conditional probability choosing location } k}.
\end{aligned} \tag{47}
$$

Thus, the probability selecting nest D_m is equal to

$$
\sum_{k\in D_m}\mu_t^{kj} = \frac{\big(\sum_{h\in D_m}\exp(\gamma_m\beta V_{t+1}^{h} - \gamma_m\tau_t^{hj})\big)^{\frac{\theta}{\gamma_m}}}{\sum_{s\in M}\big(\sum_{h\in D_s}(\exp(\gamma_s\beta V_{t+1}^{h} - \gamma_s\tau_t^{hj})\big)^{\frac{\theta}{\gamma_s}}} \tag{48}
$$

Substituting it into equation (47) produces

$$
\frac{\mu_t^{kj}}{\sum_{h\in D_m}\mu_t^{hj}}|_{k\in D_m} = \frac{\exp(\gamma_m\beta V_{t+1}^{k} - \gamma_m\tau_t^{kj})}{\sum_{h\in D_m}\exp(\gamma_m\beta V_{t+1}^{h} - \gamma_m\tau_t^{mj})}. \tag{49}
$$

• Proof of Proposition 3

PROOF It follows from Equation (47) that the migration rate to a location outside the origin nest relative to the migration rate to another outside-nest location is independent of origin's value function, V_{t+1}^{j}. Hence, all else being equal, its level won't change as V_{t+1}^{j} changes. However, if the destination k belongs to the origin location j's nest while another destination h

doesn't, then following equation (47)

$$\frac{\partial\left(\frac{\mu_t^{kj}}{\mu_t^{hj}}\right)}{\partial V_{t+1}^j} = \frac{\partial\left[\frac{\left(\sum_{f\in D_d}\exp(\gamma_d\beta V_{t+1}^f-\gamma_d\tau_t^{fj})\right)^{\frac{\theta}{\gamma_d}-1}}{\left(\sum_{m\in D_s}\exp(\gamma_s\beta V_{t+1}^m-\gamma_s\tau_t^{mj})\right)^{\frac{\theta}{\gamma_s}-1}}\frac{\exp(\gamma_d\beta V_{t+1}^k-\gamma_d\tau_t^{kj})}{\exp(\gamma_s\beta V_{t+1}^h-\gamma_s\tau_t^{hj})}\right]}{\partial V_{t+1}^j}$$

$$= (\frac{\theta}{\gamma_d}-1)\frac{\left(\sum_{f\in D_d}\exp(\gamma_d\beta V_{t+1}^f-\gamma_d\tau_t^{fj})\right)^{\frac{\theta}{\gamma_d}-2}}{\left(\sum_{m\in D_s}\exp(\gamma_s\beta V_{t+1}^m-\gamma_s\tau_t^{mj})\right)^{\frac{\theta}{\gamma_s}-1}}\frac{\exp(\gamma_d\beta V_{t+1}^k-\gamma_d\tau_t^{kj})}{\exp(\gamma_s\beta V_{t+1}^h-\gamma_s\tau_t^{hj})}\beta\gamma_d\exp(\gamma_d\beta V_{t+1}^j)$$

$$= \beta(\theta-\gamma_d)\frac{\left(\sum_{f\in D_d}\exp(\gamma_d\beta V_{t+1}^f-\gamma_d\tau_t^{fj})\right)^{\frac{\theta}{\gamma_d}-1}}{\left(\sum_{m\in D_s}\exp(\gamma_s\beta V_{t+1}^m-\gamma_s\tau_t^{mj})\right)^{\frac{\theta}{\gamma_s}-1}}\frac{\exp(\gamma_d\beta V_{t+1}^k-\gamma_d\tau_t^{kj})}{\exp(\gamma_s\beta V_{t+1}^h-\gamma_s\tau_t^{hj})}\frac{\exp(\gamma_d\beta V_{t+1}^j)}{\sum_{f\in D_d}\exp(\gamma_d\beta V_{t+1}^f-\gamma_d\tau_t^{fj})}$$

Equation (47) and (49) $\Rightarrow$

$$= \beta(\theta-\gamma_d)\frac{\mu_t^{kj}}{\mu_t^{hj}}\frac{\mu_t^{jj}}{\sum_{f\in D_d}\mu_t^{fj}}, \quad j,k\in D_d, h\notin D_d. \tag{50}$$

■

• Value function

The proof of equation (47) implies that the expected continuation value $\Phi_t \equiv \mathbf{E}[\max_k\{\beta\mathbf{E}v_{t+1}^k - \tau_t^{kj}+\ln\varepsilon_t^{kj}\}]$ can be expressed as

$$\Phi_t = \sum_k\int_0^\infty\left(\beta V_{t+1}^k-\tau_t^{kj}+\ln\varepsilon_t^{kj}\right)\exp\left[-\exp(-\theta\beta V_{t+1}^k+\theta\tau_t^{kj})(\varepsilon^{kj})^{-\theta}G(<\exp(\theta\beta V_{t+1}^m-\theta\tau_t^{mj})>)\right]$$

$$\times G_k(<\exp(\theta\beta V_{t+1}^m-\theta\tau_t^{mj})>)\theta(\varepsilon^{kj})^{-\theta-1}d\varepsilon^{kj}$$

Let $\omega \equiv \beta V_{t+1}^k-\tau_t^{kj}+\ln\varepsilon_t^{kj}$,

$$= \sum_k\int_{-\infty}^\infty\omega\exp\left(-\exp(-\theta\omega)G(<\exp(\theta\beta V_{t+1}^m-\theta\tau_t^{mj})>)\right)$$

$$\times G_k(<\exp(\theta\beta V_{t+1}^m-\theta\tau_t^{mj})>)\theta\exp(-\theta\omega)\exp(\theta\beta V_{t+1}^k-\theta\tau_t^{kj})d\omega$$

By the homogeneity of degree one of G,

$$= \int_{-\infty}^\infty\omega exp\left(-\exp(-\theta\omega)G(<\exp(\theta\beta V_{t+1}^m-\theta\tau_t^{mj})>)\right)G(<\exp(\theta\beta V_{t+1}^m-\theta\tau_t^{mj})>)\theta\exp(-\theta\omega)d\omega$$

Let $x \equiv \exp(-\theta\omega)G(<\exp(\theta\beta V_{t+1}^m-\theta\tau_t^{mj})>)$,

$$= \int_0^\infty\frac{\ln G(<\exp(\theta\beta V_{t+1}^m-\theta\tau_t^{mj})>)-\ln x}{\theta}\exp(-x)dx$$

$$= \frac{1}{\theta}\left[\ln G(<\exp(\theta\beta V_{t+1}^{m} - \theta\tau_t^{mj})>) - \int_0^{\infty} \ln x \exp(-x)dx\right]$$

The second term is equal to the Euler-Mascheroni constant, $\bar{\gamma}$.

$$= \frac{\ln G(<\exp(\theta\beta V_{t+1}^{m} - \theta\tau_t^{mj})>) + \bar{\gamma}}{\theta}$$

Plugging equation (43) into it

$$= \frac{\ln\left[\sum_{s\in M}\left(\sum_{h\in D_s}(\exp(\gamma_s\beta V_{t+1}^{h} - \gamma_s\tau_t^{hj})\right)^{\frac{\theta}{\gamma_s}}\right] + \bar{\gamma}}{\theta}. \tag{51}$$

Therefore, the representative agent's lifetime utility at location j is given by

$$V_t^j = u(C_t^j) + \frac{\ln\left[\sum_{s\in M}\left(\sum_{h\in D_s}(\exp(\gamma_s\beta V_{t+1}^{h} - \gamma_s\tau_t^{hj})\right)^{\frac{\theta}{\gamma_s}}\right] + \bar{\gamma}}{\theta}. \tag{52}$$

Substituting equation (48) into it yields

$$V_t^j = u(C_t^j) + \frac{\ln(\sum_{h\in D_m}\exp(\gamma_m\beta V_{t+1}^{h} - \gamma_m\tau_t^{hj}))}{\gamma_m} + \frac{\bar{\gamma} - \ln(\sum_{h\in D_m}\mu_t^{hj})}{\theta},$$

Plugging equation (49),

$$= u(C_t^j) - \tau_t^{kj} + \beta V_{t+1}^{k} + \frac{\ln(\sum_{h\in D_m}\mu_t^{hj}) - \ln\mu_t^{kj}}{\gamma_m} + \frac{\bar{\gamma} - \ln(\sum_{h\in D_m}\mu_t^{hj})}{\theta}, \ \ \forall k \in D_m$$

$$= u(C_t^j) - \tau_t^{kj} + \beta V_{t+1}^{k} + \frac{\theta - \gamma_m}{\gamma_m\theta}\ln(\sum_{h\in D_m}\mu_t^{hj}) - \frac{\ln\mu_t^{kj}}{\gamma_m} + \frac{\bar{\gamma}}{\theta}, \ \ \forall k \in D_m. \tag{53}$$

• The mean of idiosyncratic tastes for those migrants from location i conditional on moving to location k

$$\mathbf{E}[\ln \varepsilon_t^{kj} | k = \arg\max_{i\in\{1,..,J\}} \{\beta \mathbf{E} v_{t+1}^k - \tau_t^{kj} + \ln \varepsilon_t^{kj}\}] = \frac{\mathbf{E}[\ln \varepsilon_t^{kj} \mathbf{1}_{k=\arg\max_{i\in\{1,..,J\}}\{\beta \mathbf{E} v_{t+1}^k - \tau_t^{kj} + \ln \varepsilon_t^{kj}\}}]}{\mathbf{P}(k = \arg\max_{i\in\{1,..,J\}}\{\beta \mathbf{E} v_{t+1}^k - \tau_t^{kj} + \ln \varepsilon_t^{kj}\})}$$

$$= \frac{1}{\mathbf{P}(k = \arg\max_{i\in\{1,..,J\}}\{\beta \mathbf{E} v_{t+1}^k - \tau_t^{kj} + \ln \varepsilon_t^{kj}\})}$$

$$\times \int_0^\infty \ln \varepsilon_t^{kj} \exp\left[-\exp(-\theta\beta V_{t+1}^k + \theta \tau_t^{kj})(\varepsilon^{kj})^{-\theta} G(< \exp(\theta\beta V_{t+1}^m - \theta \tau_t^{mj}) >)\right]$$

$$\times G_k(< \exp(\theta\beta V_{t+1}^m - \theta \tau_t^{mj}) >) \theta (\varepsilon^{kj})^{-\theta-1} d\varepsilon^{kj}$$

Let $y \equiv \exp(-\theta\beta V_{t+1}^k + \theta \tau_t^{kj})(\varepsilon^{kj})^{-\theta} G(< \exp(\theta\beta V_{t+1}^m - \theta \tau_t^{mj}) >)$

$$= \frac{1}{\mathbf{P}(k = \arg\max_{i\in\{1,..,J\}}\{\beta \mathbf{E} v_{t+1}^k - \tau_t^{kj} + \ln \varepsilon_t^{kj}\})}$$

$$\times \int_0^\infty [\frac{-\ln y}{\theta} - \beta V_{t+1}^k + \tau_t^{kj} + \frac{\ln G(< \exp(\theta\beta V_{t+1}^m - \theta \tau_t^{mj}) >)}{\theta}] \exp(-y)$$

$$\times \frac{\exp(\theta\beta V_{t+1}^k - \theta \tau_t^{kj}) G_k(< \exp(\theta\beta V_{t+1}^m - \theta \tau_t^{mj}) >)}{G(< \exp(\theta\beta V_{t+1}^m - \theta \tau_t^{mj}) >)} dy$$

Equation (46) $\Rightarrow$

$$= \int_0^\infty [\frac{-\ln y}{\theta} - \beta V_{t+1}^k + \tau_t^{kj} + \frac{\ln G(< \exp(\theta\beta V_{t+1}^m - \theta \tau_t^{mj}) >)}{\theta}] \exp(-y) dy$$

$$= \int_0^\infty \frac{-\ln y}{\theta} \exp(-y) dy - \beta V_{t+1}^k + \tau_t^{kj} + \frac{\ln G(< \exp(\theta\beta V_{t+1}^m - \theta \tau_t^{mj}) >)}{\theta}$$

Based upon the proof in Equation (53)

$$= \frac{\theta - \gamma_m}{\gamma_m \theta} \ln(\sum_{h\in D_m} \mu_t^{hj}) - \frac{\ln \mu_t^{kj}}{\gamma_m} + \frac{\bar{\gamma}}{\theta} \tag{54}$$

• single-elasticity migration model

This is the equation in existing migration research that governs the motion of bilateral migration flows,

$$\mu_t^{kj} = \frac{\exp(\bar{\sigma}\beta V_{t+1}^k - \bar{\sigma}\tau_t^{kj})}{\sum_h \exp(\bar{\sigma}\beta V_{t+1}^h - \bar{\sigma}\tau_t^{hj})}, \ \forall k \tag{55}$$

where $\bar{\sigma}$ is the single migration elasticity.

• Proof of Proposition 4

PROOF Equation (55) $\Rightarrow$

$$\begin{aligned}\frac{\partial \log \mu_t^{kj}}{\partial V_{t+1}^j}|_{k\neq j} =& \frac{1}{\mu_t^{kj}} \frac{\partial \mu_t^{kj}}{\partial V_{t+1}^j} \\ =& \frac{1}{\mu_t^{kj}} \frac{\exp(\bar{\sigma}\beta V_{t+1}^k - \bar{\sigma}\tau_t^{kj})}{[\sum_h \exp(\bar{\sigma}\beta V_{t+1}^h - \bar{\sigma}\tau_t^{hj})]^2} \bar{\sigma}\beta \exp(\bar{\sigma}\beta V_{t+1}^j) \\ =& \beta\bar{\sigma}\mu_t^{jj}.\end{aligned} \tag{56}$$

■

• Proof of Proposition 5

PROOF Let $\mathscr{N}_t^{mj} \equiv \sum_{k\in D_m} \mu_t^{kj}$. If $k, j \in D_m$, equation (48) $\Rightarrow$

$$\begin{aligned}\frac{\partial \ln \mathscr{N}_t^{mj}}{\partial V_{t+1}^j} =& \frac{1}{\mathscr{N}_t^{mj}} \frac{\partial \mathscr{N}_t^{mj}}{\partial V_{t+1}^j} \\ =& \frac{1}{\mathscr{N}_t^{mj}} \Bigg[- \frac{\left(\sum_{h\in D_m} \exp(\gamma_m\beta V_{t+1}^h - \gamma_m\tau_t^{hj})\right)^{\frac{\theta}{\gamma_m}}}{\left[\sum_{s\in M}\left(\sum_{h\in D_s}(\exp(\gamma_s\beta V_{t+1}^h - \gamma_s\tau_t^{hj})\right)^{\frac{\theta}{\gamma_s}}\right]^2} \frac{\theta}{\gamma_m} \Big(\sum_{h\in D_m} \exp(\gamma_m\beta V_{t+1}^h - \gamma_m\tau_t^{hj})\Big)^{\frac{\theta}{\gamma_m}-1} \\ & \times \gamma_m\beta \exp(\gamma_m\beta V_{t+1}^j - \gamma_m\tau_t^{jj}) + \frac{\left(\sum_{h\in D_m} \exp(\gamma_m\beta V_{t+1}^h - \gamma_m\tau_t^{hj})\right)^{\frac{\theta}{\gamma_m}-1}}{\sum_{s\in M}\left(\sum_{h\in D_s}(\exp(\gamma_s\beta V_{t+1}^h - \gamma_s\tau_t^{hj})\right)^{\frac{\theta}{\gamma_s}}} \frac{\theta}{\gamma_m} \\ & \times \gamma_m\beta \exp(\gamma_m\beta V_{t+1}^j - \gamma_m\tau_t^{jj}) \Bigg] \\ =& \frac{1}{\mathscr{N}_t^{mj}} \Bigg[- \beta\theta \frac{\left(\sum_{h\in D_m} \exp(\gamma_m\beta V_{t+1}^h - \gamma_m\tau_t^{hj})\right)^{\frac{\theta}{\gamma_m}}}{\sum_{s\in M}\left(\sum_{h\in D_s}(\exp(\gamma_s\beta V_{t+1}^h - \gamma_s\tau_t^{hj})\right)^{\frac{\theta}{\gamma_s}}} \frac{\left(\sum_{h\in D_m} \exp(\gamma_m\beta V_{t+1}^h - \gamma_m\tau_t^{hj})\right)^{\frac{\theta}{\gamma_m}}}{\sum_{s\in M}\left(\sum_{h\in D_s}(\exp(\gamma_s\beta V_{t+1}^h - \gamma_s\tau_t^{hj})\right)^{\frac{\theta}{\gamma_s}}} \\ & \times \frac{\exp(\gamma_m\beta V_{t+1}^j - \gamma_m\tau_t^{jj})}{\sum_{h\in D_m} \exp(\gamma_m\beta V_{t+1}^h - \gamma_m\tau_t^{hj})} + \beta\theta \frac{\left(\sum_{h\in D_m} \exp(\gamma_m\beta V_{t+1}^h - \gamma_m\tau_t^{hj})\right)^{\frac{\theta}{\gamma_m}}}{\sum_{s\in M}\left(\sum_{h\in D_s}(\exp(\gamma_s\beta V_{t+1}^h - \gamma_s\tau_t^{hj})\right)^{\frac{\theta}{\gamma_s}}} \\ & \times \frac{\exp(\gamma_m\beta V_{t+1}^j - \gamma_m\tau_t^{jj})}{\sum_{h\in D_m} \exp(\gamma_m\beta V_{t+1}^h - \gamma_m\tau_t^{hj})} \Bigg]\end{aligned}$$

Equation (47) and (48) $\Rightarrow$

$$= \beta\theta\mu_t^{jj} \frac{1 - \mathscr{N}_t^{mj}}{\mathscr{N}_t^{mj}}. \tag{57}$$

Similarly, if $j \notin D_m$, equation (48) $\Rightarrow$

$$\frac{\partial \ln \mathscr{N}_t^{mj}}{\partial V_{t+1}^j} = -\beta\theta\mu_t^{jj}. \tag{58}$$

■

D Identification and Estimation

• Heterogeneous migration elasticity estimation strategy

Here, I assume that the moving cost is time-invariant. Equation (47) and (48) suggest that

$$\begin{aligned} L_{jt}\mu_t^{kj}|_{k\in D_m} &= \exp\left[\ln(\sum_{h\in D_m}\mu_t^{hj}) - \gamma_m\tau^{kj} + \gamma_m\beta V_{t+1}^k - \ln[\sum_{h\in D_m}\exp(\gamma_m\beta V_{t+1}^h - \gamma_m\tau^{hj})] + \ln L_{jt}\right] \\ &= \exp\left(\Gamma_{k,t} + \Phi_{j,m,t} + F_{k,j}\right). \end{aligned} \tag{59}$$

where

$$\Gamma_{k,t} = \gamma_m\beta V_{t+1}^k - \gamma_m\beta V_{t+1}^1, \tag{60}$$

$$\Phi_{j,m,t} = \ln(\sum_{h\in D_m}\mu_t^{hj}) - \ln[\sum_{h\in D_m}\exp(\gamma_m\beta V_{t+1}^h - \gamma_m\tau^{hj})] + \ln L_{jt} + \gamma_m\beta V_{t+1}^1, \tag{61}$$

$$F_{k,j} = -\gamma_m\tau^{kj}. \tag{62}$$

Because $\Gamma_{k,t}$ and $\Phi_{j,m,t}$ cannot be separately identified, without loss of generality I normalized $\Gamma_{1,t}$ to be zero.

In the case that origin j also belongs to the nest m, equation (49) suggests that

$$\sum_{h\in D_m}\exp(\gamma_m\beta V_{t+1}^h - \gamma_m\tau^{hj}) = \exp(\gamma_m\beta V_{t+1}^j - \gamma_m\tau^{jj})\frac{\sum_{h\in D_m}\mu_t^{hj}}{\mu_t^{jj}}. \tag{63}$$

Therefore,

$$\Phi_{j,m,t} = \gamma_m\tau^{jj} + \ln\mu_t^{jj} - \gamma_m\beta V_{t+1}^j + \ln L_{jt} + \gamma_m\beta V_{t+1}^1, j,k \in D_m. \tag{64}$$

Equation (53) implies that if $j,k \in D_m$

$$\begin{aligned}\Gamma_{k,t} &= \beta\gamma_m V_{t+1}^k - \gamma_m \beta V_{t+1}^1 \\ &= \beta\gamma_m u(C_{t+1}^k) - \beta\gamma_m \tau^{jk} + \beta^2 \gamma_m V_{t+2}^j + \frac{\beta(\theta-\gamma_m)}{\theta}\ln(\sum_{h\in D_m}\mu_{t+1}^{hk}) - \beta\ln\mu_{t+1}^{jk} + \frac{\beta\gamma_m\bar{\gamma}}{\theta} - \gamma_m\beta V_{t+1}^1,\end{aligned}$$

Equation (64)$\Rightarrow$

$$\begin{aligned}&= \beta\gamma_m u(C_{t+1}^k) - \beta\gamma_m\tau^{jk} + \beta[\gamma_m\tau^{jj} + \ln\mu_{t+1}^{jj} - \Phi_{j,\gamma_m,t+1} + \ln L_{jt+1} + \gamma_m\beta V_{t+2}^1] \\ &+ \frac{\beta(\theta-\gamma_m)}{\theta}\ln(\sum_{h\in D_m}\mu_{t+1}^{hk}) - \beta\ln\mu_{t+1}^{jk} + \frac{\beta\gamma_m\bar{\gamma}}{\theta} - \gamma_m\beta V_{t+1}^1. \qquad (65)\end{aligned}$$

Replacing the fixed effects with the estimated ones and rearranging this equations gives

$$\begin{aligned}\widehat{\Gamma}_{k,t} + \beta\widehat{\Phi}_{j,m,t+1} - \beta\ln L_{jt+1} &= \beta\gamma_m u(C_{t+1}^k) - \beta\gamma_m\tau^{jk} + \beta\gamma_m\tau^{jj} + \beta\ln\mu_{t+1}^{jj} - \beta\ln\mu_{t+1}^{jk} + \varepsilon_{k,j,t} \\ &+ \frac{\beta(\theta-\gamma_m)}{\theta}\ln(\sum_{h\in D_m}\mu_{t+1}^{hk}) + \frac{\beta\gamma_m\bar{\gamma}}{\theta} + \gamma_m\beta(\beta V_{t+2}^1 - V_{t+1}^1) + \varepsilon_{k,j,t}\end{aligned}$$

Under the assumption that $\gamma_m = \gamma \ \forall m$

$$\begin{aligned}&= \beta\gamma_m u(C_{t+1}^k) - \underbrace{\beta\gamma\tau^{jk} + \beta\gamma\tau^{jj}}_{\text{Origin-destination fixed effect}} + \underbrace{\frac{\beta\gamma\bar{\gamma}}{\theta} + \gamma\beta(\beta V_{t+2}^1 - V_{t+1}^1)}_{\text{time fixed effect}} - \beta\ln\ln(\frac{\mu_{t+1}^{jk}}{\mu_{t+1}^{jj}}) \\ &+ \frac{\beta(\theta-\gamma_m)}{\theta}\ln(\sum_{h\in D_m}\mu_{t+1}^{hk}) \\ &= \beta\gamma u(C_{t+1}^k) + \alpha_{kj} + \alpha_t + \alpha_1\ln(\frac{\mu_{t+1}^{jk}}{\mu_{t+1}^{jj}}) + \beta(1-\frac{\gamma}{\theta})\ln(\sum_{h\in D_m}\mu_{t+1}^{hk}) + \tilde{e}_{kjt}, \quad j,k\in D_m,\end{aligned} \qquad (66)$$

where $\tilde{e}_{kjt}$ is the error term.

• Estimation methodology in the single-elasticity model

For the migration elasticity estimation, it is assumed that τ_t^{kj} is time-invariant. Similarly,

the number of migrants, $L_{jt}\mu_t^{kj}$ can be expressed as three types of fixed effects,

$$\begin{aligned} L_{jt}\mu_t^{kj} &= \exp\left[\bar{\sigma}\beta V_t^k - \bar{\sigma}\tau_t^{kj} - \ln[\sum_h \exp(\bar{\sigma}\beta V_{t+1}^h - \bar{\sigma}\tau_t^{hj})] + \ln L_{jt}\right] \\ &= \exp(\Gamma'_{k,t} + \Phi'_{j,t} + F'_{k,j}), \\ &\text{where} \\ \Gamma'_{k,t} &= \bar{\sigma}\beta V_{t+1}^k - \bar{\sigma}\beta V_{t+1}^1 \\ \Phi'_{j,t} &= -\ln[\sum_h \exp(\bar{\sigma}\beta V_{t+1}^h - \bar{\sigma}\tau^{hj})] + \ln L_{jt} + \bar{\sigma}\beta V_{t+1}^1 \\ F'_{k,j} &= -\bar{\sigma}\tau^{kj}. \end{aligned} \tag{67}$$

$\Gamma'_{k,t}$ is the destination fixed effect, $\Phi'_{j,t}$ is the origin fixed effect, and $F_{k,j}$ is the origin-destination fixed effect.

It follows from equation (55) that

$$\ln[\sum_h \exp(\bar{\sigma}\beta V_{t+1}^h - \bar{\sigma}\tau^{hj})] = \bar{\sigma}\beta V_{t+1}^j - \bar{\sigma}\tau^{jj} - \ln\mu_t^{jj}. \tag{68}$$

Thus,

$$\Phi'_{j,t} = -\bar{\sigma}\beta V_{t+1}^j + \bar{\sigma}\tau^{jj} + \ln\mu_t^{jj} + \ln L_{jt} + \bar{\sigma}\beta V_{t+1}^1 \tag{69}$$

The lifetime utility of a representative agent in location j at time t, V_t^j, in the single-elasticity migration model is

$$V_t^j = u(C_t^j) - \tau_t^{kj} + \beta V_{t+1}^k - \frac{\ln\mu_t^{kj}}{\bar{\sigma}} + \frac{\bar{\gamma}}{\bar{\sigma}}, \forall k. \tag{70}$$

Therefore,

$$\begin{aligned}\Gamma'_{k,t} &= \bar{\sigma}\beta\left[u(C^k_{t+1}) - \tau^{jk} + \beta V^j_{t+2} - \frac{\ln \mu^{jk}_t}{\bar{\sigma}} + \frac{\bar{\gamma}}{\bar{\sigma}}\right] - \bar{\sigma}\beta V^1_{t+1} \\ &\quad \text{Substituting } \Phi'_{j,t} \text{ for } V^j_{t+2} \\ &= \beta\bar{\sigma}u(C^k_{t+1}) - \beta\bar{\sigma}\tau^{jk} - \beta\ln\mu^{jk}_{t+1} + \beta\bar{\gamma} - \bar{\sigma}\beta V^1_{t+1} \\ &\quad + \beta\left[-\Phi'_{j,t+1} + \bar{\sigma}\tau^{jj} + \ln\mu^{jj}_{t+1} + \ln L_{jt+1} + \bar{\sigma}\beta V^1_{t+2}\right].\end{aligned} \tag{71}$$

Replacing the fixed effects with the estimated ones and rearranging this equation yields

$$\begin{aligned}\widehat{\Gamma}'_{k,t} + \beta\widehat{\Phi}'_{j,t+1} - \beta\ln L_{jt+1} &= \beta\bar{\sigma}u(C^k_{t+1}) - \beta\bar{\sigma}\tau^{jk} + \beta\bar{\sigma}\tau^{jj} - \beta\ln\frac{\mu^{jk}_{t+1}}{\mu^{jj}_{t+1}} \\ &\quad + \beta\bar{\gamma} + \bar{\sigma}\beta[\beta V^1_{t+2} - V^1_{t+1}] + \varepsilon'_{kjt} \\ &= \beta\bar{\sigma}u(C^k_{t+1}) + \alpha_{kj} + \alpha_t + \alpha'_1\ln(\frac{\mu^{jk}_{t+1}}{\mu^{jj}_{t+1}}) + \varepsilon'_{kjt}.\end{aligned} \tag{72}$$

- Robustness tests for the migration elasticity estimation. I consider two scenarios.

- In the first case, I only use Infutor data over the 2014-2018 period for the estimation. The results are reported in Table 6.

	Within-nest Migration Elasticity	Cross-nest Migration Elasticity
Nested Logit Migration Model	1.92***	0.05***
	(0.5395)	(0.0097)
Single-elasticity Migration model	0.02	0.02
	(0.0918)	(0.0918)

Standard errors in parentheses. $*p < 0.1$, $**p < 0.05$, $***p < 0.01$

Table 6: Robustness Check II: Estimated Annual Migration Elasticities Using Infutor Data

- In the second case, there are endogenous local amenities. Similar to Diamond (2016), I use CZs' college worker ratios as a proxy for local endogenous amenity levels and add them into equation (20) as a controlled variable. The final estimated migration elasticities are reported in Table 7.

	Within-nest Migration Elasticity	Cross-nest Migration Elasticity
Nested Logit Migration Model	1.38***	0.03***
	(0.2100)	(0.0046)
Single-elasticity Migration Model	0.32***	0.32***
	(0.0694)	(0.0694)

Standard errors in parentheses. $*p<0.1$, $**p<0.05$, $***p<0.01$

Table 7: Robustness Check II: Estimated Annual Migration Elasticities with Endogenous Local Amenities

E Quantitative Analysis

• Proof of Proposition 6

PROOF For simplification, let $U_t^k = \exp(V_t^k)$ and $\dot{\tau}_{t+1}^{kj} = \exp(\tau_{t+1}^{kj} - \tau_t^{kj})$.

$$\dot{\mu}_{t+1}^{kj}|_{k\in D_m} \equiv \frac{\mu_{t+1}^{kj}}{\mu_t^{kj}}$$

Following equation (49)

$$= \frac{\sum_{h\in D_m}\mu_{t+1}^{hj}}{\sum_{h\in D_m}\mu_t^{hj}} \frac{\exp(\gamma_m\beta V_{t+2}^k - \gamma_m\beta V_{t+1}^k)\exp(-\gamma_m\tau_{t+1}^{kj} + \gamma_m\tau_t^{kj})}{[\sum_{h\in D_m}\exp(\gamma_m\beta V_{t+2}^h - \gamma_m\tau_{t+1}^{hj})]/[\sum_{h\in D_m}\exp(\gamma_m\beta V_{t+1}^h - \tau_t^{hj})]}$$

$$= \frac{\sum_{h\in D_m}\mu_t^{hj}\dot{\mu}_{t+1}^{hj}}{\sum_{h\in D_m}\mu_t^{hj}} \frac{(\dot{U}_{t+2}^k)^{\gamma_m\beta}(\dot{\tau}_{t+1}^{kj})^{-\gamma_m}}{\sum_{s\in D_m}\frac{\exp(\gamma_m\beta V_{t+1}^s - \gamma_m\tau_t^{sj})(\dot{U}_{t+2}^s)^{\gamma_m\beta}(\dot{\tau}_{t+1}^{sj})^{-\gamma_m}}{\sum_{h\in Dm}\exp(\gamma_m\beta V_{t+1}^h - \gamma_m\tau_t^{hj})}}$$

Equation (49) $\Rightarrow$

$$= \frac{\sum_{h\in D_m}\mu_t^{hj}\dot{\mu}_{t+1}^{hj}}{\sum_{h\in D_m}\mu_t^{hj}} \frac{(\dot{U}_{t+2}^k)^{\gamma_m\beta}(\dot{\tau}_{t+1}^{kj})^{-\gamma_m}}{\sum_{s\in D_m}\frac{\mu_t^{sj}(\dot{U}_{t+2}^s)^{\gamma_m\beta}(\dot{\tau}_{t+1}^{sj})^{-\gamma_m}}{\sum_{h\in Dm}\mu_t^{hj}}}$$

$$= \frac{\sum_{h\in D_m}\mu_t^{hj}\dot{\mu}_{t+1}^{hj}}{\sum_{s\in D_m}\mu_t^{sj}(\dot{U}_{t+2}^s)^{\gamma_m\beta}(\dot{\tau}_{t+1}^{sj})^{-\gamma_m}}(\dot{U}_{t+2}^k)^{\gamma_m\beta}(\dot{\tau}_{t+1}^{kj})^{-\gamma_m}. \tag{73}$$

Define $\mathscr{N}_t^{mj} \equiv \sum_{h\in D_m}\mu_t^{hj}$. Then equation (73) reduces to

$$\frac{\dot{\mu}_{t+1}^{kj}}{\mathscr{N}_{t+1}^{mj}}|_{k\in D_m} = \frac{(\dot{U}_{t+2}^k)^{\gamma_m\beta}(\dot{\tau}_{t+1}^{kj})^{-\gamma_m}}{\sum_{s\in D_m}\mu_t^{sj}(\dot{U}_{t+2}^s)^{\gamma_m\beta}(\dot{\tau}_{t+1}^{sj})^{-\gamma_m}}. \tag{74}$$

Therefore, equation (48) indicates that

$$\dot{\mathscr{N}}_{t+1}^{mj} = \frac{\left(\sum_{h\in D_m}\exp(\gamma_m\beta V_{t+2}^h-\gamma_m\tau_{t+1}^{hj})\right)^{\frac{\theta}{\gamma_m}}/\left(\sum_{h\in D_m}\exp(\gamma_m\beta V_{t+1}^h-\tau_t^{hj})\right)^{\frac{\theta}{\gamma_m}}}{\sum_{s\in M}\left(\sum_{h\in D_s}\exp(\gamma_s\beta V_{t+2}^h-\gamma_s\tau_{t+1}^{hj})\right)^{\frac{\theta}{\gamma_s}}/\sum_{s\in M}\left(\sum_{h\in D_s}\exp(\gamma_s\beta V_{t+1}^h-\gamma_s\tau_t^{hj})\right)^{\frac{\theta}{\gamma_s}}}$$

$$= \frac{\left[\sum_{n\in D_m}\frac{\exp(\gamma_m\beta V_{t+1}^n-\gamma_m\tau_t^{nj})(\dot{U}_{t+2}^n)^{\gamma_m\beta}(\dot{\tau}_{t+1}^{nj})^{-\gamma_m}}{\sum_{h\in D_m}\exp(\gamma_m\beta V_{t+1}^h-\tau_t^{hj})}\right]^{\frac{\theta}{\gamma_m}}}{\sum_{s\in M}\left[\frac{\left(\sum_{h\in D_s}\exp(\gamma_s\beta V_{t+1}^h-\gamma_s\tau_t^{hj})\right)^{\frac{\theta}{\gamma_s}}}{\sum_{d\in M}\left(\sum_{h\in D_d}\exp(\gamma_d\beta V_{t+1}^h-\gamma_d\tau_t^{hj})\right)^{\frac{\theta}{\gamma_d}}}\left[\sum_{n\in D_s}\frac{\exp(\gamma_s\beta V_{t+1}^n-\gamma_s\tau_t^{nj})(\dot{U}_{t+2}^n)^{\gamma_s\beta}(\dot{\tau}_{t+1}^{nj})^{-\gamma_s}}{\sum_{h\in D_s}\exp(\gamma_s\beta V_{t+1}^h-\gamma_s\tau_t^{hj})}\right]^{\frac{\theta}{\gamma_s}}\right]}$$

Equaiton (49) and (48) $\Rightarrow$

$$= \frac{\left(\sum_{n\in D_m}\frac{\mu_t^{nj}}{\mathscr{N}_t^{mj}}(\dot{U}_{t+2}^n)^{\gamma_m\beta}(\dot{\tau}_{t+1}^{nj})^{-\gamma_m}\right)^{\frac{\theta}{\gamma_m}}}{\sum_{s\in M}(\mathscr{N}_t^{sj})^{\frac{\gamma_s-\theta}{\gamma_s}}\left(\sum_{n\in D_s}\mu_t^{nj}(\dot{U}_{t+2}^n)^{\gamma_s\beta}(\dot{\tau}_{t+1}^{nj})^{-\gamma_s}\right)^{\frac{\theta}{\gamma_s}}}. \tag{75}$$

Equation (52) implies

$$\begin{aligned}
\dot{U}_{t+1}^j &\equiv \frac{\exp(V_{t+1}^j)}{\exp(V_t^j)} \\
&= \dot{\omega}^j(\dot{L}_{t+1},\dot{\Theta}_{t+1})\frac{\left[\sum_{s\in M}\left(\sum_{h\in D_s}\exp(\gamma_s\beta V_{t+2}^h-\gamma_s\tau_{t+1}^{hj})\right)^{\frac{\theta}{\gamma_s}}\right]^{\frac{1}{\theta}}}{\left[\sum_{s\in M}\left(\sum_{h\in D_s}\exp(\gamma_s\beta V_{t+1}^h-\gamma_s\tau_t^{hj})\right)^{\frac{\theta}{\gamma_s}}\right]^{\frac{1}{\theta}}} \\
&= \dot{\omega}^j(\dot{L}_{t+1},\dot{\Theta}_{t+1})\left[\sum_{n\in M}\frac{\left(\sum_{e\in D_n}\exp(\gamma_n\beta V_{t+2}^e-\gamma_n\tau_{t+1}^{ej})\right)^{\frac{\theta}{\gamma_n}}}{\sum_{s\in M}\left(\sum_{h\in D_s}\exp(\gamma_s\beta V_{t+1}^h-\gamma_s\tau_t^{hj})\right)^{\frac{\theta}{\gamma_s}}}\right]^{\frac{1}{\theta}} \\
&= \dot{\omega}^j(\dot{L}_{t+1},\dot{\Theta}_{t+1})\left[\sum_{n\in M}\frac{\left(\sum_{e\in D_n}\exp(\gamma_n\beta V_{t+1}^e-\gamma_n\tau_t^{ej})\right)^{\frac{\theta}{\gamma_n}}}{\sum_{s\in M}\left(\sum_{h\in D_s}\exp(\gamma_s\beta V_{t+1}^h-\gamma_s\tau_t^{hj})\right)^{\frac{\theta}{\gamma_s}}}\times\right. \\
&\left.\Big[\sum_{f\in D_n}\frac{\exp(\gamma_n\beta V_{t+1}^f-\gamma_n\tau_t^{fj})(\dot{U}_{t+2}^f)^{\gamma_n\beta}(\dot{\tau}_{t+1}^{fj})^{-\gamma_n}}{\sum_{e\in D_n}\exp(\gamma_n\beta V_{t+1}^e-\gamma_n\tau_t^{ej})}\Big]^{\frac{\theta}{\gamma_n}}\right]^{\frac{1}{\theta}}
\end{aligned}$$

Equation (48) and (49) $\Rightarrow$

$$\begin{aligned}
&= \dot{\omega}^j(\dot{L}_{t+1},\dot{\Theta}_{t+1})\left[\sum_{n\in M}\Big[\Big(\sum_{e\in D_n}\mu_t^{ej}\Big)\Big[\sum_{f\in D_n}\frac{\mu_t^{fj}(\dot{U}_{t+2}^f)^{\gamma_n\beta}(\dot{\tau}_{t+1}^{fj})^{-\gamma_n}}{\sum_{e\in D_n}\mu_t^{ej}}\Big]^{\frac{\theta}{\gamma_n}}\Big]\right]^{\frac{1}{\theta}}, \\
&= \dot{\omega}^j(\dot{L}_{t+1},\dot{\Theta}_{t+1})\left[\sum_{n\in M}\Big[(\mathscr{N}_t^{nj})^{\frac{\gamma_n-\theta}{\gamma_n}}\Big[\sum_{f\in D_n}\mu_t^{fj}(\dot{U}_{t+2}^f)^{\gamma_n\beta}(\dot{\tau}_{t+1}^{fj})^{-\gamma_n}\Big]^{\frac{\theta}{\gamma_n}}\Big]\right]^{\frac{1}{\theta}}.
\end{aligned} \tag{76}$$

■

• Solution Algorithm

Given an initial allocation of the economy, (L_0,μ_{-1}), and given an anticipated convergent

sequence of changes in fundamentals, $\{\dot{\Theta}_t\}_{t=1}^{\infty}$, the approach to solving the general-equilibrium model is as follows:

1. Conduct the initial guess for the path of $\{\dot{U}_{t+1}^{j}\}_{t=0}^{T}$.
2. Given the path of $\{\dot{U}_{t+1}^{j(i)}\}_{t=0}^{T}$, where the superscript (i) denotes the ith iteration, and the set of initial conditions, (L_0, μ_{-1}), solve for the path of $\{\mu_t^{kj(i)}\}_{t=0}^{T}$ and $\{\mathscr{N}_t^{kj(i)}\}_{t=0}^{T}$ using equation (74) and (75).
3. Derive the path of $\{L_{jt+1}^{(i)}\}$ using $L_{jt+1} = \sum_m \mu_t^{jm} L_{mt}, \forall j$ associated with the path of $\{\mu_t^{jm(i)}\}_{t=0}^{T}$ and L_0.
4. Use equation (76) associated with the path of $\{[\dot{G}_{t+1}^{j(i)}]^{\frac{1}{\theta}}\}_{t=0}^{T}$ and $\{L_{t+1}^{j(i)}\}$ to solve backward for $\{\dot{U}_{t+1}^{j(i+1)}\}_{t=0}^{T}$.
5. If $\{\dot{U}_{t+1}^{j(i+1)}\}_{t=0}^{T}$ does not converge to $\{\dot{U}_{t+1}^{j(i)}\}_{t=0}^{T}$, then return to Step 2 and repeat this process till the convergence.

• Proof of Proposition 7

PROOF Equation (73) $\Rightarrow$

$$\dot{\mu}_{t+1}^{'kj}|_{k\in D_m} = \frac{\sum_{h\in D_m} \mu_t^{'hj} \dot{\mu}_{t+1}^{'hj}}{\sum_{s\in D_m} \mu_t^{'sj} (\dot{U}_{t+2}^{'s})^{\gamma_m\beta} (\dot{\tau}_{t+1}^{'sj})^{-\gamma_m}} (\dot{U}_{t+2}^{'k})^{\gamma_m\beta} (\dot{\tau}_{t+1}^{'kj})^{-\gamma_m}$$

$$= \frac{\sum_{h\in D_m} \mu_t^{'hj} \dot{\mu}_{t+1}^{'hj}}{\sum_{s\in D_m} \mu_t^{'sj} (\dot{U}_{t+2}^{s})^{\gamma_m\beta} (\hat{U}_{t+2}^{s})^{\gamma_m\beta} (\dot{\tau}_{t+1}^{sj})^{-\gamma_m} (\hat{\tau}_{t+1}^{sj})^{-\gamma_m}} (\dot{U}_{t+2}^{k})^{\gamma_m\beta} (\hat{U}_{t+2}^{k})^{\gamma_m\beta} (\dot{\tau}_{t+1}^{kj})^{-\gamma_m} (\hat{\tau}_{t+1}^{kj})^{-\gamma_m}$$

Using equation (73) to replace $(\dot{U}_{t+2}^{k})^{\gamma_m\beta}$ and $(\dot{\tau}_{t+1}^{kj})^{-\gamma_m}$

$$= \frac{\sum_{h\in D_m} \mu_t^{'hj} \dot{\mu}_{t+1}^{'hj} / \sum_{h\in D_m} \mu_t^{hj} \dot{\mu}_{t+1}^{hj}}{\sum_{s\in D_m} \mu_t^{'sj} (\dot{U}_{t+2}^{s})^{\gamma_m\beta} (\hat{U}_{t+2}^{s})^{\gamma_m\beta} (\dot{\tau}_{t+1}^{sj})^{-\gamma_m} (\hat{\tau}_{t+1}^{sj})^{-\gamma_m} / \sum_{s\in D_m} \mu_t^{sj} (\dot{U}_{t+2}^{s})^{\gamma_m\beta} (\dot{\tau}_{t+1}^{sj})^{-\gamma_m}} \dot{\mu}_{t+1}^{kj} (\hat{U}_{t+2}^{k})^{\gamma_m\beta} (\hat{\tau}_{t+1}^{kj})^{-\gamma_m}$$

$$= \frac{\sum_{h\in D_m} \mu_t^{'hj} \dot{\mu}_{t+1}^{'hj} / \sum_{h\in D_m} \mu_t^{hj} \dot{\mu}_{t+1}^{hj}}{\sum_{s\in D_m} \mu_t^{'sj} \frac{(\dot{U}_{t+2}^{s})^{\gamma_m\beta} (\dot{\tau}_{t+1}^{sj})^{-\gamma_m}}{\sum_{n\in D_m} \mu_t^{nj} (\dot{U}_{t+2}^{n})^{\gamma_m\beta} (\dot{\tau}_{t+1}^{nj})^{-\gamma_m}} (\hat{U}_{t+2}^{s})^{\gamma_m\beta} (\hat{\tau}_{t+1}^{sj})^{-\gamma_m}} \dot{\mu}_{t+1}^{kj} (\hat{U}_{t+2}^{k})^{\gamma_m\beta} (\hat{\tau}_{t+1}^{kj})^{-\gamma_m}$$

Substituting equation (74) into the denominator,

$$= \frac{\sum_{h\in D_m} \mu_t^{'hj} \dot{\mu}_{t+1}^{'hj} / \sum_{h\in D_m} \mu_t^{hj} \dot{\mu}_{t+1}^{hj}}{\sum_{s\in D_m} \mu_t^{'sj} \frac{\dot{\mu}_{t+1}^{sj}}{\sum_{h\in D_m} \mu_{t+1}^{hj}} (\hat{U}_{t+2}^{s})^{\gamma_m\beta} (\hat{\tau}_{t+1}^{sj})^{-\gamma_m}} \dot{\mu}_{t+1}^{kj} (\hat{U}_{t+2}^{k})^{\gamma_m\beta} (\hat{\tau}_{t+1}^{kj})^{-\gamma_m}$$

$$= \frac{\sum_{h\in D_m} \mu_t^{'hj} \dot{\mu}_{t+1}^{'hj}}{\sum_{s\in D_m} \mu_t^{'sj} \dot{\mu}_{t+1}^{sj} (\hat{U}_{t+2}^{s})^{\gamma_m\beta} (\hat{\dot{\tau}}_{t+1}^{sj})^{-\gamma_m}} \dot{\mu}_{t+1}^{kj} (\hat{U}_{t+2}^{k})^{\gamma_m\beta} (\hat{\dot{\tau}}_{t+1}^{kj})^{-\gamma_m}. \tag{77}$$

Equation (75) suggests

$$\begin{aligned}
\hat{\mathscr{N}}_{t+1}^{mj} &= \frac{\left(\sum_{n\in D_m} \frac{\mu_t^{'nj}}{\mathscr{N}_t^{'mj}} (\dot{U}_{t+2}^{'n})^{\gamma_m\beta} (\dot{\tau}_{t+1}^{'nj})^{-\gamma_m}\right)^{\frac{\theta}{\gamma_m}} / \left(\sum_{n\in D_m} \frac{\mu_t^{nj}}{\mathscr{N}_t^{mj}} (\dot{U}_{t+2}^{n})^{\gamma_m\beta} (\dot{\tau}_{t+1}^{nj})^{-\gamma_m}\right)^{\frac{\theta}{\gamma_m}}}{\sum_{s\in M} (\mathscr{N}_t^{'sj})^{\frac{\gamma_s-\theta}{\gamma_s}} \left(\sum_{n\in D_s} \mu_t^{'nj} (\dot{U}_{t+2}^{'n})^{\gamma_s\beta} (\dot{\tau}_{t+1}^{'nj})^{-\gamma_m}\right)^{\frac{\theta}{\gamma_s}} / \sum_{s\in M} (\mathscr{N}_t^{sj})^{\frac{\gamma_s-\theta}{\gamma_s}} \left(\sum_{n\in D_s} \mu_t^{nj} (\dot{U}_{t+2}^{n})^{\gamma_s\beta} (\dot{\tau}_{t+1}^{nj})^{-\gamma_m}\right)^{\frac{\theta}{\gamma_s}}} \\
&= \frac{\left[\sum_{h\in D_m} \frac{\mu_t^{'hj}}{\mathscr{N}_t^{'mj}} (\hat{U}_{t+2}^{h})^{\gamma_m\beta} (\hat{\tau}_{t+1}^{hj})^{-\gamma_m} \frac{(\dot{U}_{t+2}^{h})^{\gamma_m\beta} (\dot{\tau}_{t+1}^{hj})^{-\gamma_m}}{\left(\sum_{n\in D_m} \frac{\mu_t^{nj}}{\mathscr{N}_{t+1}^{mj}} (\dot{U}_{t+2}^{n})^{\gamma_m\beta} (\dot{\tau}_{t+1}^{nj})^{-\gamma_m}\right)} (\dot{\mathscr{N}}_{t+1}^{mj})^{-1}\right]^{\frac{\theta}{\gamma_m}}}{\sum_{d\in M} (\mathscr{N}_t^{'dj})^{\frac{\gamma_d-\theta}{\gamma_d}} (\mathscr{N}_t^{dj})^{\frac{\theta}{\gamma_d}} \frac{\left(\sum_{n\in D_d} \frac{\mu_t^{nj}}{\mathscr{N}_t^{dj}} (\dot{U}_{t+2}^{n})^{\gamma_d\beta} (\dot{\tau}_{t+1}^{nj})^{-\gamma_d}\right)^{\frac{\theta}{\gamma_d}}}{\sum_{s\in M} (\mathscr{N}_t^{sj})^{\frac{\gamma_s-\theta}{\gamma_s}} \left(\sum_{n\in D_s} \mu_t^{nj} (\dot{U}_{t+2}^{n})^{\gamma_s\beta} (\dot{\tau}_{t+1}^{nj})^{-\gamma_s}\right)^{\frac{\theta}{\gamma_s}}} \times \Big[\\
&\quad \frac{1}{\sum_{f\in D_d} \frac{\mu_t^{'fj} (\dot{U}_{t+2}^{f})^{\gamma_d\beta} (\dot{\tau}_{t+1}^{fj})^{-\gamma_d} (\dot{U}_{t+2}^{f})^{\gamma_d\beta} (\hat{\tau}_{t+1}^{fj})^{-\gamma_d}}{\sum_{n\in D_d} \mu_t^{nj} (\dot{U}_{t+2}^{n})^{\gamma_d\beta} (\dot{\tau}_{t+1}^{nj})^{-\gamma_d}}\Big]^{\frac{\theta}{\gamma_d}}}
\end{aligned}$$

Equation (74) and (75) $\Rightarrow$

$$\begin{aligned}
&= \frac{\left[\sum_{h\in D_m} \frac{\mu_t^{'hj}}{\mathscr{N}_t^{'mj}} (\hat{U}_{t+2}^{h})^{\gamma_m\beta} (\hat{\tau}_{t+1}^{hj})^{-\gamma_m} \dot{\mu}_{t+1}^{hj} (\dot{\mathscr{N}}_{t+1}^{mj})^{-1}\right]^{\frac{\theta}{\gamma_m}}}{\sum_{d\in M} (\mathscr{N}_t^{'dj})^{\frac{\gamma_d-\theta}{\gamma_d}} (\mathscr{N}_t^{dj})^{\frac{\theta}{\gamma_d}} \dot{\mathscr{N}}_{t+1}^{dj} \left[\sum_{f\in D_d} \frac{\mu_t^{'fj} \dot{\mu}_{t+1}^{fj} (\hat{U}_{t+2}^{f})^{\gamma_d\beta} (\hat{\tau}_{t+1}^{fj})^{-\gamma_d}}{\mathscr{N}_{t+1}^{dj}}\right]^{\frac{\theta}{\gamma_d}}} \\
&= \frac{\left[\sum_{h\in D_m} \mu_t^{'hj} \dot{\mu}_{t+1}^{hj} (\hat{U}_{t+2}^{h})^{\gamma_m\beta} (\hat{\tau}_{t+1}^{hj})^{-\gamma_m}\right]^{\frac{\theta}{\gamma_m}} (\mathscr{N}_t^{'mj})^{-\frac{\theta}{\gamma_m}} (\dot{\mathscr{N}}_{t+1}^{mj})^{-\frac{\theta}{\gamma_m}}}{\sum_{d\in M} (\mathscr{N}_t^{'dj})^{\frac{\gamma_d-\theta}{\gamma_d}} (\dot{\mathscr{N}}_{t+1}^{dj})^{\frac{\gamma_d-\theta}{\gamma_d}} \left[\sum_{f\in D_d} \mu_t^{'fj} \dot{\mu}_{t+1}^{fj} (\hat{U}_{t+2}^{f})^{\gamma_d\beta} (\hat{\tau}_{t+1}^{fj})^{-\gamma_d}\right]^{\frac{\theta}{\gamma_d}}}.
\end{aligned} \tag{78}$$

Equation (76) $\Rightarrow$

$$\begin{aligned}
\hat{U}_{t+1}^{j} &= \hat{\omega}_{jt+1}(\hat{L}_{t+1}, \hat{\Theta}_{t+1}) \frac{\left[\sum_{n\in M} \left[(\mathscr{N}_t^{'nj})^{\frac{\gamma_n-\theta}{\gamma_n}} \left[\sum_{f\in D_n} \mu_t^{'fj} (\dot{U}_{t+2}^{'f})^{\gamma_n\beta} (\dot{\tau}_{t+1}^{'fj})^{-\gamma_n}\right]^{\frac{\theta}{\gamma_n}}\right]\right]^{\frac{1}{\theta}}}{\left[\sum_{n\in M} \left[(\mathscr{N}_t^{nj})^{\frac{\gamma_n-\theta}{\gamma_n}} \left[\sum_{f\in D_n} \mu_t^{fj} (\dot{U}_{t+2}^{f})^{\gamma_n\beta} (\dot{\tau}_{t+1}^{fj})^{-\gamma_n}\right]^{\frac{\theta}{\gamma_n}}\right]\right]^{\frac{1}{\theta}}} \\
&= \hat{\omega}_{jt+1}(\hat{L}_{t+1}, \hat{\Theta}_{t+1}) \left[\sum_{s\in M} \frac{\left[(\mathscr{N}_t^{'sj})^{\frac{\gamma_s-\theta}{\gamma_s}} \left[\sum_{f\in D_s} \mu_t^{'fj} (\dot{U}_{t+2}^{'f})^{\gamma_s\beta} (\dot{\tau}_{t+1}^{'fj})^{-\gamma_s}\right]^{\frac{\theta}{\gamma_s}}\right]}{\sum_{n\in M} \left[(\mathscr{N}_t^{nj})^{\frac{\gamma_n-\theta}{\gamma_n}} \left[\sum_{f\in D_n} \mu_t^{fj} (\dot{U}_{t+2}^{f})^{\gamma_n\beta} (\dot{\tau}_{t+1}^{fj})^{-\gamma_n}\right]^{\frac{\theta}{\gamma_n}}\right]}\right]^{\frac{1}{\theta}} \\
&= \hat{\omega}_{jt+1}(\hat{L}_{t+1}, \hat{\Theta}_{t+1}) \left[\sum_{s\in M} \frac{\left[(\mathscr{N}_t^{'sj})^{\frac{\gamma_s-\theta}{\gamma_s}} \left[\sum_{f\in D_s} \mu_t^{'fj} \frac{(\dot{U}_{t+2}^{f})^{\gamma_s\beta} (\dot{\tau}_{t+1}^{fj})^{-\gamma_d}}{\sum_{m\in D_s} \mu_t^{mj} (\dot{U}_{t+2}^{m})^{\gamma_s\beta} (\dot{\tau}_{t+1}^{mj})^{-\gamma_s}} (\hat{U}_{t+2}^{f})^{\gamma_s\beta} (\hat{\tau}_{t+1}^{fj})^{-\gamma_s}\right]^{\frac{\theta}{\gamma_s}}\right]}{\sum_{n\in M} \left[(\mathscr{N}_t^{nj})^{\frac{\gamma_n-\theta}{\gamma_n}} \left[\sum_{f\in D_n} \mu_t^{fj} (\dot{U}_{t+2}^{f})^{\gamma_n\beta} (\dot{\tau}_{t+1}^{fj})^{-\gamma_n}\right]^{\frac{\theta}{\gamma_n}}\right]}\right] \\
&\quad \times \Big[\sum_{m\in D_s} \mu_t^{mj} (\dot{U}_{t+2}^{m})^{\gamma_s\beta} (\dot{\tau}_{t+1}^{mj})^{-\gamma_s}\Big]^{\frac{\theta}{\gamma_s}}\Big]^{\frac{1}{\theta}}
\end{aligned}$$

Substituting equation (74) for the $\dot{U}^f_{t+2}$ term in the numerator

$$= \hat{\omega}_{jt+1}(\hat{L}_{t+1}, \hat{\Theta}_{t+1}) \Bigg[\sum_{s \in M} \frac{\big[(\mathscr{N}_t^{'sj})^{\frac{\gamma_s-\theta}{\gamma_s}} (\mathscr{N}_{t+1}^{sj})^{-\frac{\theta}{\gamma_s}} [\sum_{f \in D_s} \mu_t^{'fj} \dot{\mu}_{t+1}^{fj} (\hat{U}_{t+2}^f)^{\gamma_s \beta} (\hat{\tau}_{t+1}^{fj})^{-\gamma_s}]^{\frac{\theta}{\gamma_s}}\big]}{\sum_{n \in M} \big[(\mathscr{N}_t^{nj})^{\frac{\gamma_n-\theta}{\gamma_n}} [\sum_{f \in D_n} \mu_t^{fj} (\dot{U}_{t+2}^f)^{\gamma_n \beta} (\dot{\tau}_{t+1}^{fj})^{-\gamma_n}]^{\frac{\theta}{\gamma_n}}\big]}$$

$$\times [\sum_{m \in D_s} \mu_t^{mj} (\dot{U}_{t+2}^m)^{\gamma_s \beta} (\dot{\tau}_{t+1}^{mj})^{-\gamma_s}]^{\frac{\theta}{\gamma_s}} \Bigg]^{\frac{1}{\theta}}$$

$$= \hat{\omega}_{jt+1}(\hat{L}_{t+1}, \hat{\Theta}_{t+1}) \Bigg[\sum_{s \in M} \frac{\big[(\mathscr{N}_t^{'sj})^{\frac{\gamma_s-\theta}{\gamma_s}} (\dot{\mathscr{N}}_{t+1}^{sj})^{-\frac{\theta}{\gamma_s}} [\sum_{f \in D_s} \mu_t^{'fj} \dot{\mu}_{t+1}^{fj} (\hat{U}_{t+2}^f)^{\gamma_s \beta} (\hat{\tau}_{t+1}^{fj})^{-\gamma_s}]^{\frac{\theta}{\gamma_s}}\big]}{\sum_{n \in M} \big[(\mathscr{N}_t^{nj})^{\frac{\gamma_n-\theta}{\gamma_n}} [\sum_{f \in D_n} \mu_t^{fj} (\dot{U}_{t+2}^f)^{\gamma_n \beta} (\dot{\tau}_{t+1}^{fj})^{-\gamma_n}]^{\frac{\theta}{\gamma_n}}\big]}$$

$$\times [\sum_{m \in D_s} \frac{\mu_t^{mj}}{\mathscr{N}_t^{sj}} (\dot{U}_{t+2}^m)^{\gamma_s \beta} (\dot{\tau}_{t+1}^{mj})^{-\gamma_s}]^{\frac{\theta}{\gamma_s}} \Bigg]^{\frac{1}{\theta}}$$

$$= \hat{\omega}_{jt+1}(\hat{L}_{t+1}, \hat{\Theta}_{t+1}) \Bigg[\sum_{s \in M} \frac{[\sum_{m \in D_s} \frac{\mu_t^{mj}}{\mathscr{N}_t^{sj}} (\dot{U}_{t+2}^m)^{\gamma_s \beta} (\dot{\tau}_{t+1}^{mj})^{-\gamma_s}]^{\frac{\theta}{\gamma_s}}}{\sum_{n \in M} \big[(\mathscr{N}_t^{nj})^{\frac{\gamma_n-\theta}{\gamma_n}} [\sum_{f \in D_n} \mu_t^{fj} (\dot{U}_{t+2}^f)^{\gamma_n \beta} (\dot{\tau}_{t+1}^{fj})^{-\gamma_n}]^{\frac{\theta}{\gamma_n}}\big]}$$

$$\times \big[(\mathscr{N}_t^{'sj})^{\frac{\gamma_s-\theta}{\gamma_s}} (\dot{\mathscr{N}}_{t+1}^{sj})^{-\frac{\theta}{\gamma_s}} [\sum_{f \in D_s} \mu_t^{'fj} \dot{\mu}_{t+1}^{fj} (\hat{U}_{t+2}^f)^{\gamma_s \beta} (\hat{\tau}_{t+1}^{fj})^{-\gamma_s}]^{\frac{\theta}{\gamma_s}}\big] \Bigg]^{\frac{1}{\theta}}$$

Substituting equation (75) for the first term in the bracket

$$= \hat{\omega}_{jt+1}(\hat{L}_{t+1}, \hat{\Theta}_{t+1}) \Bigg[\sum_{s \in M} (\mathscr{N}_t^{'sj})^{\frac{\gamma_s-\theta}{\gamma_s}} (\dot{\mathscr{N}}_{t+1}^{sj})^{\frac{\gamma_s-\theta}{\gamma_s}} [\sum_{f \in D_s} \mu_t^{'fj} \dot{\mu}_{t+1}^{fj} (\hat{U}_{t+2}^f)^{\gamma_s \beta} (\hat{\tau}_{t+1}^{fj})^{-\gamma_s}]^{\frac{\theta}{\gamma_s}} \Bigg]^{\frac{1}{\theta}}. \tag{79}$$

■

• Welfare formula

PROOF Equation (53)⇒

$$\begin{aligned} V_t^j &= u(C_t^j) - \tau_t^{jj} + \beta V_{t+1}^j + \frac{\theta - \gamma_m}{\gamma_m \theta} \ln(\sum_{h \in D_m} \mu_t^{hj}) - \frac{\ln \mu_t^{jj}}{\gamma_m} + \frac{\bar{\gamma}}{\theta} \\ &= \sum_{s=t}^{\infty} \beta^{s-t} u(C_s^j) + \frac{\theta - \gamma_m}{\gamma_m \theta} \sum_{s=t}^{\infty} \beta^{s-t} \ln(\sum_{h \in D_m} \mu_s^{hj}) - \frac{1}{\gamma_m} \sum_{s=t}^{\infty} \beta^{s-t} \ln \mu_s^{jj} \\ &\quad + \frac{\bar{\gamma}}{\theta(1-\beta)}, j \in D_m \end{aligned} \tag{80}$$

Suppose that the lifetime utility in the counterfactual is

$$V_t^{'j} = \sum_{s=t}^{\infty} \beta^{s-t} u(C_s^{'j}) + \frac{\theta - \gamma_m}{\gamma_m \theta} \sum_{s=t}^{\infty} \beta^{s-t} \ln(\sum_{h \in D_m} \mu_s^{'hj}) - \frac{1}{\gamma_m} \sum_{s=t}^{\infty} \beta^{s-t} \ln \mu_s^{'jj} + \frac{\bar{\gamma}}{\theta(1-\beta)}. \tag{81}$$

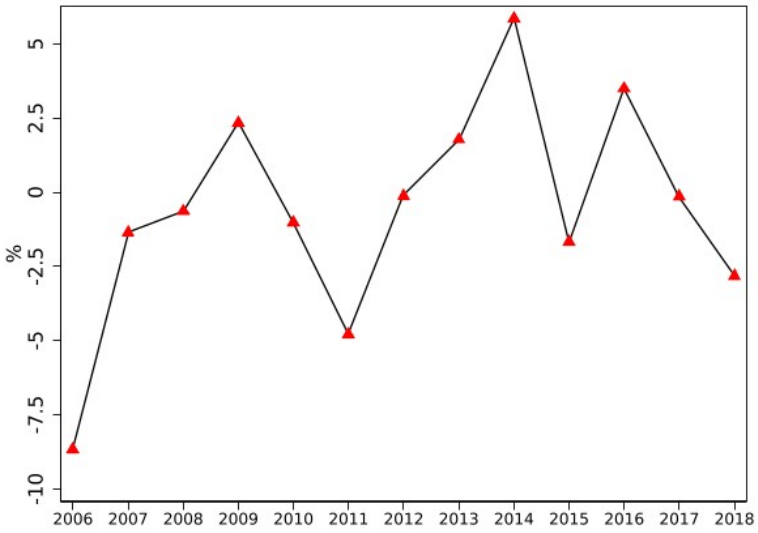


Figure 17: Real Wage Change in New Orleans based on Annual ACS data

We define the compensating variation in consumption at $t = 0$ for location j to be the scalar δ^j such that

$$V_0^{'j} = V_0^j + \sum_{s=0}^{\infty} \beta^s \ln(\delta^j). \tag{82}$$

Under logarithmic preference, equation (80) and (81) imply that

$$\begin{aligned}
\ln(\delta^j) &= (1-\beta)\Big[\sum_{s=0}^{\infty} \beta^s \ln\Big(\frac{C_s^{'j}/C_s^j}{(\mu_s^{'jj}/\mu_s^{jj})^{1/\gamma_m}}\Big) + \frac{\theta-\gamma_m}{\gamma_m\theta}\sum_{s=0}^{\infty}\beta^s \ln\frac{\sum_{h\in D_m}\mu_s^{'hj}}{\sum_{h\in D_m}\mu_s^{hj}}\Big] \\
&= \ln\Big(\frac{C_0^{'j}/C_0^j}{(\mu_0^{'jj}/\mu_0^{jj})^{1/\gamma_m}}\Big) + \sum_{s=1}^{\infty}\beta^s \ln\Big(\frac{(C_s^{'j}/C_{s-1}^{'j})/(C_s^j/C_{s-1}^j)}{((\mu_s^{'jj}/\mu_{s-1}^{'jj})/(\mu_s^{jj}/\mu_{s-1}^{jj}))^{1/\gamma_m}}\Big) \\
&\quad - \frac{\theta-\gamma_m}{\gamma_m\theta}\ln\frac{\sum_{h\in D_m}\mu_0^{'hj}}{\sum_{h\in D_m}\mu_0^{hj}} + \frac{\theta-\gamma_m}{\gamma_m\theta}\sum_{s=1}^{\infty}\beta^s \ln\frac{\sum_{h\in D_m}\mu_s^{'hj}/\sum_{h\in D_m}\mu_{s-1}^{'hj}}{\sum_{h\in D_m}\mu_s^{hj}/\sum_{h\in D_m}\mu_{s-1}^{hj}},
\end{aligned}$$

Since the initial state is the same, by the definition of $\hat{C}_t$, $\hat{\mu}_t$ and $\mathscr{N}_t^{mj}$

$$= \sum_{s=1}^{\infty}\beta^s \ln\Big(\frac{\hat{C}_s^j}{(\hat{\mu}_s^{jj})^{1/\gamma_m}}\Big) + \frac{\theta-\gamma_m}{\gamma_m\theta}\sum_{s=1}^{\infty}\beta^s \ln\big(\hat{\mathscr{N}}_s^{mj}\big), \quad j \in D_m. \tag{83}$$

■

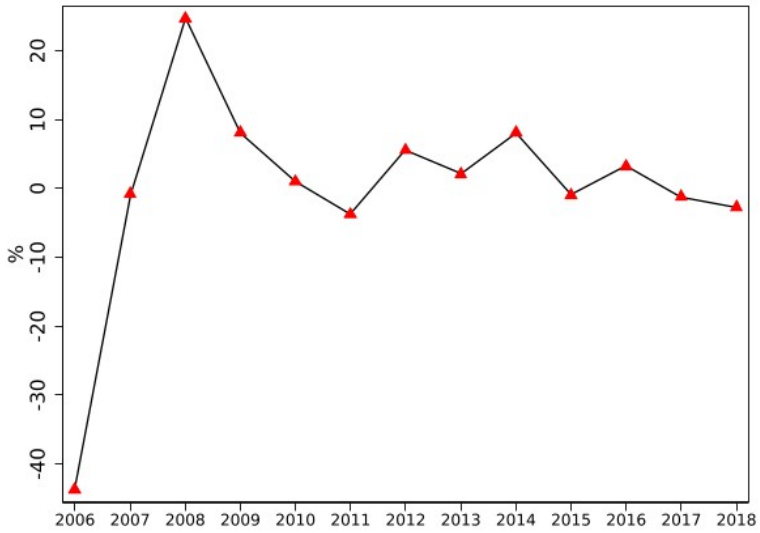
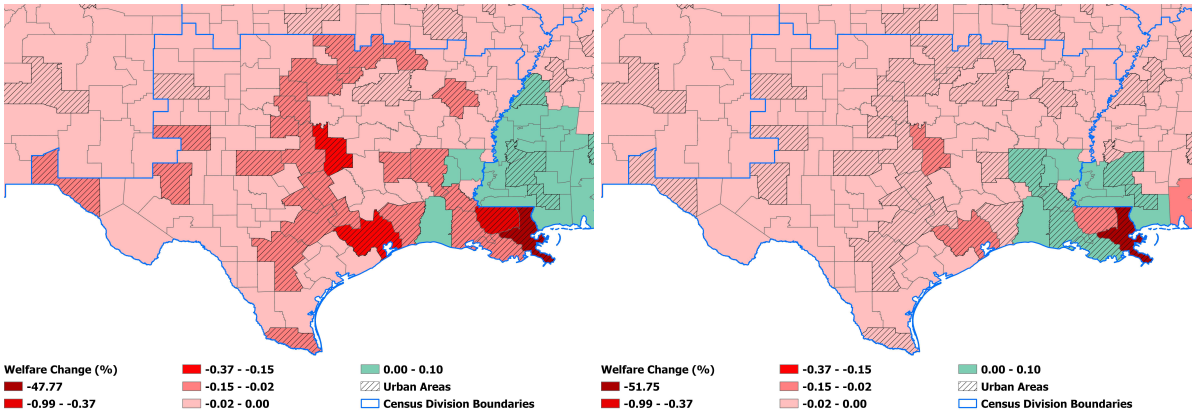


Figure 18: Productivity Change in New Orleans based on Model Inversion



(a) My Model (b) Conventional Model

Figure 19: Welfare Change in the South of United State (Katrina Case)

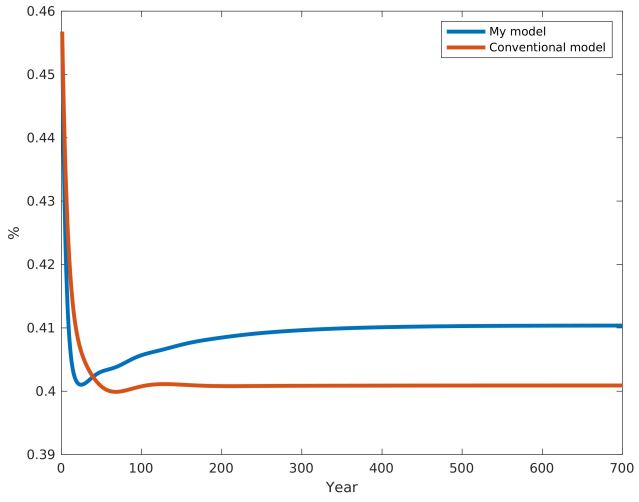


Figure 20: New Orleans Population in the Katrina Case

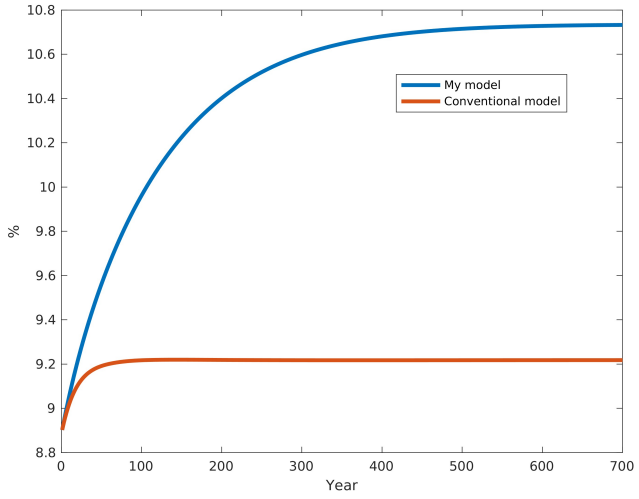


Figure 21: New Orleans Nest Population in the Katrina Case

F Multi-sectors and Capital Dynamics

In this section, I extend the economy to allow for a wider range of general-equilibrium mechanisms such as costly tradable products, multiple sectors, input-output linkages, and capital dynamics.

F.1 Households

The local aggregate consumption C_{jt} for a representative hand-to-mouth agent in location j at period t is now a Cobb-Douglas aggregator of consumption across K different sectors with expenditure share α_s:

$$C_{jt} = \Pi_{s \in K} (\frac{c^s_{jt}}{\alpha_s})^{\alpha_s}, \tag{84}$$

where c^s_{jt} denotes the sector s local aggregator; and α_s is the expenditure share in sector s goods.

Here, individual i in location j at time t can endogenously choose her employment status, *employed* or *unemployed*, depending on the employment benefits, $w_{jt}\varepsilon^e_{it}$, and the non-employment benefits, $b_{jt}\varepsilon^u_{it}$. ε^e_{it} and ε^u_{it} denote the idiosyncratic efficiency units of labor and non-employment income potential, respectively. They are independently drawn from a Frechet

distribution with shape parameter ϕ each period. Therefore, we can derive the employment rate in location j with efficient labor wage w_{jt} and the non-employment benefits b_{jt}, n_{jt}, which is

$$n_{jt} = \frac{w_{jt}^{\phi}}{w_{jt}^{\phi} + b_{jt}^{\phi}}. \tag{85}$$

The conditional mean of efficient labor units for those who are employed in location j, l_{jt}^{E}, is given by

$$\begin{aligned}
l_{jt}^{E} &= \mathbf{E}[\varepsilon_{it}^{e} | e = argmax_k\{b_{jt}\varepsilon_i^{u}, w_{jt}\varepsilon_i^{e}\}] \\
&= \frac{\int_0^{\infty} \varepsilon \exp\big(-(\frac{w_{jt}}{b_{jt}}\varepsilon)^{-\phi}\big)\phi\varepsilon^{-\phi-1}\exp(-\varepsilon^{-\phi})d\varepsilon}{n_{jt}} \\
&= \frac{\int_0^{\infty} \varepsilon \exp\big(-(\frac{b_{jt}^{\phi}+w_{jt}^{\phi}}{w_{jt}^{\phi}})\varepsilon^{-\phi}\big)\phi\varepsilon^{-\phi-1}d\varepsilon}{n_{jt}} \\
&\text{Let } x = (b_{jt}^{\phi} + w_{jt}^{\phi})^{-\frac{1}{\phi}} w_{jt}\varepsilon \\
&= \frac{\int_0^{\infty} \exp(-x^{-\phi})\phi x^{-\phi}(b_{jt}^{\phi} + w_{jt}^{\phi})^{\frac{1}{\phi}-1} w_{jt}^{\phi-1} dx}{n_{jt}} \\
&= \frac{(b_{jt}^{\phi} + w_{jt}^{\phi})^{\frac{1}{\phi}-1} w_{jt}^{\phi-1}}{n_{jt}} \Gamma(1-\frac{1}{\phi}).
\end{aligned} \tag{86}$$

Similarly, the expected non-employment income potential, l_{jt}^{U}, is

$$l_{jt}^{U} = \frac{(b_{jt}^{\phi} + w_{jt}^{\phi})^{\frac{1}{\phi}-1} b_{jt}^{\phi-1}}{u_{jt}} \Gamma(1-\frac{1}{\phi}), \;\; u_{jt} = 1 - n_{jt}. \tag{87}$$

In addition to making choices about consumption and employment, individuals make migration decisions each period. Here, I assume that only after they have moved to their migration destination can individuals observe their realized idiosyncratic efficiency units of labor and decide their employment status in that destination. Therefore, when they choose their optimal place for the next period, $t+1$, it is the expected wage over the idiosyncratic efficient labor supply distribution, denoted as w_{jt+1}^{E}, in destination j instead of either the employed wage or non-employment benefits alone that affects individuals' migration behavior. Based upon equation

(86) and (87), we can obtain the expected wage, w_{jt}^E, which is equal to

$$\begin{aligned} w_{jt}^E &= n_{jt} w_{jt} l_{jt}^E + (1 - n_{jt}) b_{jt} l_{jt}^U \\ &= (b_{jt}^\phi + w_{jt}^\phi)^{\frac{1}{\phi}} \Gamma(1 - \frac{1}{\phi}). \end{aligned} \tag{88}$$

Replacing $(b_{jt}^\phi + w_{jt}^\phi)^{\frac{1}{\phi}}$ with equation (85), we have

$$w_{jt}^E = w_{jt} n_{jt}^{-\frac{1}{\phi}} \Gamma(1 - \frac{1}{\phi}). \tag{89}$$

The total number of efficient labor units in location j with population L_{jt}, denoted as L_{jt}^s, is given by

$$L_{jt}^s = L_{jt} n_{jt} l_{jt}^E = L_{jt} (b_{jt}^\phi + w_{jt}^\phi)^{\frac{1}{\phi}-1} w_{jt}^{\phi-1} \Gamma(1 - \frac{1}{\phi}) = L_{jt} n_{jt}^{1-\frac{1}{\phi}} \Gamma(1 - \frac{1}{\phi}). \tag{90}$$

Then the total wage income, W_{jt}^R, is equal to

$$W_{jt}^R = w_{jt} L_{jt}^s = w_{jt} L_{jt} n_{jt} l_{jt}^E = w_{jt} L_{jt} n_{jt}^{1-\frac{1}{\phi}} \Gamma(1 - \frac{1}{\phi}). \tag{91}$$

F.2 Production

In the goods market, there are multiple sectors featuring Eaton and Kortum (2002)-style production technology associated with input-output linkage.

Firms in each sector and place produce differentiated intermediate goods. The production technology requires labor, structure, and intermediate goods. Total factor productivity (TFP) consists of a time-varying sectoral-location component, the location's agglomeration forces, and firm-specific productivity. Specifically, the tradable intermediate good producer i in sector s and location j owns the following technology:

$$q_{jit}^s = z_{jit}^s (A_{jt}^s k_{jit}^\alpha (l_{jit}^e)^{1-\alpha})^{\gamma_j^s} \Pi_{d \in K} (M_{jt}^{ds})^{(1-\gamma_j^s)\xi_j^{ds}} \left(\frac{n_{jt}}{1 - n_{jt}}\right)^\psi \tag{92}$$

where k_{jit} and l_{jit}^e are physical capital and efficient labor inputs, respectively; and M_{jt}^{ds} is the

sector d aggregator demanded by firm i in sector s. γ_j^s is the sector-specific share of value added in total output. α is the capital share in value added. A_{jt}^s is the sectoral productivity in location j, while z_{jit}^s is the firm-specific productivity independently drawn from a Frechet distribution with shape parameter υ^s. The final factor, $(\frac{n_{jt}}{1-n_{jt}})^{\psi}$, is used to capture various agglomeration forces in a reduced-form way as in Adao et al. (2019).

Let r_{jt} denote the rental prices of local structures. The unit price of an input bundle in location j and sector s is

$$x_{jt}^s = B^s (r_{jt}^{\alpha} w_{jt}^{1-\alpha})^{\gamma_j^s} \Pi_{s \in K} (P_{jt}^s)^{(1-\gamma_j^s)\xi_j^{sj}}, \tag{93}$$

where B^s is a constant and P_{jt}^s is the sector s price index in location j. Hence, the unit cost of intermediate good z_{ji}^s is equal to

$$\frac{x_{jt}^s}{z_{jit}^s (A_j^s)^{\gamma_j^s} (\frac{n_{jt}}{1-n_{jt}})^{\psi}}. \tag{94}$$

Similar to Caliendo et al. (2019), I assume there is a non-tradable local sectoral good denoted by Q, which aggregates intermediate goods demand from sector s and from all places. Let Q_{jt}^s be the quantity of aggregate sectoral goods s produced in location j and $q(z_t^s)$ be the quantity of an intermediate good of a given variety demanded from the lowest-cost supplier. Then the production of local sectoral goods is given by

$$Q_{jt}^s = \left(\int q(z_t^s)^{1-1/\zeta^s} d\phi(z^s) \right)^{\zeta^s/(\zeta^s-1)}, \tag{95}$$

where $\phi(z^s) = \exp(-\sum_{k \in J} (z_r^s)^{-\upsilon^s})$ is the multivariate Fréchet distribution over the vector z^s, with the marginal distribution given by $\exp(-z_r^s)^{\upsilon^s}$. It follows from the Fréchet distribution that the sectoral aggregate price index, P_{jt}^s, is

$$P_{jt}^s = \Gamma(1 + (1-\zeta^s)/\upsilon^s) \left(\sum_{f \in J} (x_{ft}^s \kappa_{fmt}^s)^{-\upsilon^s} (A_{ft}^s)^{\gamma_{ft}^s \upsilon^s} \left(\frac{n_{ft}}{1-n_{ft}} \right)^{\psi \upsilon^s} \right)^{-\frac{1}{\upsilon^s}}, \tag{96}$$

where κ_{fjt}^s is the trade cost for importing intermediate goods in sector s from location f to j

and $\Gamma(1+(1-\zeta^s)/\upsilon^s)$ is a constant.[30] We can also solve for the share of total expenditure in location j on goods s imported from location h, π^s_{hmt}, which is

$$\pi^s_{hmt} = \frac{(x^s_{ht}\kappa^s_{hmt})^{-\upsilon^s}(A^s_{ht})^{\gamma^s_h\upsilon^s}\left(\frac{n_{ht}}{1-n_{ht}}\right)^{\psi\upsilon^s}}{\sum_{f\in J}(x^s_{ft}\kappa^s_{fmt})^{-\upsilon^s}(A^s_{ft})^{\gamma^s_f\upsilon^s}\left(\frac{n_{ft}}{1-n_{ft}}\right)^{\psi\upsilon^s}}. \tag{97}$$

F.3 Capital accumulation

Similar to Kleinman et al. (2023), I assume that landlords have access to an investment technology for accumulating local physical capital and that their investment is determined by an intertemporal consumption-investment problem. Concretely, a representative landlord l in location j at time t chooses her consumption and investment to solve for her intertemporal optimization problem according to

$$v^l_{jt} = \mathbf{E}\sum_{s=0}^{\infty}\beta^s_k \log C^l_{mt+s}, \tag{98}$$

$$s.t.\ \ r_{jt}k^l_{jt} = P_{jt}(C^l_{jt} + k^l_{jt+1} - (1-\delta)k^l_{jt}), \tag{99}$$

where β_k is the landlord's discount factor; C^l_{jt+1} is the local aggregator in region j; $P_{jt}(\equiv \Pi_{s\in K}(P^s_{jt})^{\alpha_s})$ is the local price index; and δ is the capital depreciation rate. The budget constraint, equation (99), implicitly assumes that one unit of the local consumption aggregator can produce one unit of capital.

The guess-and-verify approach shows that the optimal saving rate for landlord l is a constant that is equal to the discount rate, β_k. Hence, landlords' optimal saving and investment decisions are given by

$$k^l_{jt+1} = \beta_k R_{jt}k^l_{jt},\ \ R_{jt} \equiv 1-\delta+r_{jt}/P_{jt}. \tag{100}$$

F.4 Trade imbalance

I follow the standard assumption in the quantitative trade literature that trade imbalances, D_{jt}, are exogenous. I assume that there is a global government that levies a labor income tax at

[30] To obtain equation (96), I assume that $1+\upsilon^s > \zeta^s$.

rate χ and then redistributes the tax revenues in a way that each location receives a constant portion. Let location j's portion be $\iota_j \sum_{h\in J} \chi W_{ht}^R$, where $\sum_{h\in J} \chi W_{ht}^R$ is the total tax revenue; and $\sum_{h\in J} \iota_h = 1$. This redistribution guarantees that the difference between the received transfer and the levied labor income tax in each place will generate trade imbalances. Formally,

$$D_{jt} = \sum_{s\in K}\sum_{r\in J} \pi_{jrt}^s X_{rt}^s - \sum_{s\in K}\sum_{r\in J} \pi_{rjt}^s X_{jt}^s, \tag{101}$$

$$\iota_j = \frac{\chi W_{jt}^R - D_{jt}}{\sum_{h\in J} \chi W_{ht}^R}. \tag{102}$$

F.5 Market clearing

Let X_{jt}^s denote the total expenditure on sector s good in location j. Then the market clearing condition implies

$$X_{jt}^s = \sum_{s\in K} (1-\gamma_j^s)\xi_j^{js} \sum_{r\in R} \pi_{jrt}^s X_{rt}^s + \alpha^s((1-\chi)W_{jt}^R + r_{jt}k_{jt} + + \iota_j \sum_{h\in J} \chi W_{ht}^R), \tag{103}$$

where the first term in $R.H.S$ represents the value of the total demand for sector j goods across all sectors and regions. The second term, which consists of post-tax labor income, capital income, and government transfer, is the value of the total demand as the final consumption of goods in region j. α^s denotes the share of the consumption expenditure on sector s goods.

The labor market clearing in location j indicates that

$$L_{jt}^s = \frac{\sum_{h\in K}\sum_{r\in J}(1-\alpha)\gamma_j^h \pi_{mrt}^h X_{rt}^h}{w_{jt}}. \tag{104}$$

The structure market clearing in location j satisfies

$$k_{jt} r_{jt} = \frac{\alpha}{1-\alpha} w_{jt} L_{jt}^s. \tag{105}$$

F.6 Static hat algebra

This subsection shows how to use hat algebra to solve for the static equilibrium. Let $\dot{y}_{t+1} \equiv y_{t+1}/y_t$. We also assume that unemployment benefits' component b_{jt} in location j is exoge-

nously given.

Equation (100)⇒

$$k_{jt+1} = \beta_k R_{jt} k_{jt}. \tag{106}$$

Equation (85) ⇒

$$\dot{n}_{jt+1} = \frac{\dot{w}^{\phi}_{jt+1}}{(1-n_{jt}) + n_{jt}\dot{w}^{\phi}_{jt+1}}, \;\; \dot{u}_{jt+1} = \frac{1}{(1-n_{jt}) + n_{jt}\dot{w}^{\phi}_{jt+1}}. \tag{107}$$

Replacing r_{jt} with $r_{jt} = \frac{\alpha(w_{jt}L^s_{jt})}{(1-\alpha)k_{jt}}$ based on equation (105), equation (93) ⇒

$$\dot{x}^s_{jt+1} = \dot{w}^{\gamma^s_j}_{jt+1} \left(\frac{\dot{L}^s_{jt+1}}{\dot{k}_{jt+1}}\right)^{\alpha\gamma^s_j} \Pi_{s\in K} (\dot{P}^s_{jt+1})^{(1-\gamma^s_j)\xi^{sj}_j}. \tag{108}$$

Equation (106) ⇒

$$\dot{x}^s_{jt+1} = \dot{w}^{\gamma^s_j}_{jt+1} \left(\frac{\dot{L}^s_{jt+1}}{\beta_k R_{jt}}\right)^{\alpha\gamma^s_j} \Pi_{s\in K} (\dot{P}^s_{jt+1})^{(1-\gamma^s_j)\xi^{sj}_j}. \tag{109}$$

Equation (90) ⇒

$$\dot{L}^s_{jt+1} = \dot{L}_{jt+1} \dot{n}^{1-\frac{1}{\phi}}_{jt+1}. \tag{110}$$

Equation (89) ⇒

$$\dot{w}^E_{jt+1} = \dot{w}_{jt+1} (\dot{n}_{jt+1})^{-\frac{1}{\phi}}. \tag{111}$$

Equation (96) and (97) ⇒

$$\dot{P}^s_{jt+1} = \left(\sum_{f\in J} \pi^s_{fmt} (\dot{x}^s_{ft+1} \dot{\kappa}^s_{fmt+1})^{-\upsilon^s} (\dot{A}^s_{ft+1})^{\gamma^s_f \upsilon^s} \left(\frac{\dot{n}_{ft+1}}{\dot{u}_{ft+1}}\right)^{\psi\upsilon^s} \right)^{-\frac{1}{\upsilon^s}}. \tag{112}$$

Equation (97) and (112) $\Rightarrow$

$$\dot{\pi}^s_{hmt+1} = \frac{(\dot{x}^s_{ht+1}\dot{\kappa}^s_{hmt+1})^{-\upsilon^s}(\dot{A}^s_{ht+1})^{\gamma^s_h\upsilon^s}\left(\frac{\dot{n}_{ht+1}}{\dot{u}_{ht+1}}\right)^{\psi\upsilon^s}}{(\dot{P}^s_{jt+1})^{-\upsilon^s}}. \tag{113}$$

Dividing equation (105) at time $t+1$ by its counterpart at time t and replacing r_{jt+1} in (105) with R_{jt+1} in (100), we obtain

$$(R_{jt+1}-(1-\delta)) = (R_{jt}-(1-\delta))\frac{\dot{w}_{jt+1}\dot{L}^s_{jt+1}}{\dot{P}_{jt+1}\dot{k}_{jt+1}}. \tag{114}$$

It follows from equation (106) that capital's law of motion is

$$(R_{jt+1}-(1-\delta)) = (R_{jt}-(1-\delta))\frac{\dot{w}_{jt+1}\dot{L}^s_{jt+1}}{\dot{P}_{jt+1}\beta_k R_{jt}}. \tag{115}$$

Equation (91) and (103) $\Rightarrow$

$$\begin{aligned} X^s_{jt+1} = &\sum_{h\in K}(1-\gamma^h_j)\xi^{jh}_m\sum_{r\in J}\pi^h_{mrt+1}X^h_{rt+1} \\ &+\alpha^s((1-\chi+\frac{\alpha}{1-\alpha})\dot{w}_{jt+1}\dot{L}^s_{jt+1}w_{jt}L^s_{jt}+\iota_j\sum_{h\in J}\chi\dot{w}_{ht+1}\dot{L}^s_{ht+1}w_{ht}L^s_{ht}). \end{aligned} \tag{116}$$

In the labor market, it follows from equation (104) that

$$\dot{w}_{jt+1}\dot{L}^s_{jt+1}w_{jt}L^s_{jt} = \sum_{h\in K}(1-\alpha)\gamma^h_j\sum_{r\in J}\pi^h_{mrt+1}X^h_{rt+1}. \tag{117}$$

Finally, location j's aggregate price index is

$$\dot{P}_{jt+1} = \Pi_{s\in K}(\dot{P}^s_{jt+1})^{\alpha_s}. \tag{118}$$

F.7 Simple Example

In this simple economy, there are five locations: four commuting zones (CZs) belonging to the same country and one place outside the country. People are mobile within a country but not across countries. Of the four CZs, two are in the northern region and the other two in the

Parameter	Value
Capital depreciation rate δ	0.05
Capital share α	0.35
Labor income tax rate χ	0.2
Landlord's discount factor β_k	0.90
Trade elasticity υ	5
Value-added share γ	0.5

Table 8: Parameterization

southern part. There are two sectors in the economy. The intermediate goods in one sector are tradable both within and across countries, but they are not tradable in the other sector. Both sectors use each sector's local aggregator as the intermediate goods input in their intermediate goods production based on the input-output linkage.

Households' expenditure share in the tradable sector is equal to 0.85. Following Adao et al. (2019), I set the efficient labor supply elasticity ϕ to 4.4 and the agglomeration forces ϕ to 0.05. Other parameters are presented in Table 8.

Based on Propositions 6 and 7 associated with the static-hat algebra in Subsection F.6, I first calculate the common steady state for both my model and the single-elasticity framework under this multisector background. It serves as the baseline economy. Then I simulate a scenario in which the tradable sector's productivity unexpectedly declines 10% in CZ 1 in my dynamic nested logit setting and in the conventional setting, respectively. In my framework, the nest is defined as the region. Within-region CZs are more substitutable with each other than cross-region ones. Finally, I compare the counterfactuals with the baseline economy.[31]

Figure 22 presents CZ 1's outflows' percentage change relative to the steady state. The blue line is my model's result, while the red line is the conventional model's one. Clearly, the flow to CZ 2 that belongs to CZ 1's nest adjusts faster than the flow to either of the two outside-nest CZs in my framework. However, all flows in the single-elasticity model (excluding that of non-migrants) scale up at the same proportion. Therefore, such a difference in the migration response between my framework and the conventional one implies that even if I were to introduce more richness in both the household and production sides and allow for capital dynamics, we would still observe the crucial fact in Section 6 that heterogeneity in

[31] Simulation details are available upon request.

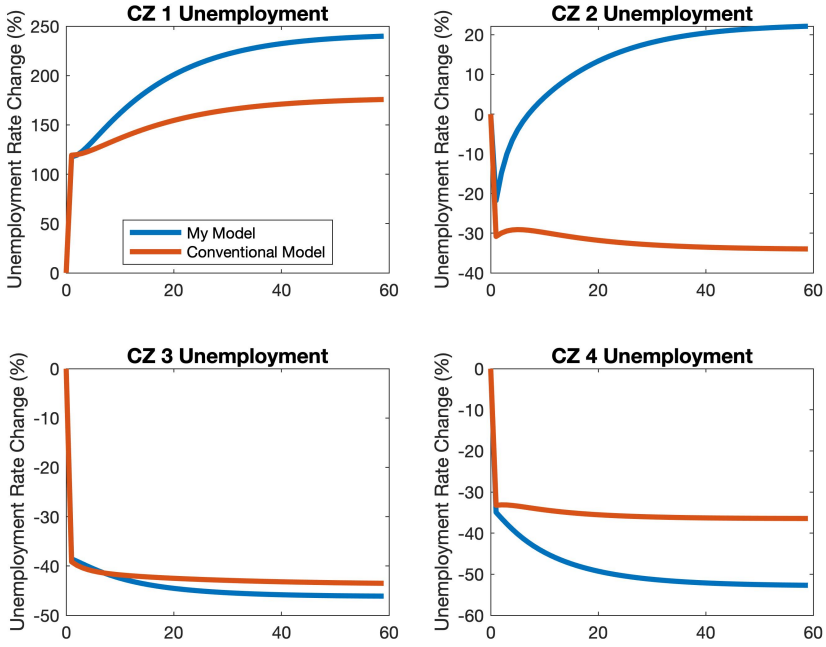


Figure 22: Outflow Change in CZ 1 (%)

migration elasticities may lead to disproportionate post-shock migration responses, whereas the single elasticity fails to do the same.

Furthermore, as seen in Figure 23, these two models deliver different welfare implications. Similar to our observations in Section 6, the welfare loss is concentrated in the within-nest destination CZ 2. It is also true that, as evident in Figure 24, the adjustment to the shock is slower in my dynamic nested logit framework than than it is in the conventional model.

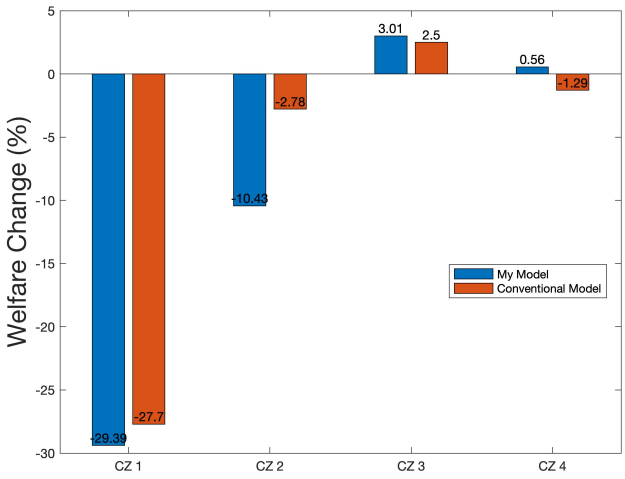


Figure 23: Welfare Change (%)

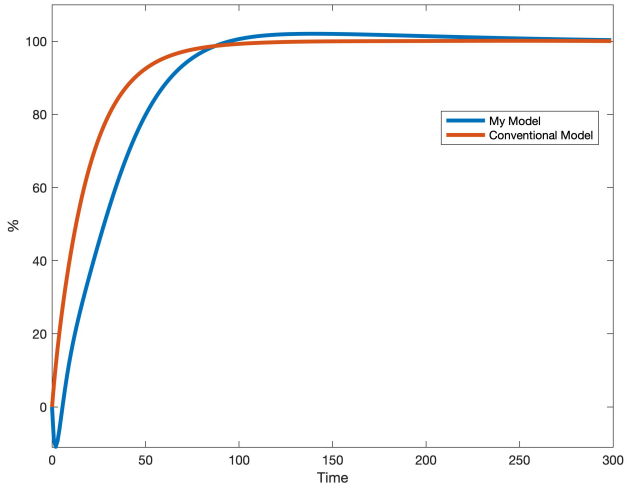


Figure 24: Population Adjustment in CZ 1's Nest (%)